# 大規模火山災害時の避難所空港選択モデルに関する研究

# Muroran IT

## Muroran Institute of Technology

DISSERTATION:

STUDY ON SHELTER AIRPORT UTILIZATION MODELS DURING LARGE-SCALE VOLCANIC DISASTERS

Saharat Arreeras
19096002
March 2022

# STUDY ON SHELTER AIRPORT UTILIZATION MODELS DURING LARGE-SCALE VOLCANIC DISASTERS

By

Saharat ARREERAS

A dissertation submitted in partial fulfilment of the requirements for the degree of
Doctor of Engineering

| | |
|---|---|
| Examination Committee: | Prof. Nakatsugawa Makoto |
| | Prof. Kimura Katsutoshi |
| | Prof. Mikiharu Arimura (Chairman) |
| | |
| Nationality: | Thai |
| | |
| Previous Degree: | Bachelor of Information Science |
| | Suranaree University of Technology, Thailand |
| | Master of Information Technology |
| | Suranaree University of Technology, Thailand |
| | |
| Scholarship Donor: | Japan Student Services Organization (JASSO) Scholarship |
| | Muroran Institute of Technology Scholarship |

Muroran Institute of Technology
Division of Sustainable and Environmental Engineering
Japan

# Acknowledgement

| Topic: | Study on Shelter Airport Utilization Models During Large-Scale Volcanic Disasters |
|---|---|
| Author: | Saharat ARREERAS |
| Degree: | Doctor of Engineering |
| Course: | Course of Advanced Sustainable and Environmental Engineering |
| Advisor: | Professor Mikiharu ARIMURA |

# ABSTRACT

Air transport supports economic growth and prosperity through the movement of passengers and goods. As it grows more extensive and more complex, the more vulnerable its operations to unexpected natural disasters (e.g., typhoons and volcanic eruptions) will become. In Japan, many active volcanos are affecting its airspace and are considered a threat to the national air transportation and critical aviation equipment such as aircraft. The study is primarily concerned with resolving the issue of shelter airport selection during an aircraft evacuation during a volcanic eruption. The shelter airport selection model was constructed using the airside, airline, and historical data. Later, it was applied to a genetic algorithm (GA) to find an approximate solution for aircraft evacuation with the least amount of flight time and the best suitability for shelter airport selection criteria.

Moreover, the study has extended to provide a strategy for resolving the issue of aircraft stand use at shelter airports during emergencies. The suggested aircraft stand utilization for aircraft assignment employs a two-dimensional bin packing (2DBP) technique combined with a heuristic approach to maximize the aircraft handling capability of the airport while minimizing stand usage. The performance of the proposed model was compared to the conventional aircraft assignment in a case study of Japanese airspace, which has endured various natural disasters, including earthquakes and volcanic eruptions, that endanger national air transport infrastructure. In addition, both the proposed aircraft and the conventional aircraft stand assignment models were employed to assess the capabilities and potential of shelter airports to handle various scenarios of affected aircraft.

This dissertation addressed three contribution studies to the acknowledgement of aviation disaster prevention, which consists of; 1) a study on shelter airport selection during large-scale volcanic disasters using carats open dataset, 2) an improvement on shelter airport selection model during large-scale volcanic disasters: a case study of Hakoneyama Japan, and 3) aircraft parking stand utilization for aircraft evacuation using two-dimensional bin packing algorithm. Hence, a stack of varying viewpoints research provided a comprehensive review and suggestion throughout significant results. Therefore, the contribution of this dissertation could be an advantage for emergency strategy and policies planner to recognize alternative solutions leading to better aviation disaster prevention.

**Keyword:** Genetic algorithm (GA), Large-scale volcanic disasters, Shelter airport selection criterions, Evacuation, Aircraft stand utilization, Two-dimensional bin packing (2DBP).

| 題目: | 大規模火山災害時の避難所空港選択モデルに関する研究 |
|---|---|
| 氏 名: | サハラート　アレーラス |
| 学位: | 博士（工学） |
| コース: | 先端環境創生工学コース |
| 主任指導教員氏名: | 有村　幹治 教授 |

# 論文内容の要旨

　　　　航空輸送は乗客と物流を通じて経済成長と繁栄を支えている。航空輸送がより広範かつ複雑に成長するにつれ、予期しない自然災害（台風や火山の噴火等）に対して、航空機の運用はより脆弱となる。日本では多くの活火山が管制領域に影響を及ぼしており、国の航空輸送や航空機等の重要な航空機器の運用に対する脅威と見なされている。この研究は主に火山噴火に対する航空機の避難所となる空港選択の問題の解決を目的とする。避難所空港選択モデルは、エアサイド、航空会社、および運用履歴データを使用して構築された。その後、遺伝的アルゴリズム（GA）を適用し、飛行時間が最小となる避難所の空港選択基準に最も適した航空機の避難方法を探索した。

　　　　さらに本研究では、緊急時の避難所空港の航空機駐機位置問題を解決する戦略を提供するようにモデルを拡張した。航空機の割り当てに推奨される航空機駐機位置の使用率の効率化のために、2次元ビンパッキング（2DBP）手法とヒューリスティックなアプローチを組み合わせて、駐機位置の使用量を最小限に抑えながら空港の航空機運用能力を最大化する。提案されたモデルの性能について、国の航空輸送インフラを危険にさらす地震や火山噴火などの様々な自然災害に耐えてきた日本の空域をケーススタディとして、従来の航空機駐機位置の割り当てモデルと比較した。さらに提案された航空機と従来の航空機駐機位置割り当てモデルの両方を使用して、影響を受けた航空機の様々なシナリオを処理する避難所空港の能力と可能性を評価した。

　　　　本論文は、航空防災に貢献する 3 つの関連する研究として、1）CARATS オープンデータセットを用いた大規模火山災害時の避難所選択に関する研究、2）大規模火山災害時の避難所空港選択モデルの改善：日本の箱根山の事例研究、3）航空機避難のための二次元ビンパッキングアルゴリズムを使用した航空機駐機位置の活用、以上から構成される。本論文では上記の様々な視点からの研究蓄積と重要な成果を通して包括的なレビューと提案を提供した。本論文の貢献は、航空機避難に関する緊急戦略の策定およびより良い航空防災につながる代替解決策を政策立案者に認識させる点にある。

キーワード: 遺伝的アルゴリズム（GA）、大規模な火山災害、避難所の空港選択基準、避難、航空機スタンドの利用、2次元ビンパッキング（2DBP）

# CONTENTS INDEX

# LIST OF FIGURES

# LIST OF TABLES

# LIST OF APPENDIX TABLES

# CHAPTER 1

Introduction and Background

## 1.1.   AIR TRANSPORTATION SUPPORT ECONOMY GROWTH

Air transport supports economic growth and prosperity through movement of passengers and goods. With low fare of low-cost carrier airlines (LCC) and stronger economies, the worldwide air passenger numbers have exceeded four billion in 2017 (IATA, 2018) for the first time and has thus grew continuously.

Globally, passenger growth improves but the trend remains moderate Year-on-year growth in industry-wide revenue passenger kilometers (RPKs) edged up to 4.5% in August. Despite the difficult economic conditions in several key markets, the moderate upward trend in passenger traffic continues. According to IATA annual report in June 2019, Japan, the world's fifth-largest airline industry and one of the busiest airspaces in the world. Japan, annual growth in domestic RPKs slowed to 3.8% in August compared to global trend, but still higher that the same period in 2018 at 2.6%. Economic growth was revised downwards in Q2 for Japan and weakness in the global economy also impact passenger travel, see Figure 1.1.



<div align="center">(a)                                                        (b)</div>
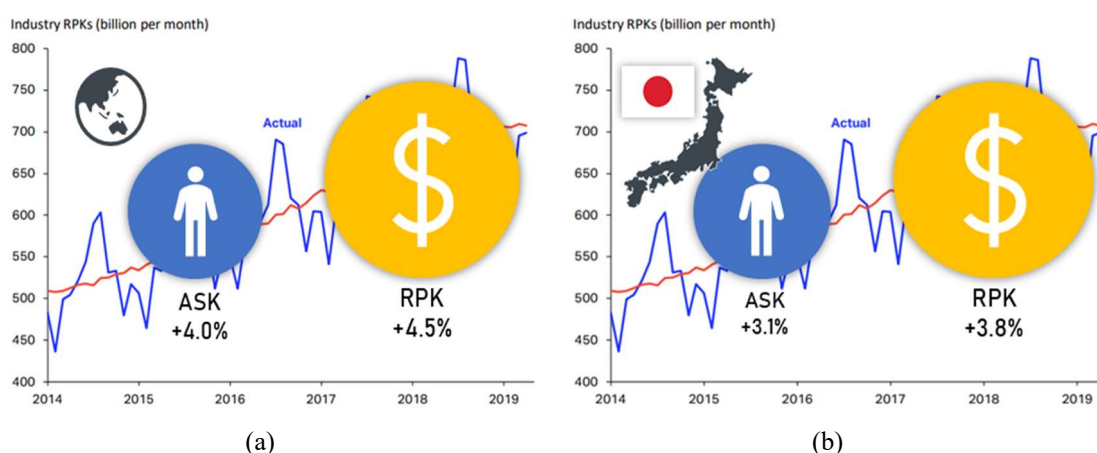
**Figure 1.1** Global (a) and Japan (b) passenger air transport growth rate.

<div align="right">ASK: Available Seat Kilometers, RPK: Revenue Passer<br>Sources: Air Passenger Market Analysis, IATA Economics, IATA Monthly Statistics</div>

## 1.2.   DISASTERS WEAKEN AIR TRANSPORT NETWORK

Airports are the critical aviation infrastructure and essential to their regions' economic activities and even more critical during the disaster (Smith, 2010) such as earthquakes, volcanic eruptions, and human-made disasters. Recently, the airline industry had encountered the uncertain situations of volcanic eruption and its ash cloud when the Eyjafefjallajökull and Merapi Volcano erupted in 2010, which had significantly disrupted air transport and economy in Europe and Indonesia's central (Langmann et al., 2012; Mazzocchi et al., 2010; Picquout et al., 2013). In Japan, the volcanic eruption is one of the national air transportation threats as there are more than 100 active volcanos, and many of them are in the busy airspace and large hub/regional airports.

The International Civil Aviation Organization (ICAO) and the Japan Meteorological Agency established guidelines for the safe operation of all aviation parties during natural disasters and volcanic eruptions (JMA).
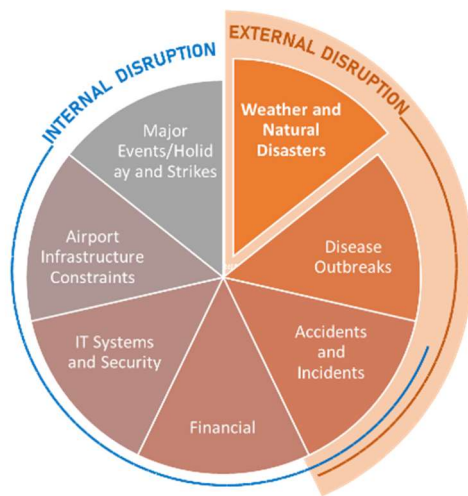
"Flight disruption"

Defined as 'situations where a scheduled flight is cancelled, or delayed for two hours or more, within 48 hours of the original scheduled departure time'. Disruptions in aviation cost airlines and their customers up to $60 billion per year, or about 8% of worldwide airline revenue.

Source: Amadeus, Travel Technology Research Ltd. (2016)
Airport Council International (ACI)

**Recent Global-scale volcanic disaster in Iceland 2010**

Disturbed European and north America airspace, and global air transportation. 95,000 flights have been cancelled during the eruption, impact on 100k of passengers
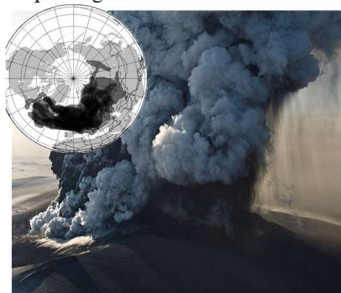


**Hazards to aviation from volcanic ash cloud**

Airport Emergency Planning during disaster has suggested to evacuate aircraft both in-flight and on-ground to the safe facility outside impacted area as soon as possible.



ICAO Annex 14 and doc-9173 part 7
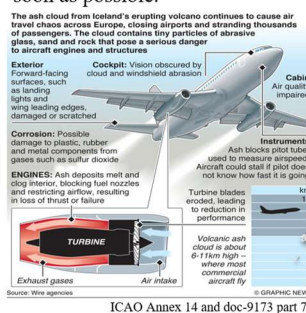
**Volcanos in the busiest airspace of Japan**

100 active volcanos and the busiest airspace, in 100km range from active volcano "Hakoneyama"

Kanto: the busiest airspace and airports in Japan, handle 30% of all traffic.
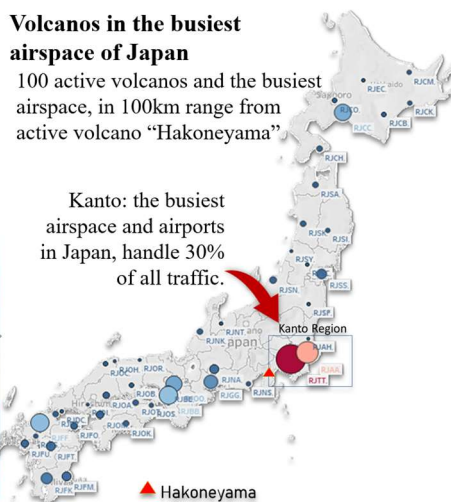


## 1.3.    AIRCRAFT AND AIRPORT MANAGEMENT DURING DISASTER

In the disaster times, the surrounding unaffected airports are expected to quickly respond and fulfill the affected airports' loss capacity to reduce the disaster's wide-effect (Button et al., 2010; HANAOKA et al., 2013). The Japan catastrophic earthquake in March 2011 caused the loss of Sendai international airport, one of the major air transportation hubs in East Japan. Other regional and smaller local airports' role became more important on bypassing, maintaining the connections between remaining airports, and securing the unoperated equipment included aircraft (Cidell, 2006; Kita et al., 2005). These unforeseeable conditions can reduce the level of airport operation performance, create air traffic congestion, and put pressure on airport resources from limited resource utilization (Harsha, 2003).

The airport's practical resource utilization could be achieved by integrating various operations, including aircraft maintenance, flight operations, ground handling, fueling services, airside services, and air traffic control (Harriman et al., 2009). Madas and Zografos studied airport

slot allocation under the situation of air traffic congestion by airport's classification, capacity and size, and air traffic demand to measure the airport handling capability before choosing the suitable slot allocation for aircraft (Madas and Zografos, 2010). The other studies showed that Airport capacity, alliance/partner airline operations, and airline operations at the designated airport are all factors that have a substantial impact on aircraft and passenger relocation during a disruption, according to the study (Hu et al., 2016; Lordan et al., 2015, 2014; Lordan and Klophaus, 2017). Hence, the large airports (hub and regional airports) are expected to become emergency airports in surging air traffic demands during the disaster from their operations and capacities readiness.



The capacity of an airport relates to its ability to manage its whole operation. However, the majority of definitions define airport capacity in terms of runway and apron area. Additionally, capacity is defined as the maximum number of operations done in a specified amount of time and on a continuous basis on the ground and in the air (de Neufville and Odoni, 2013; Idrissi and Li, 2006). During a disaster, an unexpected surge of various types of aircraft, including non-operational flights, evacuated flights, and humanitarian planes, can easily exceed the airport's capacity. As a result, airports are likely to operate faster and more quickly to aid in local and national disaster relief efforts. Therefore, proper operation and infrastructure planning are crucial for the smooth operation of airport disaster management and response operations.

Airport disaster management (ADM) studies have put the focusing on the airport resources capacity utilization on both landside and airside, which airside capacity is defined into three parts: runway(s), taxiway(s), and apron area (the aircraft stands area for loading, unloading, and refueling) within the airport capacity constraints (Jimenez Serrano and Kazda, 2017). In particular, the aircraft stands allocation (SA) for accommodating the affected aircraft but rarely the study on SA during the disaster. Instead, a bundle of studies on airport gate assignment problem (AGAP) is available. Most of them had set on the four main minimization objectives, i.e., the passenger's walking distance, the number of ungated flights, dispersion of idle gate periods, passenger travel time, and the number of flights exceeds the number of available gates.

Many studies had applied various meta-heuristic algorithms to solve these optimization problems on aircraft stand allocation and proved to be necessary to solve such NP-hardness of the optimization problem as SA (Guépet et al., 2015). Those applied meta-heuristic algorithms included simulated annealing (Cheng et al., 2012; Ding et al., 2005), bee colony optimization (Dell'Orco et al., 2017; Marinelli et al., 2015), tabu search, and genetic algorithm (Aktel et al., 2017; Cheng et al., 2012; Ding et al., 2005; Liu and Kozan, 2016; Marinelli et al., 2015). Although the studies mentioned above did not intend to solve airport selection and aircraft assignment during the disaster. However, they had given a big picture of the concerning factors on airport disaster management, resource utilization, and optimization algorithms, which can develop the computational optimization model on shelter airport selection for aircraft evacuation during the natural disaster.

## 1.4.   OPTIMIZATION MODEL FOR AIRCRAFT AND AIRPORT MANAGEMENT DURING DISASTER

In principle, the optimization model for shelter location selection was built for large-scale emergencies to select shelters from the exited safe and suitable locations according to both evacuee and shelter location criteria. The main goals are responsiveness and cost-efficiency by minimizing total evacuation cost, time, and the entire transport distance between demand points (an affected area and candidate facilities). Regularly, the evacuation is evaluated its efficiency by distance or time (Toregas et al., 1971). Thus, the first objective function aims to focus on the travel distance and time criterion. The minimization of total or minisum formulation had widely applied to the optimization models on the facility selection of humanitarian relief supply distribution in the various natural disasters, i.e., hurricane and earthquake (Horner and Downs, 2010; Lin et al., 2012). The metaheuristic approach, such as the genetic algorithm (GA), has recently introduced to the complex multi-criteria objective optimization problems of optimal shelter selection on the flooding evacuation planning, earthquake shelter location selection, and the facility location selection in response to large-scale emergencies (Hu et al., 2014; Kongsomsaksakul et al., 2005).

Additionally, aircraft recovery research began in 1984 (Teodorović and Guberinić, 1984), when a disruption event and optimization model were simulated if one or more aircraft became unavailable for flight. Later that year, Argüello et al. introduced a metaheuristic approach to aircraft recovery optimization by utilizing a Greedy Randomized Adaptive Search Procedure (GRASP) to reconstruct aircraft flight routes following the grounding of one or more aircraft. Additionally, aircraft recovery problems have been addressed using the metaheuristic method based on tabu and local search (Andersson, 2006; Løve et al., 2001). These models enabled the development of a novel solution that met the study's objective and constraints. Furthermore, the stand allocation problem (SAP) operation disruptions studies were examined, and the underlying assumptions and methodologies used to address operational disruptions caused by arrival and departure uncertainty were discussed (Skorupski and Żarów, 2021). The problem was commonly referred to as the gate re-assignment problem, and several models were proposed and evaluated using metaheuristic algorithms in conjunction with gate assignment constraints for addressing when an incoming aircraft's delay causes subsequent incoming aircraft to arrive at the assigned gate late (Gu and Chung, 1999; Narciso and Piera, 2015; Şeker and Noyan, 2012; van Schaijk and Visser, 2017; Yan and Tang, 2007). However, the system for selecting a shelter airport for aircraft evacuation and aircraft stand utilization due to surging aircraft parking demand during disaster are infrequently available.

## 1.5.   AIMS OF THIS STUDY AND RESEARCH QUESTIONS

The first phase of this study had aimed to propose an airport selection model for aircrafts evacuation in a volcanic eruption situation by considering the airport's available aircraft stands capacity, aircraft size, and enclosed area to avoid volcanic ash cloud. Then, the proposed improved model, which could help design a more practical shelter airport option for airline recovery following a disruption event. This study aimed to improve shelter airport selection during a disaster or airline recovery operation by combining additional airline data and generating new model restrictions. This research contributes by creating a model for selecting a shelter airport for affected aircraft assignment in emergency evacuation planning during the disaster with extended airport and airline limits.

Later, to overcome the surging demand of aircraft parking space during emergency, an aircraft stand utilization model based on two-dimensional bin packing was developed to extend airport aircraft handling capacity, space utilization, and minimizing the number of aircraft stands required to accommodate aircraft evacuation without further airport infrastructure investment and impairing regular flying operations at selected aircraft during an emergency.

Question 1: Chapter 2

How to select shelter airport for aircraft evacuation with approximate solution?

Question 2: Chapter 3

How to improve the shelter airport selection model to suitable shelter airport which could help airport and airline perform their operations during and after the disaster?

Question 3: Chapter 4

How can airport utilize it aircraft parking capacity to handle more grounded aircraft during the disaster without invest more on expanding their facility?

## 1.6. MATERIALS AND METHODS

In this study, the historical flight dataset "the collaborative actions for the renovation of air traffic systems (CARATS)", airport infrastructure, airline schedule flight data had been used to determine and simulate; possible disaster impacted and safe area for shelter airport, and number of affected aircrafts and their profiles. And also, airport and aircraft regulations and restriction, which had been used as shelter airport selection constraints in model construction and validation. At the early part of this book on shelter airport selection,

The proposed model has been developed and applied to the genetic algorithm (GA), then analyzed its performance according to the study's objective and subject. The study also compared GA's performance with the Greedy Randomized Adaptive Search Procedure (GRASP), the basic multi-start meta-heuristic algorithm on the same developed model. Although GRASP does not equip with the crossover and mutation operators like in GA. GRASP has a similar mechanism to GA in its ability to randomly generate initial solutions, evaluate, select the better solution, and replace it with a better new local optimal solution in each iteration. Even though both GA and GRASP may or may not promise the global-optimal results, their procedures could ensure that the best result or approximate results will be generated at the end of all running iterations. Therefore, their results could suggest aviation authorities and related parties, e.g., air traffic control agencies, airports, and airlines, on which airport could be the critical shelter airports for aircraft evacuation of the volcanic eruption minimize effected of the event.

Later, the proposed model employed the two-dimensional bin packing algorithm (2DBP) to assign affected aircraft to available aircraft stands at shelter airports. In 2DBP, packing techniques such as the maximal rectangles split (MAXRECT) and the first fit decreasing algorithm (FFD) are used. The bins and items represent the available aircraft parking stands and the affected aircraft of different sizes. The proposed model aimed to extend aircraft parking stand space utilization, which enabled airports to accommodate more aircraft within their limited capacity. Figure 1.2 illustrates of the study construction conceptual framework.
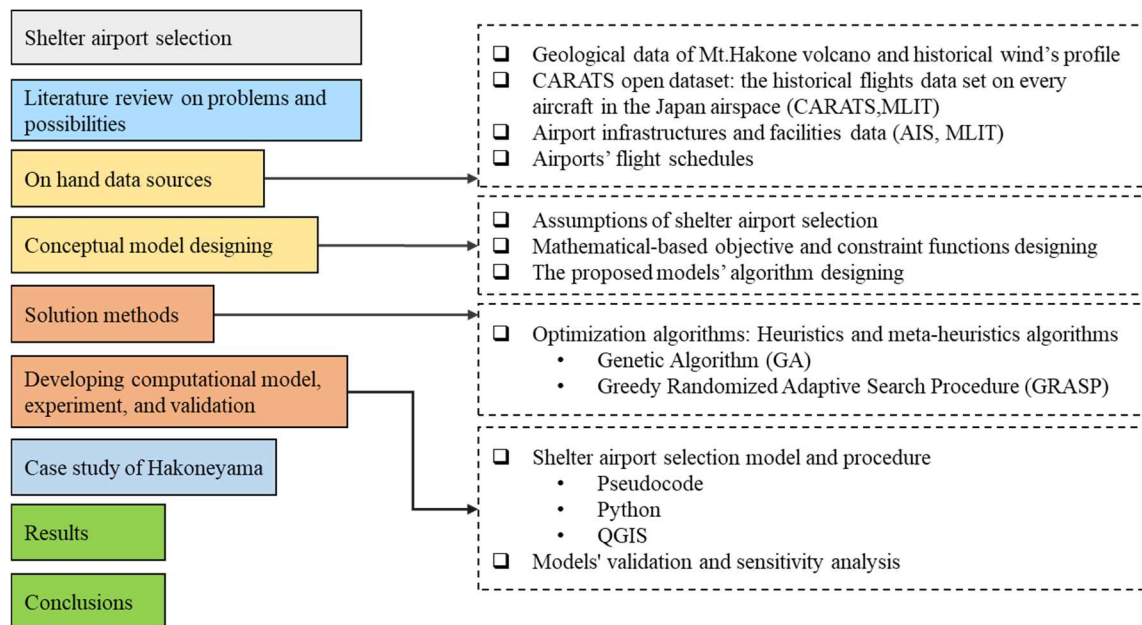
**Figure 1.2** Conceptual framework of the study.

## 1.1. CONTRIBUTION OF THE STUDY

TRC: Therefore, their results could suggest aviation authorities and related parties, e.g., air traffic control agencies, airports, and airlines, on which airport could be the critical shelter airports for aircraft evacuation of the volcanic eruption minimize effected of the event.

EASTS/ATS: This research contributes by creating a model for selecting a shelter airport for aircraft utilized in emergency evacuation planning during volcanic eruptions with extended airport and airline limits. The new proposed model might give aviation authorities and other stakeholders, such as air traffic control agencies, airports, and airlines, a realistic and viable option for aircraft evacuation.

JATM: This study contributes to existing research by giving aviation authorities and related parties, such as air traffic control agencies, airports, and airlines, practical and realistic advice for aircraft stand utilization and critical airports that can accommodate a significant number of affected aircraft during aircraft evacuation.

## 1.7. STUDY STRUCTURES

This book is organized as follows: chapter 2 presents the methodology, dataset, and proposed mathematical model for shelter airport selection under basic measure of evacuation constraints (Evacuation time/distance, aircraft sizes, and shelter airport capacity) applied with Genetic Algorithm (GA). The model was applied on a case study of Mt.Hakone, later compared the result with Greedy Randomized Adaptive Search Procedure (GRASP). In chapter 3, the model from chapter 2 was improved using additional airport and airline constraints, which could allow model to select more appropriate shelter airport with beneficial for airport and aircraft at all stage from evacuation until recovery.

The concerning of aircraft parking demand during disaster may lead to insufficient aircraft parking at the shelter airport. Numbers of airport must be designated as shelter airport, which may lead to difficulty in airport and airlines management. Chapter 4 had proposed the model for airport capacity expansion for grounded airport during disaster without airport investment on its infrastructure. The model was adopted airport and aircraft parking regulation and restrictions applied with Two-dimensional Bin Packing algorithm (2DBP) to achieve the goal. Finally, the conclusion, future research suggestions, and research limitations are presented in chapter 5 as illustrated in Figure 1.3.
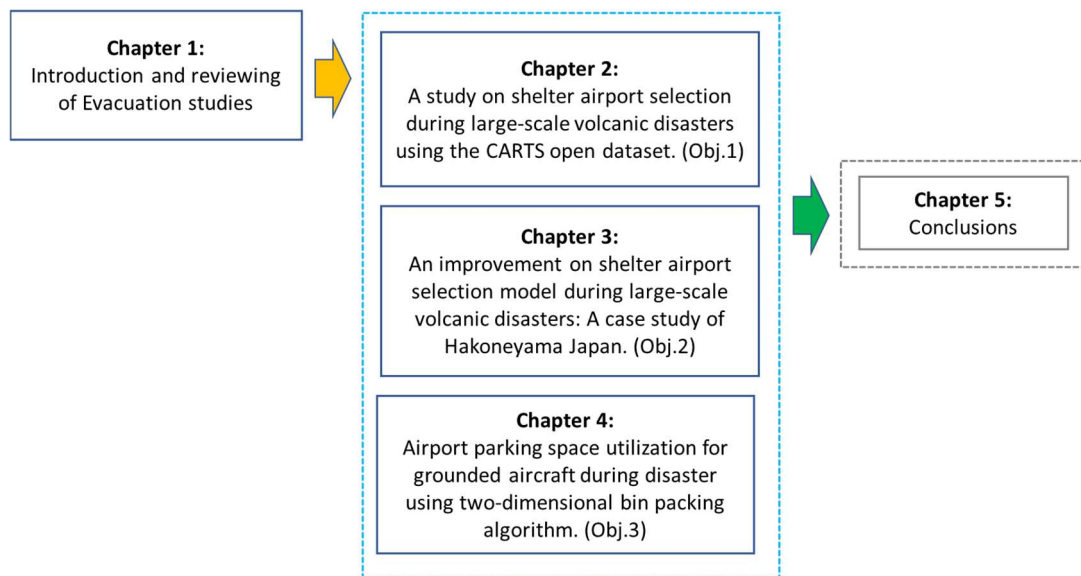


**Figure 1.3** Book's chapters organizing.

## REFERENCES

Aktel, A., Yagmahan, B., Özcan, T., Yenisey, M.M., Sansarcı, E., 2017. The comparison of the metaheuristic algorithms performances on airport gate assignment problem. Transportation Research Procedia 22, 469–478. https://doi.org/10.1016/j.trpro.2017.03.061

Andersson, T., 2006. Solving the flight perturbation problem with meta heuristics. Journal of Heuristics 12, 37–53. https://doi.org/10.1007/s10732-006-4833-4

Button, K., Vega, H., Nijkamp, P., 2010. A Dictionary Of Transport Analysis, A Dictionary of Transport Analysis. https://doi.org/10.4337/9781849804714

Cheng, C.H., Ho, S.C., Kwan, C.L., 2012. The use of meta-heuristics for airport gate assignment. Expert Systems with Applications 39, 12430–12437. https://doi.org/10.1016/j.eswa.2012.04.071

Cidell, J., 2006. Regional cooperation and the regionalization of air travel in Central New England. Journal of Transport Geography 14, 23–34. https://doi.org/10.1016/j.jtrangeo.2004.10.003

de Neufville, R., Odoni, A.R., 2013. Airport Systems: Planning, Design, and Management. McGraw-Hill Education.

Dell'Orco, M., Marinelli, M., Altieri, M.G., 2017. Solving the gate assignment problem through the Fuzzy Bee Colony Optimization. Transportation Research Part C: Emerging Technologies 80, 424–438. https://doi.org/10.1016/j.trc.2017.03.019

Ding, H., Lim, A., Rodrigues, B., Zhu, Y., 2005. The over-constrained airport gate assignment problem. Computers & Operations Research 32, 1867–1880. https://doi.org/10.1016/j.cor.2003.12.003

Gu, Y., Chung, C.A., 1999. Genetic algorithm approach to aircraft gate reassignment problem. Journal of Transportation Engineering 125, 384–389. https://doi.org/10.1061/(ASCE)0733-947X(1999)125:5(384)

Guépet, J., Acuna-Agost, R., Briant, O., Gayon, J.P., 2015. Exact and heuristic approaches to the airport stand allocation problem. European Journal of Operational Research 246, 597–608. https://doi.org/10.1016/j.ejor.2015.04.040

Hanaoka, S., Indo, Y., Hirata, T., Todoroki, T., Aratani, T., Osada, T., 2013. Lessons and challenges in airport operation during a disaster: case studies on Iwate Hanamaki airport, Yamagata airport, and Fukushima airport during the great east Japan earthquake. Journal of JSCE 1, 286–297. https://doi.org/10.2208/journalofjsce.1.1_286

Harriman, S., Fanjoy, R., Petrin, D., 2009. Small General Aviation Airport Emergency Preparedness and the Perceived Risks of Very Light Jet Operations. Journal of Aviation/Aerospace Education & Research. https://doi.org/10.15394/jaaer.2009.1382

Harsha, P., 2003. Mitigating Airport Congestion: Market Mechanisms and Airline Response Models. Massachusetts Institute of Technology.

Horner, M.W., Downs, J.A., 2010. Optimizing hurricane disaster relief goods distribution: Model development and application with respect to planning strategies. Disasters. https://doi.org/10.1111/j.1467-7717.2010.01171.x

Hu, F., Yang, S., Xu, W., 2014. A non-dominated sorting genetic algorithm for the location and districting planning of earthquake shelters. International Journal of Geographical Information Science. https://doi.org/10.1080/13658816.2014.894638

Hu, Y., Song, Y., Zhao, K., Xu, B., 2016. Integrated recovery of aircraft and passengers after airline operation disruption based on a GRASP algorithm. Transportation Research Part E: Logistics and Transportation Review 87, 97–112. https://doi.org/10.1016/j.tre.2016.01.002

IATA, 2018. the Annual Review 2018. IATA Journal 68.

Idrissi, A., Li, C.M., 2006. Modeling and optimization of the capacity allocation problem with constraints, in: Proceedings of the 4th IEEE International Conference on Research, Innovation and Vision for the Future, RIVF'06. pp. 107–116. https://doi.org/10.1109/RIVF.2006.1696426

Jimenez Serrano, F.J., Kazda, A., 2017. Airline disruption management: Yesterday, today and tomorrow, in: Transportation Research Procedia. Elsevier, pp. 3–10. https://doi.org/10.1016/j.trpro.2017.12.162

Kita, H., Koike, A., Tanimoto, K., 2005. Air Service Development of Local Airports and its Influence on the Formation of Aviation Networks. Research in Transportation Economics. https://doi.org/10.1016/S0739-8859(05)13011-X

Kongsomsaksakul, S., Yang, C., Chen, A., 2005. Shelter location-allocation model for flood evacuation planning. Journal of the Eastern Asia Society for Transportation Studies.

Langmann, B., Folch, A., Hensch, M., Matthias, V., 2012. Volcanic ash over Europe during the eruption of Eyjafjallajökull on Iceland, April-May 2010. Atmospheric Environment 48, 1–8. https://doi.org/10.1016/j.atmosenv.2011.03.054

Lin, Y.H., Batta, R., Rogerson, P.A., Blatt, A., Flanigan, M., 2012. Location of temporary depots to facilitate relief operations after an earthquake. Socio-Economic Planning Sciences 46, 112–123. https://doi.org/10.1016/j.seps.2012.01.001

Liu, S.Q., Kozan, E., 2016. Parallel-identical-machine job-shop scheduling with different stage-dependent buffering requirements. Computers and Operations Research 74, 31–41. https://doi.org/10.1016/j.cor.2016.04.023

Lordan, O., Klophaus, R., 2017. Measuring the vulnerability of global airline alliances to member exits. Transportation Research Procedia 25, 7–16. https://doi.org/10.1016/j.trpro.2017.05.189

Lordan, O., Sallan, J.M., Simo, P., 2014. Study of the topology and robustness of airline route networks from the complex network approach: A survey and research agenda. Journal of Transport Geography 37, 112–120. https://doi.org/10.1016/j.jtrangeo.2014.04.015

Lordan, O., Sallan, J.M., Simo, P., Gonzalez-Prieto, D., 2015. Robustness of airline alliance route networks. Communications in Nonlinear Science and Numerical Simulation 22, 587–595. https://doi.org/10.1016/j.cnsns.2014.07.019

Løve, M., Sørensen, K., Larsen, J., Clausen, J., 2001. Using heuristics to solve the dedicated aircraft recovery problem, Optimization Online.

Madas, M.A., Zografos, K.G., 2010. Airport slot allocation: A time for change? Transport Policy 17, 274–285. https://doi.org/10.1016/j.tranpol.2010.02.002

Marinelli, M., Palmisano, G., Dell'Orco, M., Ottomanelli, M., 2015. Fusion of Two Metaheuristic Approaches to Solve the Flight Gate Assignment Problem. Transportation Research Procedia 10, 920–930. https://doi.org/10.1016/j.trpro.2015.09.045

Mazzocchi, M., Hansstein, F., Ragona, M., 2010. The 2010 volcanic ash cloud and its financial impact on the European airline industry. CESifo Forum.

Narciso, M.E., Piera, M.A., 2015. Robust gate assignment procedures from an airport management perspective. Omega 50, 82–95. https://doi.org/10.1016/j.omega.2014.06.003

Picquout, A., Lavigne, F., Mei, E.T.W., Grancher, D., Noer, C., Vidal, C.M., Hadmoko, D.S., 2013. Air traffic disturbance due to the 2010 Merapi volcano eruption. Journal of Volcanology and Geothermal Research 261, 366–375. https://doi.org/10.1016/j.jvolgeores.2013.04.005

Şeker, M., Noyan, N., 2012. Stochastic optimization models for the airport gate assignment problem. Transportation Research Part E: Logistics and Transportation Review 48, 438–459. https://doi.org/10.1016/j.tre.2011.10.008

Skorupski, J., Żarów, P., 2021. Dynamic management of aircraft stand allocation. Journal of Air Transport Management 90, 101964. https://doi.org/10.1016/j.jairtraman.2020.101964

Smith, J.F., 2010. Regional Cooperation, Coordination, and Communication between Airports during Disasters. Transportation Research Record: Journal of the Transportation Research Board 2177, 132–140. https://doi.org/10.3141/2177-16

Teodorović, D., Guberinić, S., 1984. Optimal dispatching strategy on an airline network after a schedule perturbation. European Journal of Operational Research 15, 178–182. https://doi.org/10.1016/0377-2217(84)90207-8

Toregas, C., Swain, R., ReVelle, C., Bergman, L., 1971. The Location of Emergency Service Facilities. Operations Research. https://doi.org/10.1287/opre.19.6.1363

van Schaijk, O.R.P., Visser, H.G., 2017. Robust flight-to-gate assignment using flight presence probabilities. Transportation Planning and Technology 40, 928–945. https://doi.org/10.1080/03081060.2017.1355887

Yan, S., Tang, C.H., 2007. A heuristic approach for airport gate assignments for stochastic flight delays. European Journal of Operational Research 180, 547–567. https://doi.org/10.1016/j.ejor.2006.05.002

# CHAPTER 2

A Study on Shelter Airport Selection during Large-scale Volcanic Disasters using CARATS Open Dataset

# A Study on Shelter Airport Selection during Large-scale Volcanic Disasters using CARATS Open Dataset

## ABSTRACT

Air transport supports economic growth and prosperity through the movement of passengers and goods. As it grows more extensive and more complex, the more vulnerable its operations to unexpected natural disasters (e.g., typhoon and volcanic eruption) will become. In Japan, many active volcanos are affecting its airspace and considered a threat to the national air transportation and critical aviation equipment such as aircraft. The study focuses on solving the evacuation of the affected aircraft during the volcanic eruption by proposed the shelter airport selection model using the historical data of volcanic eruption, aircraft movement, and airports data in Japan. The model was applied to the genetic algorithm (GA), the metaheuristic algorithm to provide the approximate solution of the suitable shelter airport with minimum flight time and no exceeded shelter airports' capacities for the aircraft evacuation.

## KEYWORDS

genetic algorithm, large-scale volcanic disasters, shelter airport selection

**Motivations:**

- ❏ Impact of natural disaster on air transportation in Japan, especially volcanic eruption.
- ❏ Aircraft engine is vulnerable to volcanic ash particles, aircraft evacuation to the safe airport is crucial.
- ❏ Historical flight dataset and airport facility information pave the way to accurate aircraft positions and shelter airport candidates.
- ❏ Meta-heuristic algorithm has capability in finding the approximate solution under setting constraints of aircraft assignment and airport selection.

**Objectives:**

The study aims to develop shelter airport selection model, which could select the suitable shelter airport for aircraft evacuation with mini flight time. Under basic airport selection constraints using historical flight data and airport facility information applied on Genetic Algorithm and compare its performance to another similar algorithm on the same setting.

**Case study:** Hakonayama, Japan

**Study gaps:**

Historical flight data used in the study came from 2016 which may not reflect the current situation of air traffic volume (before COVID-19 pandemic). Airport facility information especially size and capacity were difficult of extract from aviation information service center (AIS) provided by MLIT.

**Data collections:**

- ❏ CARATS flight dataset on March 7th-13rd, 2016 provided by MLIT (the latest data available at the time of study)
- ❏ Japan airport information provided by aviation Information Service Center (AIS), MLIT
- ❏ Sakurajima and Hakoneyama ash fall and ash cloud observation, Japan Metrological Agency.
- ❏ Annual wind profile in March 2016 provided by National Centers for Environmental Information (NCEI)

**Methodologies:**

- ❏ Model development
- ❏ Genetic Algorithm (GA) and Greedy Randomized Adaptive Search Procedure (GRASP)
- ❏ Model validation and comparison
- ❏ Sensitivity analysis

## 2.1.    INTRODUCTION AND BACKGROUND

Airports are the critical aviation infrastructure and essential to their regions' economic activities and even more critical during the disaster (Smith, 2010) such as earthquakes, volcanic eruptions, and human-made disasters. Recently, the airline industry had encountered the uncertain situations of volcanic eruption and its ash cloud when the Eyjafefjallajökull and Merapi Volcano erupted in 2010, which had significantly disrupted air transport and economy in Europe and Indonesia's central (Langmann et al., 2012; Mazzocchi et al., 2010; Picquout et al., 2013). In Japan, the volcanic eruption is one of the national air transportation threats as there are more than 100 active volcanos, and many of them are located in the busy airspace and large hub/regional airports. Although the safety operation regulations during the volcanic eruption have been established by ICAO and Japan Meteorological Agency (JMA), there is no shelter airport selection system with integrated air flight and airport data available, which is considered as a problem in this study. Therefore, we aim to develop a shelter airport selection model for the event of a volcanic eruption.

In the disaster times, the surrounding unaffected airports are expected to quickly respond and fulfill the affected airports' loss capacity to reduce the disaster's wide effect (Button et al., 2010; HANAOKA et al., 2013). The Japan catastrophic earthquake in March 2011 caused the loss of Sendai international airport, one of the major air transportation hubs in East Japan. Other regional and smaller local airports' role became more important on bypassing, maintaining the connections between remaining airports, and securing the unoperated equipment included aircraft (Cidell, 2006; Kita et al., 2005). These unforeseeable conditions can reduce the level of airport operation performance, create air traffic congestion, and put pressure on airport resources from limited resource utilization (Harsha, 2003).

The airport's practical resource utilization could be achieved by integrating various operations, including aircraft maintenance, flight operations, ground handling, fueling services, airside services, and air traffic control (Harriman et al., 2009). Madas and Zografos studied airport slot allocation under the situation of air traffic congestion by airport's classification, capacity and size, and air traffic demand to measure the airport handling capability before choosing the suitable slot allocation for aircraft (Madas and Zografos, 2010). The other studies showed that airport capacity had a significant impact on aircraft and passenger relocation in the event of disruptions, which was also mentioned in other studies concerning airport slot allocation problems (Hu et al., 2016; Lordan et al., 2015, 2014; Lordan and Klophaus, 2017). Hence, the large airports (hub and regional airports) are expected to become emergency airports in surging air traffic demands during the disaster from their operations and capacities readiness.

Airport disaster management (ADM) studies have put the focusing on the airport resources capacity utilization on both landside and airside, which airside capacity is defined into three parts: runway(s), taxiway(s), and apron area (the aircraft stands area for loading, unloading, and refueling) within the airport capacity constraints (Jimenez Serrano and Kazda, 2017). In particular, the aircraft stands allocation (SA) for accommodating the affected aircraft but rarely the study on SA during the disaster. Instead, a bundle of studies on airport gate assignment problem (AGAP) is available. Most of them had set on the four main minimization objectives, i.e., the passenger's walking distance, the number of ungated flights, dispersion of idle gate periods, passenger travel time, and the number of flights exceeds the number of available gates. Many studies had applied various meta-heuristic algorithms to solve these optimization problems on aircraft stand allocation and proved to be necessary to solve such NP-hardness of the optimization problem as SA (Guépet et al., 2015). Those applied meta-heuristic algorithms included simulated annealing (Cheng et al., 2012; Ding et al., 2005), bee colony optimization (Dell'Orco et al., 2017; Marinelli et al., 2015), tabu search, and genetic algorithm (Aktel et al.,

2017; Cheng et al., 2012; Ding et al., 2005; Liu and Kozan, 2016; Marinelli et al., 2015). Although the studies mentioned above did not intend to solve airport selection and aircraft assignment during the disaster. However, they had given a big picture of the concerning factors on airport disaster management, resource utilization, and optimization algorithms, which can develop the computational optimization model on shelter airport selection for aircraft evacuation during the natural disaster.

In principle, the optimization model for shelter location selection was built for large-scale emergencies to select shelters from the exited safe and suitable locations according to both evacuee and shelter location criteria. The main goals are responsiveness and cost-efficiency by minimizing total evacuation cost, time, and the entire transport distance between demand points (an affected area and candidate facilities). Regularly, the evacuation is evaluated its efficiency by distance or time (Toregas et al., 1971). Thus, the first objective function aims to focus on the travel distance and time criterion. The minimization of total or minisum formulation had widely applied to the optimization models on the facility selection of humanitarian relief supply distribution in the various natural disasters, i.e., hurricane and earthquake (Horner and Downs, 2010; Lin et al., 2012). The metaheuristic approach, such as the genetic algorithm (GA), has recently introduced to the complex multi-criteria objective optimization problems of optimal shelter selection on the flooding evacuation planning, earthquake shelter location selection, and the facility location selection in response to large-scale emergencies (Hu et al., 2014; Kongsomsaksakul et al., 2005).

Therefore, this study aims to propose an airport selection model for aircrafts evacuation in a volcanic eruption situation by considering the airport's available aircraft stands capacity, aircraft size, and enclosed area to avoid volcanic ash cloud. The proposed model has been developed and applied to the genetic algorithm (GA), then analyzed its performance according to the study's objective and subject. The study also compared GA's performance with the Greedy Randomized Adaptive Search Procedure (GRASP), the basic multi-start meta-heuristic algorithm on the same developed model. Although GRASP does not equip with the crossover and mutation operators like in GA. GRASP has a similar mechanism to GA in its ability to randomly generate initial solutions, evaluate, select the better solution, and replace it with a better new local optimal solution in each iteration. Even though both GA and GRASP may or may not promise the global-optimal results, their procedures could ensure that the best result or approximate results will be generated at the end of all running iterations. Therefore, their results could suggest aviation authorities and related parties, e.g., air traffic control agencies, airports, and airlines, on which airport could be the critical shelter airports for aircraft evacuation of the volcanic eruption minimize effected of the event.

This paper's remainder is organized as follows: Section 2.2 presents the methodology, dataset, and proposed mathematical model of research. The case study of Mt.Hakone is presented in section 2.3 with models' validations in section 2.4 and computational results in section 2.5. Finally, the conclusion, future research suggestions, and research limitations are presented at the end of the study.

## 2.2.    METHODS AND MATERIALS

This section discusses a conceptual model and assumption, Genetic algorithm (GA) and Greedy Randomized Adaptive Search Procedure (GRASP), the collaborative actions for the renovation of air traffic systems (CARATS) flight dataset, and the proposed mathematical model and its pseudocodes as follows:

### 2.2.1 Genetic algorithm (GA) and Greedy Randomized Adaptive Search Procedure (GRASP)

Genetic Algorithm (GA) is a type of evaluation algorithm. Darwin's theory of evolution is an optimization method based on concepts of natural selection and genetics. They work with individuals' populations; each evolves by adapting itself to the environment, repeating crossover, mutation, and selecting a possible solution to a given environment's conditions or problem. The appropriate solution can be found by using the series of numerical computation. GA typically works by iteratively generating and evaluating individuals using an evaluation function. The basic process flow of GA is shown in Figure 2.1.

The performance of the model applied on GA is compared with the basic meta-heuristic algorithm, Greedy Randomized Adaptive Search Procedure (GRASP). GRASP is the basic multi-start meta-heuristic algorithm for combinatorial optimization problems proposed by Feo and Resende in 1995 (Feo and Resende, 1995). In each running iteration of the GRASP algorithm consists of two steps: construction and local search. In the construction step, a feasible candidate solution is built using randomized greedy heuristic. The second step, the solution is used as the initial solution for the local search procedure. If an improved solution is found in the local search, the best candidates or *restricted candidate list* (RCL) will be replaced by the better one, see Figure 2.2.
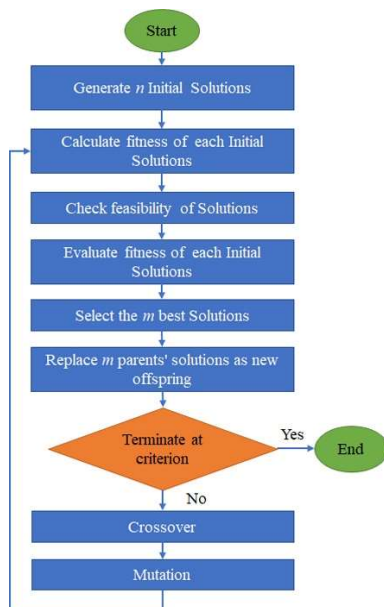


**Figure 2.1.** The process flow of the Genetic Algorithm (GA).
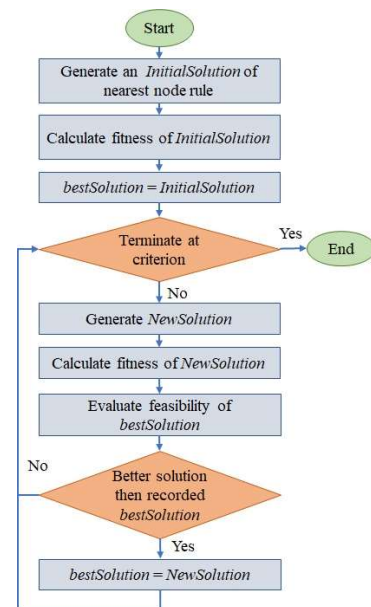
**Figure 2.2.** The process flow of the Greedy Randomized Adaptive Search Procedure (GRASP)

Moreover, the study adopted the haversine formula for distance and flight time calculation. Since the study's distance is the geodesics or curve line between two points on earth's surface using Latitude and Longitude of given aircraft $I$ and shelter airport $J$ set. The flight time of any affected aircrafts took from their current position to the safe shelter airports was calculated by flying distance divided average cruising speed of commercial aircraft at 880 km/hr. It helps to measure the solution's performance, so-called *fitness* value for both algorithms. When termination

criterion is met, such as the maximum number of iterations or the optimal solution has been found, the algorithm will be terminated and return the best solution.

$$d_{ij} = 2r \, archsin\left(\sqrt{sin^2\left(\frac{\varphi_2 - \varphi_1}{2}\right) + cos(\varphi_1)cos(\varphi_2)sin^2\left(\frac{\lambda_2 - \lambda_1}{2}\right)}\right)$$

where:

$d$ is the distance between the two points ($I, J$) along a great circle of the sphere
$r$ is the radius of the Earth's sphere $\approx$ 6,371 km (the WGS84 ellipsoid).
$\varphi_1$, $\varphi_2$ are the latitude of point $I$ and latitude of point $J$ (in radians),
$\lambda_1$, $\lambda_2$ are the longitude of point $I$ and longitude of point $J$ (in radians).

**Table 2.1** Example of CARATS flight dataset provided by Japan MLIT.

| Time | Flight_ no. | Latitude | Longitude | Altitude | AC_type | Latitude | Longitude |
|---|---|---|---|---|---|---|---|
| 00:03.9 | FLT1861 | 27.420048 | 124.383047 | 38000 | B77W | 27°25'12.17 | 124°22'58.97 |
| 00:13.9 | FLT1861 | 27.408566 | 124.369262 | 38000 | B77W | 27°24'30.84 | 124°22'09.34 |
| 00:23.9 | FLT1861 | 27.396312 | 124.353317 | 38000 | B77W | 27°23'46.72 | 124°21'11.94 |
| 00:33.9 | FLT1861 | 27.384821 | 124.339389 | 38000 | B77W | 27°23'05.36 | 124°20'21.80 |
| 00:43.9 | FLT1861 | 27.373473 | 124.326036 | 38000 | B77W | 27°22'24.50 | 124°19'33.73 |

### 2.2.2 The Collaborative Actions for Renovation of Air Traffic Systems (CARATS) flight dataset

The Collaborative Actions for Renovation of Air Traffic Systems (CARATS) dataset is a historical flight record cover all Japan's area control centers; Sapporo, Tokyo, and Fukuoka Area Control Center (ACC), consist of raw flight data of individual aircraft, i.e., date, timestamp of 10sec interval, latitude, longitude, altitude, and model of aircraft (e.g., B777 and A322) provided by Japan MLIT (MLIT, 2018) as shown in Table 2.1.

### 2.3. PROPOSED MODELS

The Computational model for genetic algorithm (GA) and Greedy Randomized Adaptive Search Procedure (GRASP) is proposed for shelter airport selection and evacuation planning. The developed models' objective is to minimize the total flight time of aircrafts taken from their current position to safe shelter airports. The models had considered the limitation of shelter airport accommodation capacity by the number of available aircraft stands and their sizes, and the affected aircraft sizes. The assumptions of the problem on model construction, indices, parameters, decision variables, objective function, constraints, genetic algorithm's operators, including GA and GRASP pseudocodes in Algorithm 1 and Algorithm 2, are described as follows:

### 2.3.1 The assumptions of the problem on model construction

According to ICAO's volcanic ash effect on aircraft engine's performance, all aircraft must avoid contact with volcanic ash particles and rocks by flying into or park inside the volcanic eruption affected areas and airspace in any ash cloud density level. It can be assumed that at any volcanic eruption, warning level has been delivered both airborne and on-ground ($I$) need to avoid those

areas by rerouting, rescheduling, or cancel their schedules and evacuate to the safe shelter airports; $J$, at all causes.

1. Since volcanic ash particles can cause severe damage an aircraft's engine, no shelter airport can be located within the affected area; F, is allowed.
2. Each shelter airport has limited capacity to accommodate the evacuation demand, the limited number of aircraft handling by sizes of aircraft, and the runway's length. The maximum occupancy rate of aircraft stands (OCj) were used to determine the maximum number of occupied stands at the affected airport (considered as the number of affected on-ground aircrafts), and available stands at the shelter airports. The occupancy rate can be calculated using; the maximum cumulative number of arrival and departure flights in one hour during the busiest day of the airport and its maximum number of aircraft stands.
3. The aircrafts assignment to available aircraft stands will be in sequential according to their size and available stands by aircraft sizes at the shelter airport. Each aircraft size: small, medium, large, and extra-large aircraft has its specific handling equipment and size defined by ICAO. Even though all available aircraft stand can accommodate various sizes and types of aircraft, selecting the most appropriate one will cost the airport less to accommodate those aircrafts in an emergency. Each airport also has its specific aircraft handling capacity by which size of aircraft it could handle by wingspan (ICAO, 2019, 2016). See detail of runway length by aircraft wingspan detail in Table A2-5. Hence, an affected aircraft will be assigned to an aircraft stand that matched its size as a primary assignment, i.e., a small aircraft to a small-size stand, a medium-size aircraft to a medium-large size stand, a large and extra-large size aircraft to a large size stand. If the size-matched stand is fully occupied, an aircraft could be assigned to the next larger size stand, i.e., a small-size aircraft to a medium-large size stand. The sequence of aircraft stands assignment for each aircraft's sizes is shown in Figure 2.3.
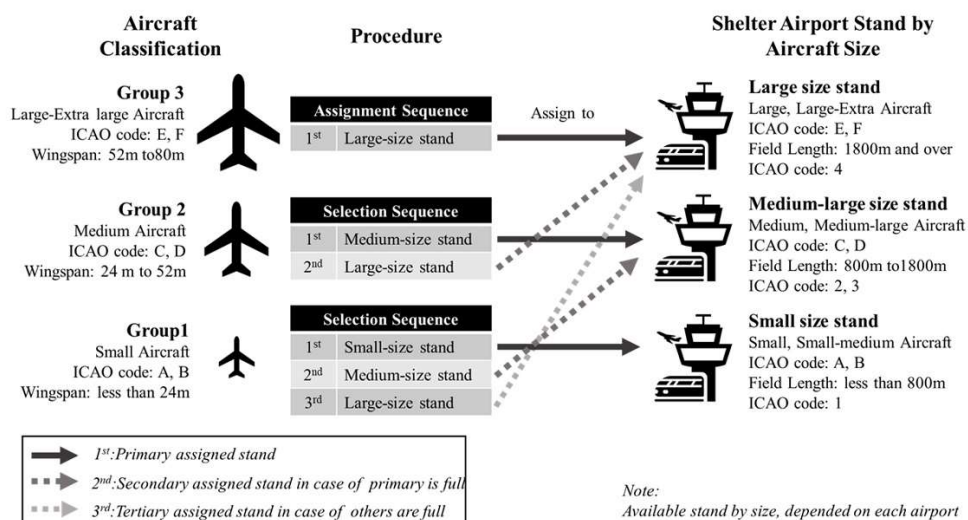


**Figure 2.3**. The sequence of aircraft stands assignment for each aircraft's sizes matching, airport available aircraft stands, and field (runway) length.

### Index sets

$I$      Set of affected aircrafts; $i \in I$

$J$      Set of candidates shelter airports; $j \in J$

$S$      Set of affected aircraft sizes; $s \in \xi$, associated with $I$

     $F$ Set of affected airports; $f \in F$

### Parameters

$M_j$      Maximum number of aircraft stands of selected shelter airport; $j \in J$

$D_{ij}$      Distance (km) from the current position of affected aircrafts $i \in I$, to shelter airport $j \in J$

$OC_j$      Occupancy rate of the aircraft stands' maximum number $M_j$ at candidate shelter airports $j \in J$

$NC_j$      Non-occupancy rate of the aircraft stands' maximum number $M_j$ at candidate shelter airports $j \in J$

$P(\rho)_j$      Available medium-size aircraft stands, at shelter airport $j \in J$

$P(\tau)_j$      Available large-size aircraft stands, at shelter airport $j \in J$

$\rho_{sj}$      Equal to 1 if a medium-size aircraft $s \in \xi$ been assigned to a medium or large-size aircraft stand at shelter airport $j \in J$, 0 otherwise.

$\tau_{sj}$      Equal to 1 if a large-size aircraft $s \in \xi$ been assigned to a large-sized aircraft stand at shelter airport $j \in J$, 0 otherwise.

$\varsigma_{sj}$      Equal to 1 if a small-size aircraft $s \in \xi$ been assigned to any stand at shelter airport $j \in J$, 0 otherwise.

$h_j$      Penalty value or additional flight time (hr) value gives a candidate shelter airport $j \in J$ according to the number of aircraft $i \in I$, which has been exceeded assign from the airport's available capacity.

$t_{ij}$      Flight time (hr) of each affected aircraft $i \in I$ to shelter airport $j \in J$; $t_{ij} = D_{ij} \div 880(km/hr)$

### Decision variables

$X_j$      Equal to 1 if the selected shelter airport $j \in J$ is in the affected airports $f \in F$, 0 otherwise.

$E_{ij}$      Equal to 1 if assigned aircraft $i \in I$ to shelter airport $j \in J$ with the correct size of stand, 0 otherwise.

$T$      Total flight time of all assigned aircrafts $i \in I$.

### Objective function

Minimize total flight time of all affected aircrafts $i \in I$ to safe shelter airports $j \in J$

$$minT = \sum_j \sum_i t_{ij} + h_j \qquad\qquad \forall i,j \qquad (1)$$

### Subjective to

*Evacuate to the airport in the safe zone:* selected shelter airport must not be located in the affected area, or the affected airport set $F$.

$$X_j \notin F \qquad\qquad \forall j \qquad (2a)$$

$$\sum_{j \in J} X_j = 0 \qquad\qquad \forall j \qquad (2b)$$

*Candidate shelter airport capacity limitation by aircraft stand sizes:* according to aircraft assignment by sizes in section 2.3.1 and Figure 2.3, each affected aircraft could be assigned to the same or larger sizes of the stand to its size. The aircraft stand size constraint has focused on the medium and large aircraft to the smaller size of the aircraft, unlike the small-size aircraft, which could be assigned to any size of available stands as shown in equation 3b to 3d. However, constraint 3e and 3f states the total number of assigned aircraft of all sizes must not exceed the available or non-occupied aircraft stands (3a); $NC_j$, of the shelter airport of $j \in J$.

$$NC_j = (1 - OC_j) * M_j \qquad\qquad \forall j \qquad (3a)$$

$$\sum_{s \in \xi} \varsigma_{sj} \leq NC_j \qquad\qquad \forall j \qquad (3b)$$

$$\sum_{s \in \xi} \rho_{sj} \leq P(\rho)_j \vee P(\tau)_j \qquad\qquad \forall j \qquad (3c)$$

$$\sum_{s \in \xi} \tau_{sj} \leq P(\tau)_j \qquad\qquad \forall j \qquad (3d)$$

$$\sum_{i \in I} E_{ij} = \sum_{s \in \xi} \tau_{sj} + \sum_{s \in \xi} \rho_{sj} + \sum_{s \in \xi} \varsigma_{sj} \qquad\qquad \forall j \qquad (3e)$$

$$\sum_{i \in I} E_{ij} \leq NC_j \qquad\qquad \forall j \qquad (3f)$$

### 2.3.2 Penalty function

In this study, the penalty function has been used to penalize infeasible solutions on the genetic algorithm by disadvantage to its individual's fitness value, force the algorithm to avoid constraint violation. Giving an additional flight time to each violation solution depended on the degree of constraint violation (number of available or non-occupied aircraft stands violation) to control the number of assigned aircraft at shelter airport not to exceed its available capacity. It can be done by assigning constant value $h_j$ to its flight time to disadvantage its fitness according to the degree of constraint violation. Thus, the degree of constraint violation can be calculated from the difference between the total number of assigned aircrafts $\sum_{i \in I} E_{ij}$ at shelter airport $j \in J$ with the correct size of aircraft and stand, and non-occupied aircraft stands $NC_j$ of shelter airport $j \in J$ multiply by constant $a$ where $a \geq 1$ according to ~1 hour (65 mins) of the average duration on the landing take-off cycle (LTO) and turnaround operations of an aircraft. The LTO cycle contains four operations involved take-off, climb, approach, and taxi with an average duration of 33mins (ICAO, 2013). Moreover, 44 mins on average of turnaround time (minimum 29 and maximum 55 mins) depend on the size of the aircraft, which included some of these activities; unload and reload its passenger, baggage and cargo, potable, and wastewater, and refueling (Airbus, 2005; Costea, 2011; Mota et al., 2017).

$$\delta_j = \sum_{i \in I} E_{ij} - NC_j \qquad\qquad a \geq 1, \forall j \qquad (4a)$$

$$h_j = a * max(\delta_j, 0) \begin{cases} \delta_j, & \delta_j \leq 0 \\ 0, & otherwise \end{cases} \qquad a \geq 1, \forall j \qquad (4b)$$

### 2.3.3 Genetic algorithm operators

In this study, an evaluation algorithm was based on DEAP, a Python operation framework for evaluation algorithm for primary operators and settings (De Rainville et al., 2012). The value of each operator based on the case study used in this study gives the example of operators' values. However, these values are adjustable to different study cases. The details of GA process flow and sitting are shown in Figure 2.1.

*Chromosome encoding*: the chromosome *N* represents a list of destination shelter airports *j* ∈ *J* for all affected aircraft *i* ∈ *I*. Each chromosome consists of *I* genes, which refer to the number of affected aircrafts *I* and contain one random number of possible shelter airports *j* ∈ *J*. Hence each gene is represented by two elements *i* and *j*. For instance, in this study, 261 affected aircrafts needed to evacuate to any 42 possible safe shelter airports. The randomly generated chromosome is shown in Figure 2.4. A single chromosome will be consisted of 261 genes.
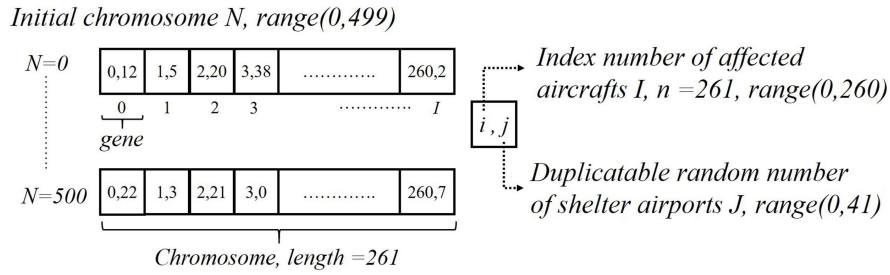


**Figure 2.4.** The GA's chromosome encoding.

Where

> *I* is the number of observable affected aircraft, e.g., 261 aircrafts.
> *J* is the duplicatable number of available shelter airports, e.g., 42 airports.
> *N* is the number of initial chromosome population, e.g., 500 chromosomes.

*Initial population*: The initial population represents the number of parents' chromosomes at the start point of the algorithms, which equal to or greater than the toursize value as mentioned in the following "Chromosome replacement". The larger number of initial populations could lead to less running iteration for GA to find an approximate solution. However, it could cause a longer calculation duration in each iteration as well. Refer to DEAP: basic setting for the number of initial populations, this study had set the number of initial chromosome population *N* to 500 chromosomes.

*Chromosome evaluation and fitness function*: the chromosome was evaluated by the total flight time of every gene calculated using a haversine distance formula divided by average aircraft speed per hour in the form of fitness value. It was also evaluated by the total number of each assigned shelter airport number against the airport's available capacity constraint. For capacity evaluation, the penalty function was used to give the capacity violation genes a disadvantage by giving additional flight time to aircraft if it exceeded-assigned to the airport capacity as defined in section 2.3.2 penalty method.

*Crossover and mutation*: the crossover method in this study is based on the two-points crossover operator (cxTwoPoints) (De Rainville et al., 2012), the random gene sequence integer i in I selection to select two crossover positions *i* within chromosome N and exchange genes between two parents, which reserved original genes values in the chromosome and give diversity to the offspring (child chromosome). Unlike crossover operation, the mutation method used the "mutUniformInt" operator (low=0, up=41, inpb=0.05), which performs an integer replacement between lower and upper bound values probability 5% uniformly, caused the value of gene to change from the original value within the range of the candidate shelter airport *J*.

*Chromosome replacement*: the study used the steady-state approach in which the population size remains constant according to the number of initially generated chromosomes. This process was done through the chromosome replacement using the "selTurnament" operator equal to 3, in

which the 3 best suitable solutions from offspring replaced the 3 initial parent chromosomes. This process has led to better fitness value on the next generation of offspring in each new running iterations until the GA process was terminated at the end of the setting iteration.

*Chromosome decoding*: at the termination phase at iteration = 500, the chromosome with the smallest fitness value (the minimum flight time according to objective) is selected as the best chromosome/solution. The chromosome is an array of selected shelter airports $j \in J$ for affected aircraft $i \in I$, which can be translated into the best-selected shelter airports for each affected aircraft with the nearest distance and shortest flight time from their current position.

**Algorithm 1** Proposed model pseudocode for Genetic Algorithm (GA).

| | |
|---|---|
| | **Input** : $J$, a set of candidate airport locations; $M$, a set of candidate airport locations capacity; and $I$, a set of affected aircraft locations;<br>**Output :** A list of the nearest $X_j$ selected shelter airports for each $E_{ij}$ affected aircraft;<br>**Initialize Populations:** 500 solutions of all affected aircraft $i \in I$ with 42 random candidate airports $j \in J$ as candidate solutions. |
| 1 | **Evaluate** each solution's fitness using the minimum total flight of the solution **do** |
| 2 |     **compute** flight time, the distances between each affected aircraft $i \in I$ and all candidate shelter airport $j \in J$; using haversine formula; |
| 3 | **Repeat Until** termination condition is satisfied; 500 iterations **do** |
| 4 |   **Select** parents; 3 solutions parents |
| 6 |   **Crossover** pairs of parents using two-points crossover operator; |
| 7 |   **Mutate the offspring** using the mutUniformInt operator to change the solution's value randomly; |
| 8 |   **Evaluate** each solution's fitness using the minimum total flight of the solution **do** |
| 9 |     **compute** flight time from the distances between $i$ and all $j \in J$ for each population $E_{ij}$; |
| 10 |     **Foreach** $E_{ij}$, aircraft $i$ to candidate airport $j$ **do** |
| 11 |       **check** sum of assigned aircraft at shelter airport $j$; $\sum_j E_{ij}$, compare to $NC_j$, the available stands and stands' sizes at airport $j$ ; |
| 12 |       **if** $\sum_j E_{ij} \leq NC_j$; exit; |
| 13 |         **else then**<br>          **compute** add additional flight time (penalty) according to number of exceeded aircraft at airport $j$ to the solution; $h_j = \lvert a * (\sum_{i \in I} E_{ij} - NC_j) \rvert$; exit; |
| 14 |     End for |
| 15 |   **Select** the 3 best solutions: minimum fitness by total flight time |
| 16 |   **Store** the results in a list of selected airports |
| 17 |   **Add** the new best solution to the population list for the next iteration |
| 18 | **Terminate** |

**Algorithm 2** Model pseudocode with limited airport capacity constraint for Greedy Randomized Adaptive Search Procedure (GRASP).

| | |
|---|---|
| | **Input** : $J$, a set of candidate airport locations; $M$, a set of candidate airport locations capacity; and $I$, a set of affected aircraft locations;<br>**Output :** A list of the nearest selected shelter airports $X_j$ for each $E_{ij}$ affected aircrafts; |
| 1 | **Initialize Solution:** a set of all affected aircraft $i \in I$ population with 42 random candidate airports $j \in J$ as candidate solutions. **the total number of selected candidate airports in each population set must not exceed maximum handling capacity by aircraft size of each airport; capacity by aircraft size: small, medium, and large. |
| 2 |   **Foreach** affected aircraft $i \in I$ **do** |
| 3 |     **compute** flight time, the distances between each affected aircraft $i \in I$ and all candidate shelter airport $j \in J$; using great-circle distance; |
| 4 |   **sort** the computed flight time, smallest to largest; |
| 5 |   **select** the nearest airport by the shortest flight time; |
| 6 |   **Foreach** affected aircraft $i$ to candidate airport $j$ **do** |
| 7 |     **check** sum of assigned aircraft at shelter airport $j$; $\sum_j E_{ij}$, compare to $NC_j$, the available stands and stands' sizes at airport $j$ ; |

| | |
|---|---|
| 8 | **if** $\sum_j E_{ij} < NC_j$ then |
| 9 | assign aircraft $i$ to the candidate shelter airport $j$; exit; |
| 10 | **else then** |
| | **select** the new next nearest shelter airport $j+1$; |
| 11 | End for |
| 12 | End for |
| 13 | **Evaluate** a solution's fitness using minimum total flight time of the solution **do** |
| 14 | **Store** the results in a list of selected airports if fitness value better than min(fitness) of all previous solution in the list |
| 15 | **Repeat Until** termination condition is satisfied; *500* iterations **do** |
| | Generate a new solution by randomly select airports with distance and capacity constraints the same as items 1-15. |
| 16 | **Terminate** |

## 2.4.    CASE STUDY

This section presents a case study of a volcanic eruption, applying the mentioned approaches to a real situation of Mt.Hakone in Kanto peninsula, Kanagawa, Japan. One of Japan's most active volcanoes (JMA, 2019a) located in the middle of the busiest airspace and near air transportation hubs of Japan (i.e., Haneda and Narita airport international airport). The historical data observation from many sources included volcanic ash cloud pattern, and flight dataset (CARATS) was used to determine the affected area, airport, and aircraft from Mt.Hakone eruption. The data present in this section will be used in the proposed model validation (section 2.4) and computational results (section 2.5).
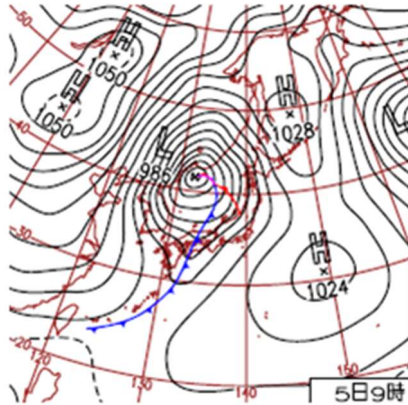


In Spring (March-April-May: the period of this study), migratory cyclones and anticyclones that alternately move eastward prevail across Japan. Temperature increases (decreases) in front (back) of cyclonic systems due to warm southerly (cold northerly) flow. Temperature in Kanto/Koshin rises gradually with large short-term variations. The sunshine duration is long in the second half of spring due to the predominance of anticyclonic systems. Temperatures rose all over Japan due to northward warm air inflow in front of a cyclonic system.

**Figure 2.5** Overview of Kanto seasonal wind's profile: March-April-May, (JMA, 2019b).

### 2.4.1    The affected airports

From the ashfall observation on Mt.Sakurajima located in South of Japan during the year 2009 to 2015 had discovered the pattern of ashfall during the period of eruption, typical plume height of explosion was between 2-5km with the traceable of ashfall at least 70 km up to hundreds of kilometer away from the vent (JMA, 2019c). The ashfall direction and distribution were highly non-uniform, influenced by seasonal winds (Poulidis et al., 2018). During the selected period of the study in March, according to the latest CARATS flight dataset of March 2016 provided by Japan MLIT, wind's direction in the Kanto peninsula moves toward the East across this area. However, the wind profile's possible direction can be varied toward North-east and South-east to Pacific ocean with vary windspeed during day-time and night-time from 9.3km/hr. to 30km/hr.

(JMA, 2019b). Based on these observations, the affected area was simulated by using geocoordinate (Latitude and Longitude) with the start point at Mt.Hakone volcano (35°14'00" N, 139°01'15" E) with varied direction toward North-east and South-east to the Pacific Ocean from 45°NE to 45°SE as shown in Figure 2.6b.

The number of affected airports has increased related to the volcanic ash cloud's direction and coverage area/airspace. The simulated affected area and the CARATS dataset were used to determine the affected airports and the affected aircraft in the following sections. There were 5 airports within the simulated direction of ashfall; 3 of them were in the minimum range of ashfall, i.e., Oshima, Chofu, and Haneda (Tokyo) airport and others 2 airports within 200km range from the vent. They could get impact from ashfall after the eruption within 2-7hrs and 5-16hrs, respectively. The 2 out of 5 airports are also Japan's major domestic and international airports: Haneda and Narita international airport, as shown in Figure 2.6.
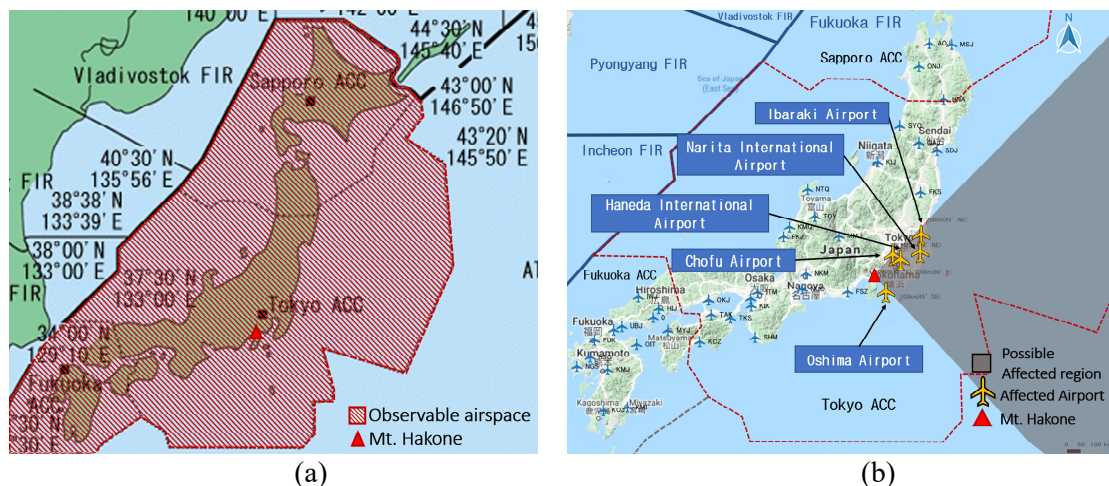


**Figure 2.6.** Observable airspace according to CARATS flight dataset(a) and Map of possible affected area and airports (b), Japan Civil Aviation Bureau (JCAB), Ministry of Land, Infrastructure, Transport and Tourism (MLIT)

## 2.4.2 The affected aircrafts

*Airborne aircraft*: this study assumed that, at the moment of volcanic eruption, all pending departure aircraft with their itineraries to the affected airports would reroute their flight's itineraries to other safe airports to avoid the impact from a volcanic eruption. Therefore, the study was considered only airborne aircrafts with their possible inbound to the affected airports. From the latest CARATS flight data on March 2016 observation, the week's busiest day was on Sunday between 10:00 am – 9:00 pm. There were 7,383 airborne aircrafts in the Japan airspace, with an average of 671 flights per hour. Among those flights, 15.8% or 107 aircrafts were inbound flights to the affected airports, which needed to be rerouted to safe shelter airports, and others were outbound or safe itinerary aircrafts. See Table 2.2.

*On-ground aircraft*: In this study, the maximum occupancy rate ($OCj$) was used to determine the number of affected aircraft and the affected airports. Those data were obtained from the flight schedule on June 2020 during the busiest period from 10:00 am – 9:00 pm of each affected airport; RJTO, RJTF, RJTT, RJAA, and RJAH at ~11%, 17%, 20%, 38%, and 20%, respectively (Central-Air, 2020; HND, 2020; IBR, 2020; NRT, 2020). Therefore, the number of affected on-ground

aircraft at 5 airports was 154 aircrafts from their overall capacities at 535. The total number of observables affected aircraft from both airborne and on-ground were 261 aircrafts, Table 2.3.

## 2.4.3    The shelter airports

This study has focused on shelter airport selection using the assumptions mention in section 2.3.1 to ensure aircraft handling capabilities of the selected shelter airports during the evacuation and recovering in particularly suitability for the sizes of affected aircrafts. From the observation on 107 airborne aircrafts with an inbound itinerary to the affected airports, we had discovered that 54.7% of aircraft were in group C with the wingspan of 24 m up to (but less than) 36 m, which needed more than 1,200 m up to (but less than) 1,800 m of field length—followed by group E (29.2%), and D (14.2%), which need longer runway up to 3,200m. The ratio by wingspan of 107 airborne aircraft also identical to the 7,383 observed aircrafts in the Japan airspace in the same time frame as shown in Table 2.2.

**Table 2.2** Aircraft size classification ratio by wingspan of 7,383 observable aircrafts in Japan airspace and 107 inbound airborne aircrafts to the affected airspace and airports

| Size Categories | 7,383 Observable airborne aircrafts: CARATS dataset[1] | | | Airborne Aircrafts[2] | | |
|---|---|---|---|---|---|---|
| | ICAO Size Code_Letter | Number of aircraft | % of Total aircraft | ICAO Size Code_Letter | Number of aircraft | % of Total aircraft |
| Small | B | 281 | 3.80% | B | 2 | 1.90% |
| Medium | C | 4,134 | 56.00% | C | 58 | 54.70% |
| | D | 783 | 10.60% | D | 14 | 14.20% |
| Large | E | 2,082 | 28.20% | E | 32 | 29.20% |
| | F | 103 | 1.40% | F | 0 | 0.00% |
| | **Total** | **7,383** | **100.00%** | **Total** | **107** | **100.00%** |

[1]*Total flight from the CARATS flight data on March 2016, the busiest day of the week, Sunday between 10:00 am – 9:00 pm*

[2]*calculated from an average 671 flights per hour, 15.8% was an inbound flight to 5 affected airports from 7,383 observed aircraft on Sunday during 10:00 am-9:00 pm (the busiest day and time)*

Overall, 98.13% of 107 inbound airborne aircrafts needed a field length of 1,200 m and up to more than 3,000 m to perform landing and taking off. We could assume that 154 on-ground aircrafts at the affected airports were at the same ratio as shown in Table 2.3. According to Japan's airports information provided by AIS, 82 from 94 airports or 88.3% of all Japan's airports could accommodate aircraft with code letter from C - F (medium - the larger-size of aircraft). The study is also considered airport connectivity, the capability of transferring affected crews and passengers to nearby accommodation facilities or nearby airports. Airport connectivity aims to allow affected crews and passengers be able to reach their final destinations. This study has chosen 42 airports on the mainland of Japan out of 94 airports outside the ash cloud affected area as the shelter airport candidates to maintain changing mode of transportation and connectivity capability (Smith and Arnedos, 2007), with an available capacity of up to 925 aircraft stands (all sizes), see Table A2-4. The available capacity used assumption of the average of maximum cumulative occupancy aircraft stands ($OC_j$) between the arrival and departure aircraft at 5 affected to determine number of the available aircraft stands at the 42 airports. The result shows that 21% of aircraft stands were occupied on average per hour during the busiest period, which could be assumed that 79% of airport capacity is non-occupancy or available aircraft stands rate ($NC_j$). See details in Table A2 2.

**Table 2.3** Maximum number of observed affected aircraft using in the study provided by AIS and CARATS.

| Observed Location | Airport | ICAO Code | Maximum aircraft stands[3] | Max_Occupancy per hour[4] | Affected aircraft (Occupied stands) | Affected aircraft by Aircraft's size[5] | | | Total |
|---|---|---|---|---|---|---|---|---|---|
| | | | | | | Large | Medium | Small | |
| | | | | | | 29% | 69% | 2% | |
| On-ground: at affected airports (AIS) | Oshima | RJTO | 9 | 11% | 1 | 0 | 1 | 0 | |
| | Chofu | RJTF | 24 | 17% | 4 | 1 | 3 | 0 | |
| | Tokyo | RJTT | 228 | 20% | 46 | 13 | 32 | 1 | 154 |
| | Narita | RJAA | 266 | 38% | 101 | 29 | 70 | 2 | |
| | Ibaraki | RJAH | 8 | 20% | 2 | 1 | 1 | 0 | |
| Airborne (CARATS), | Inbound Affected aircraft | | - | | | 31 | 74 | 2 | 107 |
| | | | | | | | **Grand Total** | | 261 |

[3]*Civil Aircraft: private and commercial aircraft*
[4]*Refer to Appendix A Table A2 2*
[5]*According to aircraft size ratio from observed historical flight data CARATS 7,383 aircrafts*

## 2.5.    MODELS VALIDATION

The sensitivity analysis is the process to validate the behavior and outcome of the proposed models on GA and GRASP in this study using various values of specific parameter configurations used in the models. The validation and sensitivity analysis used the same dataset of the selected case study of Mt.Hakoke Japan in section 2.4, with 261 affected aircrafts, 42 shelter airport candidates (5 affected airports excluded). The goal was to ensure that the proposed models could perform and give valid results according to the study's objective, subjective, and constraints on the various inputs.

   The results have shown that both algorithms could perform and gave valid results as they had been designed in the proposed model. The details on the sensitivity analysis have been given in the followings:

### 2.5.1    Genetic Algorithm: Model Validation and Sensitivity Analysis

In the genetic algorithm sensitivity analysis, the various values of specific parameter configurations: 1) crossover probability (CRXPB) and mutation probability (MUTPB), and 2) the ratio of affected aircraft, is investigated on the aircraft assigning pattern and outcomes. The suitable parameters which give the best result are used as the base-parameters configuration in this study to ensure it could perform and give a valid result.

   *Crossover and mutation probability parameters sensibility analysis:* the various crossover and mutation probability parameters were used as shown in Table 2.4. The study had revealed that increasing crossover probability number from 0.0 to 1.0 had decreased the fitness value (minimum total flight time) and the number of the exceeded-capacity airport. Thus, increasing mutation probability from 0.0 to 1.0 had risen the fitness value of each generation caused by increased genes variation of the best-selected populations' offspring until all the genes within its chromosome were utterly different from its parents at the probability of 1.0. As a result, the algorithm assigned aircraft to fewer shelter airports until it had violated the airport capacity's

constraint, which triggered penalty function to give the additional flight time to those solutions to get rid of them on the evaluation process. Consequently, higher mutation probability had given high fitness value: high total flight time and a higher number of exceeded-capacity airports that could not be used for aircraft evacuation, as shown in Figure 2.7(b).

**Table 2.4** Parameters setting for the proposed model on genetic algorithm validation.

| Parameter | Minimum value | Maximum value | (+) Incremental or (-) Decremental |
|---|---|---|---|
| Initial population | - | 500 | - |
| Crossover probability | 0.00 | 1.00 | +0.05 |
| Mutation probability | 0.00 | 1.00 | +0.05 |
| Number of iterations | - | 500 | - |

From the observation on crossover and mutation probabilities effect on GA outcome's behaviors, the acceptable range of the crossover and mutation probability numbers give low in total flight time, and a number of the capacity-exceeded airport could be varied between 0.50-1.00 and 0.10-0.60 respectively. According to the study's objective and subjective, the best crossover and mutation probability configuration was at 1.0 and 0.45, respectively, which gave the best fitness value of the lowest total flight time and not exceeding airport capacity. These probabilities were later used as the base configuration for GA. See Figure 2.7(a) and Figure 2.8(a) and (b).
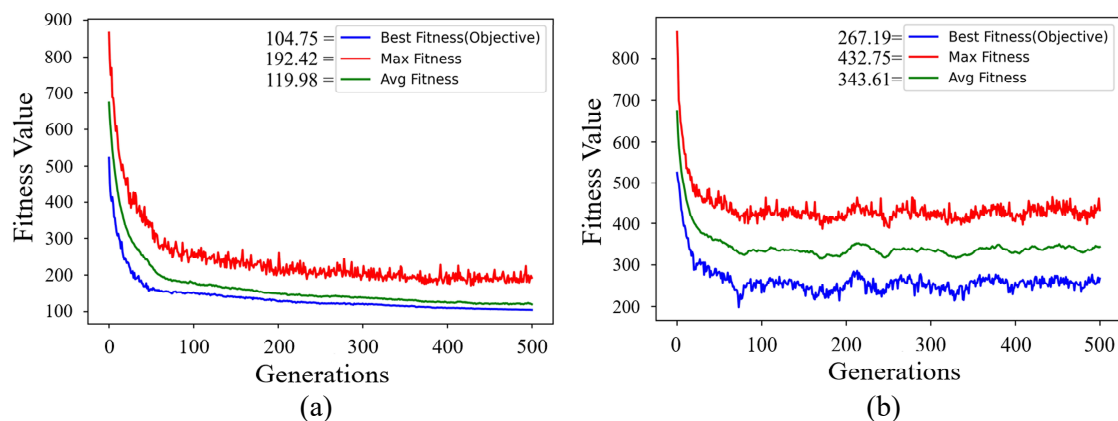


**Figure 2.7.** GA performance at CRXPB 1.0 and MUTPB 0.45, 500 iterations: best result (a), and the highest result of the MUTPB at 1.0 (b).

*Airport's occupancy rate sensitivity analysis*: The varied airport occupancy rate was set to simulate the air traffic congestion level, reflecting on the airport's aircraft occupancy and availability rate. The airport's occupancy rate ($OC_j$) was set within the range of -20% to +20% of the baseline rate with an incremental and decremental rate of ±5%. See details in Table A2 3 and Table A2-4. Consequentially, increasing the shelter airport occupancy rate had increased the number of affected aircraft, which decreased the available aircraft stands for evacuation. It also indicated increasing air traffic congestion level and vice versa.

The sensitivity study has shown increasing occupancy rate ($OC_j$) by +20% of the baseline from 21% to 25.2%, decreasing the total number of non-occupancy rate ($NC_j$) of 42 shelter airports 925 to 856 stands or from 79% to 75%. The increasing $OC_j$ rate also increased the congestion level in airspace and airport, which raised the total number of affected aircraft from 261 to 312 aircrafts, as shown in Table A2 3. Decreasing the non-occupancy stands at each shelter airport

candidates forced the system to select further and more airports from 27 airports at baseline to 40 airports to accommodate the increased number of affected aircraft, as shown in Figure 2.9(b). As reflected on the objective function's value, the total flight time has increased from baseline at 104.75hr to 168.16hr, see Figure 2.9(a).

(a)

(b)
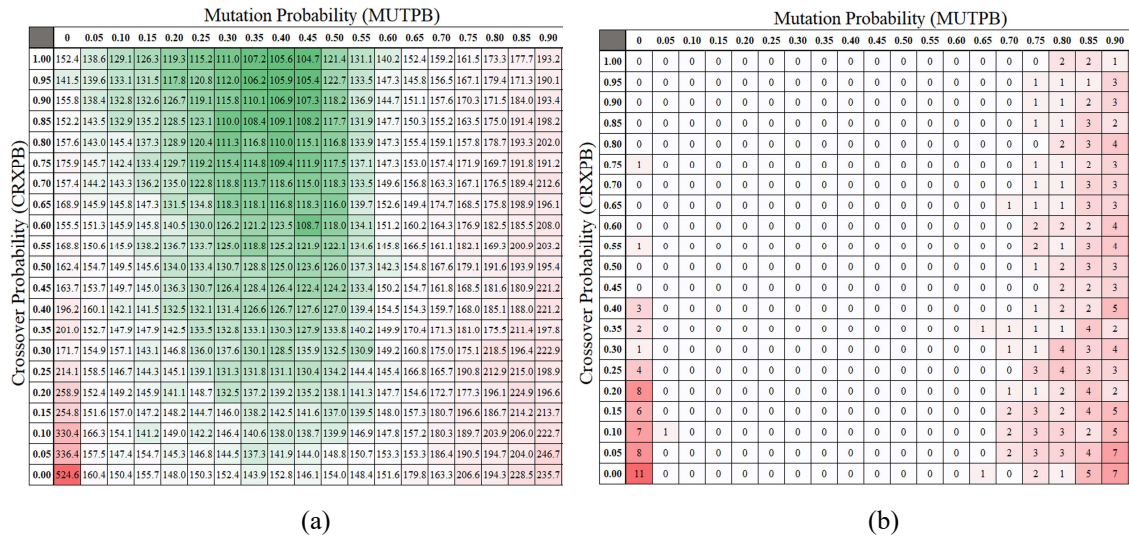
**Figure 2.8.** Results of sensitivity analysis on various crossover and mutation probabilities: total flight time (a) and the number of the exceeded-capacity airport (b). The best result at minimum total flight time was 104.75hr, and the number of the exceeded-capacity airport was 0 at crossover and mutation probability 1.0 and 0.45, respectively.

(a)

(b)
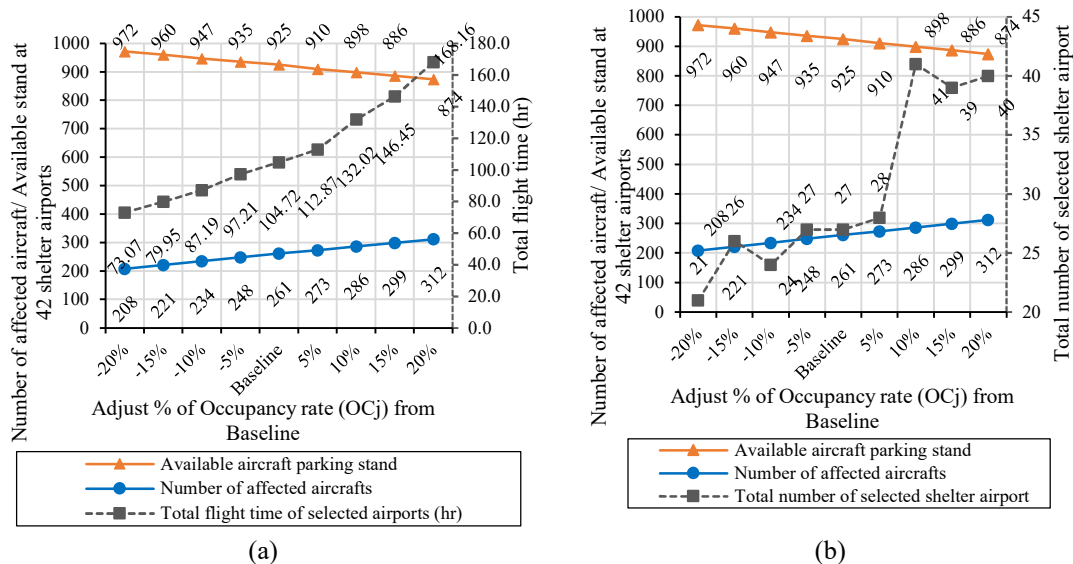
**Figure 2.9.** The GA's results on a various simulated number of affected aircraft between -20% to +20% of baseline with decrement/increment rate at ±5%: (a) total flight time and (b) number of selected shelter airports.

In contrast, decreasing the occupancy rate by -20% had increased the total number of the non-occupancy stand from 925 to 972 stands or 79% to 83%, respectively, which decreased the

number of affected aircraft to 208 from baseline. The objective function value also dropped from baseline to 73.07hr. An increasing number of available stands at each shelter airport candidate close to the affected aircraft positions reduced the number of selected shelter airports from 27 to 21 airports. From the study, the proposed model applied to GA was able to perform and gave valid results in assigning aircraft to the nearest airports without exceeding their capacities by aircraft size through both baseline dataset and the various rate of occupied stand settings, as shown in Figure 2.9.

## 2.5.2    GRASP: model validation and sensitivity analysis

The first goal was the outcome validation, whether it could give the results according to the proposed model. According to the study dataset, the study's objective and subjective through baseline setting; the number of affected aircrafts, and available aircraft stands. The second goal was to investigate the model's behavior and outcome through the various value of inputs and the various ratio of the occupied stand settings used in GA; see detail in Table A2 3.
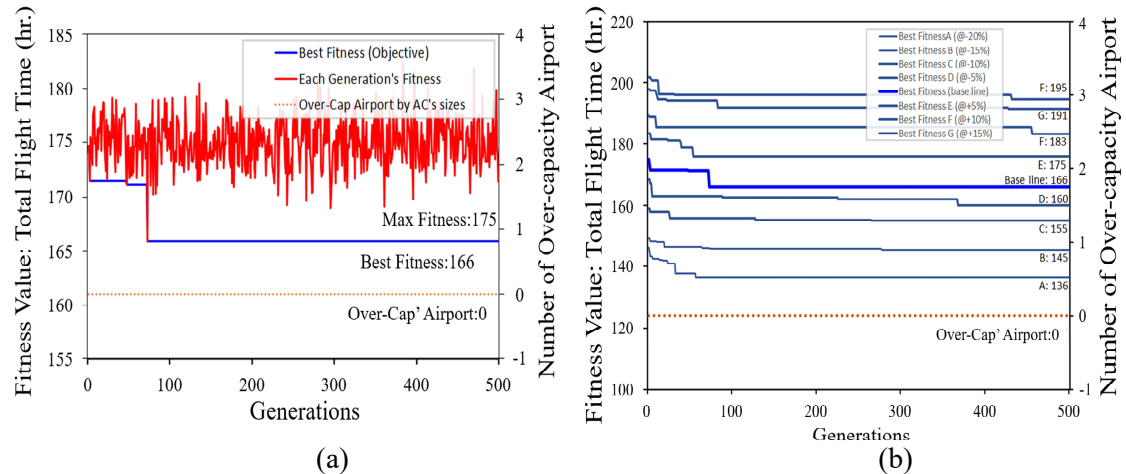


**Figure 2.10**. GRASP's result for baseline affected aircraft (a), and the results of a various simulated number of affected aircraft between -20% to +20% of baseline with decrement/increment rate at ±5% (b)

From the study, the proposed model was able to perform and gave valid results according to objective and subjective of the research in assigning aircraft to the nearest airports without exceeding their capacities by aircraft size on both baseline dataset and the various rate of the occupied aircraft stand. The result had shown the best solutions were selected through the process of randomly creating an initial solution, evaluating the solution against the subjective and constraints, comparing with the previous iteration's best solution before selection, and recording the better solution over 500 running iterations as it had been designed with decreased in the minimum number of total flight time and no exceeded-capacity airport as shows in Figure 2.10(a) and (b)

## 2.5.3    Computational Results

In this section, the proposed models applied on Genetic Algorithm (GA) and Greedy Randomized Adaptive Search Procedure (GRASP) were analyzed and compared their performances according to the study's objective and subjective mentioned in Section 2.3.1, included minimum in total

flight time and shelter airport's capacity constraint by aircraft stands and affected aircrafts' sizes. The details of each algorithms' results and comparison have been presented as followed:

### A. The Genetic Algorithms

In GAs, the affected aircrafts had been assigned to the nearest available shelter airport, similar to GRASP. Unlike the GRASP random mechanism, GA had a different mechanism through crossover and mutation called "the evolution mechanism". From the beginning of the process, 500 solutions of chromosomes were randomly generated, then evaluated their fitness against objective (1) and subjective (2)(3) along with penalty function in equation (4) to keep the model's solution from violating those subjective. Before selecting parents for the next generation, the reproduction through gene crossover and mutation to produce new alternative offspring could preserve and the alternate possibility of a solution before going through the fitness test's evaluation as the best solution for the objective's problem.



(a)                                                                            (b)
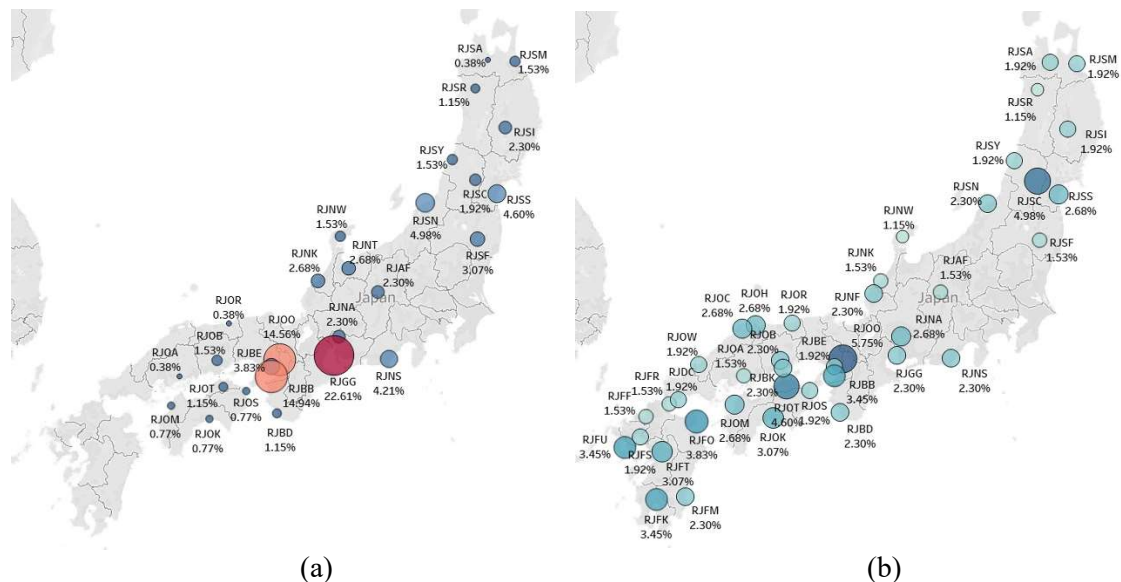
**Figure 2.11.** Mapping of assigned aircrafts to shelter airport by using Genetic algorithms (a), Mapping of aircrafts distribution to shelter airport by using GRASP (b)

As a result, 27 out of 42 shelter airports have been selected for accommodating the aircrafts with a total flight time for evacuation of 104.75 hours from 500 running iterations (duration 4.16mins), as shown in Table 2.5. Therefore, the time for each aircraft's evacuation was between 0.18-0.84 hours, with an average of 0.44 hours. The aircraft distribution was between 0.4% to 22.6%, with 3.7% on average of the total number of affected aircrafts. The maximum capacity usage at the selected shelter airports had been utilized between 5.9 and 92.2%, with the average at 42.3% of their available stands (non-occupancy stands). According to the airport's capacity based on the aircraft sizes constraint within penalty function, there was no exceeded the number of affected aircraft assigned to any selected shelter airport. The model also addressed the first 5 critical airports on the scenario, which accommodates 61.7% of the affected aircraft population. They were Chūbu centrair international airport (RJGG) 22.6%, Kansai international airport (RJBB) 14.9%, Osaka international airport (RJOO) 14.6%, Niigata airport (RJSN) 4.98%, and Sendai airport (RJSS) 4.60%, as shown in Figure 2.11(a) and Table A2-1.

## B. The Greedy Randomized Adaptive Search Procedure (GRASP)

In GRASP, the affected aircrafts had been assigned to the nearest shelter airport available by using the distance from the current position of each affected aircrafts. Moreover, the airport's capacity by aircraft size was considered to prevent the algorithm from assigning aircraft to the selected airport, as shown in Table A2-1. GRASP has the mechanism of searching, evaluating, selecting the best solution, and generating a new solution through the random number process. It can search and replace the better solution from the given conditions and constraints. From 500 running iterations, 2.21 minutes were used to search for the best solution against total flight time and shelter airport capacities by aircraft size constraints with the best solution of 166.32 hours in Table 2.5.

The results on shelter airport selection and aircraft distribution had shown that 41 shelter airports had been selected for accommodating affected aircrafts with a small distribution rate between 1.0% to 7.3% of the total number of affected aircrafts with no exceeded capacity at selected shelter airports. The algorithm had also addressed the first 5 critical airports, which accommodate 26.8% of the affected aircraft population. There were New Chitose airport (RJCC) 7.28%, Nagasaki airport (RJFU) 5.36%, Kansai international airport (RJBB) 4.98%, Chubu centrair international airport (RJGG), and Osaka international airport (RJOO) at 4.6%, as shown in see Figure 2.11(b), and more details in Table A2-1.

**Table 2.5.** Performance comparison between GA and GRASP.

| Performance Criteria | GA | GRASP | Differentiation Rate (GA/GRASP) |
|---|---|---|---|
| Running Iterations | | 500 | - |
| number of Aircraft | | 261 | - |
| Number of Candidate shelter airports | | 42 | - |
| Available aircraft aircrafts | | 925 | - |
| Actual Total Flight Time by Distance | 104.75 | 166.32 | -63.0% |
| Number of Selected Airport | 27 | 41 | -66.0% |
| Number of Exceed-capacity Airport | 0 | 0 | - |
| Searching Duration (min) | 4.16 | 2.21 | +188.2% |
| $\mu$ : mean of flight Time(hr) | 0.44 | 0.64 | -68.80% |
| Minimum flight Time(hr) | 0.18 | 0.06 | +300.00% |
| Maximum flight Time(hr) | 0.84 | 1.29 | -65.10% |
| Median | 0.41 | 0.62 | -66.10% |
| $\sigma$ : STD | 0.12 | 0.31 | -38.70% |
| 50th Percentile | 0.41 | 0.62 | -66.10% |
| 80th Percentile | 0.56 | 0.97 | -57.70% |
| 90th Percentile | 0.56 | 1.14 | -49.10% |

## C. Algorithm's performances comparison

From the performance results of the proposed models applied on Genetic Algorithm (GA) and Greedy Randomized Adaptive Search Procedure (GRASP), the study has shown the same algorithm iterations of 500 with the same set of total affected aircraft number, shelter airports, and capacity constraint by aircraft's sizes according to the study and algorithms' objective and subjective. The proposed model using GA could generate the better solution for aircrafts assignment to shelter airports with 104.75 hours of total flight time (TFT) or -63.0% compared to 166.32 hrs. from GRASP. Both algorithms can search for the solution with no over-capacity at the selected shelter airport even though GRASP searching duration was twice faster than in GA at 2.21 mins to 4.16 mins. Moreover, the study had tried to the extended iteration of GRASP to a critical of 200,000 iterations. At this critical iteration, the best result that GRASP could give was 161.34 hrs. or 2.99% better than the result at 500 iterations. Thus, GRASP could not find a better

solution than the proposed model on GA at the same running iterations or on the extended one in this study. The GRASP and GA performance comparison is shown below.

## 2.6.    CONCLUSION

- **CARATS helped to simulated more accuracy** in term of affected aircraft positions' simulation compared to actual position of aircraft on flight route over Japan airspace.

- **GA had capabilities in finding the approximate solution** of assigning aircrafts to shelter airports with distance, capacity's constraints and shelter airport utilization. **It was also given to better result compared to GRASP as The Evolution VS. Randomized optimization algorithm.**

- **The proposed algorithm could address the critical shelter airports for evacuation** in the event of volcanic eruption.

- Sensitivity analysis had shown the relationship between air traffic congestion level, the available aircraft stand at the airports, and number of affected aircraft, **suggested that the critical point of congestion level for Japan airspace could happened at +10% above the baseline.**

### Discussion and further study:
- ❑ CARATS and AIS dataset (offline data) did not provide sufficient details of each aircraft, its direction and airport capacity in deep details. Other sources of airport, aircraft, airline, flight schedules, and online data may pave the way to more accuracy of evacuation simulation.
- ❑ **More of airline and airport regulations should be studies** and used as additional shelter airport selection constraint, which may help airport and airline operations during and post-stage of disaster.

This study has proposed the conceptual models for shelter airport selection for aircraft evacuation in a volcanic eruption by considering evacuation flight time and maximum shelter airport capacity. The models have been tested with a case study of a volcanic eruption at Mt. Hakone in Japan's central and the latest air traffic data in March 2016 (CARATS open dataset) provided by MLIT. The airport facilities data by AIS, and airlines flight schedules at each airport are also used to determine the number of the affected area, airports, the number of affected aircrafts and the available aircraft stands for evacuation during the event. The 261 affected aircrafts of both airborne and on-ground have been simulated their current positions and select the appropriate shelter airports for evacuation. For this study, 42 out of 94 airports had been chosen as shelter airports by criteria of location on the mainland of Japan for maintaining connectivity with other modes of transportations, outside ash cloud affected area, and sufficient runway's length for accommodating affected aircraft with 925 available aircraft stands (non-occupancy stands).

The proposed models had been applied to the Genetic Algorithm (GA) and Greedy Randomized Adaptive Search Procedure (GRASP)to find the approximate solution of shelter airport selection. Both algorithms proved their capabilities of searching for the approximate solution according to the study objective and subjective of the assigned aircraft to shelter airport with minimum total flight time, and not exceeding selected airports' capacities. With the same logical model of aircrafts assignment and running iteration, GA had outperformed GRASP to find less in total flight time solution for the overall population with fewer selected shelter airports on the case study. Since they were different in the best solution selection mechanism as mentioned in the computational results section, this gave GA's mechanism the advantage in preserving and passing on the previous best solution to its offspring through crossover operation.

Nevertheless, the study had also revealed the critical shelter airports for aircrafts evacuation. The larger-size airport with a large number of available aircraft stands is likely to act as the critical shelter airport during the disaster event, as shown in Appendix A-Table A2-1. The alternative adjustment of the proportion of available aircraft stands at shelter airports, along with the

proportion of affected aircrafts, will give flexibility to the algorithms' output, which gives the better suggestion on which shelter airports could accommodate a reasonable number of aircraft according to their capacities.

The study could act as a suggestion for the authorities for the airport and aircraft emergency evacuation planning. However, this study could give a conceptual model of shelter airport selection solution for aircrafts evacuation in the volcanic eruption event using the nearest distances and airport capacity by aircraft size constraints. It still has limitations depending on the regulation's complexity at the airport, airline, and air traffic management, as mentioned earlier. The further applications on airport selection may need to set up more objectives and constraints for the shelter airport selection algorithm to effectively provide a more realistic selection from the beginning of evacuation until recovering for all sections of aircraft, passengers, and cargo and flight crew scheduling.

## LIMITATIONS

This study's main limitations were subject to the unavailable data as follows: the accurate number of affected aircraft and their itineraries data for both airborne and on-ground, historical data of volcanic ash cloud coverage area, and its range from Mt.Hakone.

Although the number of affected aircraft were observed from the historical data before the pandemic, the aircraft stand occupancy rate and available of aircraft stands at candidate shelter airports in this study may not represent the normal air traffic situation of this region during the COVID-19 pandemic, which caused declined in most airline and airport operations by 90% (ICAO, 2020). Hence, the historical flight schedule data of shelter airports before the pandemic are required for the occupancy rate calculation accuracy to reflect the air traffic level's normal situation. However, this study's proposed model has allowed the occupancy rate adjustment to reflecting air traffic congestion level close to the level before the pandemic.

Furthermore, the unavailable ash cloud historical data of Mt.Hakone, the Sakurajima's volcanic ashfall, and ash cloud were studied to understand the ash cloud's behavior, which was used to predict and determine the possible ash cloud coverage area in the case study.

## ACKNOWLEDGEMENTS

## REFERENCES

Airbus, 2005. Airbus A320 Aircraft Characteristics, Airport and Maintenance Planning. Airbus S.A.S. 1–387.

Aktel, A., Yagmahan, B., Özcan, T., Yenisey, M.M., Sansarcı, E., 2017. The comparison of the metaheuristic algorithms performances on airport gate assignment problem. Transportation Research Procedia 22, 469–478. https://doi.org/10.1016/j.trpro.2017.03.061

Button, K., Vega, H., Nijkamp, P., 2010. A Dictionary Of Transport Analysis, A Dictionary of Transport Analysis. https://doi.org/10.4337/9781849804714

Central-Air, 2020. 新中央航空株式会社 Time Table [WWW Document]. URL https://www.central-air.co.jp/en/timetable.html (accessed 2.13.20).

Cheng, C.H., Ho, S.C., Kwan, C.L., 2012. The use of meta-heuristics for airport gate assignment. Expert Systems with Applications 39, 12430–12437. https://doi.org/10.1016/j.eswa.2012.04.071

Cidell, J., 2006. Regional cooperation and the regionalization of air travel in Central New England. Journal of Transport Geography 14, 23–34. https://doi.org/10.1016/j.jtrangeo.2004.10.003

Costea, O., 2011. AIRBUS A380 AIRCRAFT CHARACTERISTICS AIRPORT AND MAINTENANCE PLANNING AC.

De Rainville, F.-M., Fortin, F.-A., Gardner, M.-A., Parizeau, M., Gagné, C., 2012. DEAP, in: Proceedings of the Fourteenth International Conference on Genetic and Evolutionary Computation Conference Companion - GECCO Companion '12. ACM Press, New York, New York, USA, p. 85. https://doi.org/10.1145/2330784.2330799

Dell'Orco, M., Marinelli, M., Altieri, M.G., 2017. Solving the gate assignment problem through the Fuzzy Bee Colony Optimization. Transportation Research Part C: Emerging Technologies 80, 424–438. https://doi.org/10.1016/j.trc.2017.03.019

Ding, H., Lim, A., Rodrigues, B., Zhu, Y., 2005. The over-constrained airport gate assignment problem. Computers & Operations Research 32, 1867–1880. https://doi.org/10.1016/j.cor.2003.12.003

Feo, T.A., Resende, M.G.C., 1995. Greedy Randomized Adaptive Search Procedures. Journal of Global Optimization 6, 109–133. https://doi.org/10.1007/BF01096763

Guépet, J., Acuna-Agost, R., Briant, O., Gayon, J.P., 2015. Exact and heuristic approaches to the airport stand allocation problem. European Journal of Operational Research 246, 597–608. https://doi.org/10.1016/j.ejor.2015.04.040

Hanaoka, S., Indo, Y., Hirata, T., Todoroki, T., Aratani, T., Osada, T., 2013. Lessons and challenges in airport operation during a disaster: case studies on Iwate Hanamaki airport, Yamagata airport, and Fukushima airport during the great east Japan earthquake. Journal Of Jsce 1, 286–297. Https://Doi.Org/10.2208/Journalofjsce.1.1_286

Harriman, S., Fanjoy, R., Petrin, D., 2009. Small General Aviation Airport Emergency Preparedness and the Perceived Risks of Very Light Jet Operations. Journal of Aviation/Aerospace Education & Research. https://doi.org/10.15394/jaaer.2009.1382

Harsha, P., 2003. Mitigating Airport Congestion: Market Mechanisms and Airline Response Models. Massachusetts Institute of Technology.

HND, 2020. Tokyo Haneda International Airport (HND/RJTT) | Arrivals, Departures & Routes | Flightradar24 [WWW Document]. URL https://www.flightradar24.com/data/airports/hnd (accessed 2.13.20).

Horner, M.W., Downs, J.A., 2010. Optimizing hurricane disaster relief goods distribution: Model development and application with respect to planning strategies. Disasters. https://doi.org/10.1111/j.1467-7717.2010.01171.x

Hu, F., Yang, S., Xu, W., 2014. A non-dominated sorting genetic algorithm for the location and districting planning of earthquake shelters. International Journal of Geographical Information Science. https://doi.org/10.1080/13658816.2014.894638

Hu, Y., Song, Y., Zhao, K., Xu, B., 2016. Integrated recovery of aircraft and passengers after airline operation disruption based on a GRASP algorithm. Transportation Research Part E: Logistics and Transportation Review 87, 97–112. https://doi.org/10.1016/j.tre.2016.01.002

IBR, 2020. Flight information | Ibaraki Airport [WWW Document]. URL http://www.ibaraki-airport.net/en/flight.html (accessed 2.12.20).

ICAO, 2020. FEB 2020 : Air Transport Monthly Monitor FEB 2020 : Air Transport Monthly Monitor 2019–2020.

ICAO, 2019. ASSEMBLY-40TH SESSION EXECUTIVE COMMITTEE Agenda Item 26: Other high-level policy issues to be considered by the Executive Committee GET AIRPORT READY FOR DISASTER.

ICAO, 2016. Annex 14: Aerodrome Design and Operations Seventh Edition, International Civil Aviation Organization.

ICAO, 2013. ICAO Environmental Report 2013. ICAO Environmental Report 2013.

Jimenez Serrano, F.J., Kazda, A., 2017. Airline disruption management: Yesterday, today and tomorrow, in: Transportation Research Procedia. Elsevier, pp. 3–10. https://doi.org/10.1016/j.trpro.2017.12.162

JMA, 2019a. Volcanic Warning [WWW Document]. Japan Meteorological Angency. URL https://www.jma.go.jp/en/volcano/ (accessed 6.1.19).

JMA, 2019b. Climat of Kanto/Koshin district [WWW Document]. Janpan Meteorological Agency. URL https://www.data.jma.go.jp/gmd/cpd/longfcst/en/tourist/file/Kanto_Koshin.html (accessed 9.15.19).

JMA, 2019c. Sakurajima Continuously Monitored [WWW Document]. Janpan Meteorological Agency. URL https://www.data.jma.go.jp/svd/vois/data/tokyo/STOCK/souran_eng/volcanoes/090_sakurajima.pdf (accessed 8.26.19).

Kita, H., Koike, A., Tanimoto, K., 2005. Air Service Development of Local Airports and its Influence on the Formation of Aviation Networks. Research in Transportation Economics. https://doi.org/10.1016/S0739-8859(05)13011-X

Kongsomsaksakul, S., Yang, C., Chen, A., 2005. Shelter location-allocation model for flood evacuation planning. Journal of the Eastern Asia Society for Transportation Studies.

Langmann, B., Folch, A., Hensch, M., Matthias, V., 2012. Volcanic ash over Europe during the eruption of Eyjafjallajökull on Iceland, April-May 2010. Atmospheric Environment 48, 1–8. https://doi.org/10.1016/j.atmosenv.2011.03.054

Lin, Y.H., Batta, R., Rogerson, P.A., Blatt, A., Flanigan, M., 2012. Location of temporary depots to facilitate relief operations after an earthquake. Socio-Economic Planning Sciences 46, 112–123. https://doi.org/10.1016/j.seps.2012.01.001

Liu, S.Q., Kozan, E., 2016. Parallel-identical-machine job-shop scheduling with different stage-dependent buffering requirements. Computers and Operations Research 74, 31–41. https://doi.org/10.1016/j.cor.2016.04.023

Lordan, O., Klophaus, R., 2017. Measuring the vulnerability of global airline alliances to member exits. Transportation Research Procedia 25, 7–16. https://doi.org/10.1016/j.trpro.2017.05.189

Lordan, O., Sallan, J.M., Simo, P., 2014. Study of the topology and robustness of airline route networks from the complex network approach: A survey and research agenda. Journal of Transport Geography 37, 112–120. https://doi.org/10.1016/j.jtrangeo.2014.04.015

Lordan, O., Sallan, J.M., Simo, P., Gonzalez-Prieto, D., 2015. Robustness of airline alliance route networks. Communications in Nonlinear Science and Numerical Simulation 22, 587–595. https://doi.org/10.1016/j.cnsns.2014.07.019

Madas, M.A., Zografos, K.G., 2010. Airport slot allocation: A time for change? Transport Policy 17, 274–285. https://doi.org/10.1016/j.tranpol.2010.02.002

Marinelli, M., Palmisano, G., Dell'Orco, M., Ottomanelli, M., 2015. Fusion of Two Metaheuristic Approaches to Solve the Flight Gate Assignment Problem. Transportation Research Procedia 10, 920–930. https://doi.org/10.1016/j.trpro.2015.09.045

Mazzocchi, M., Hansstein, F., Ragona, M., 2010. The 2010 volcanic ash cloud and its financial impact on the European airline industry. CESifo Forum.

MLIT, 2018. Collaborative Actions for Renovation of Air Traffic Systems (CARATS) [WWW Document]. Ministry of land, Infrastructure and transport. URL http://www.mlit.go.jp/common/001046514.pdf (accessed 6.1.19).

Mota, M.M., Boosten, G., De Bock, N., Jimenez, E., de Sousa, J.P., 2017. Simulation-based turnaround evaluation for Lelystad Airport. Journal of Air Transport Management 64, 21–32. https://doi.org/10.1016/j.jairtraman.2017.06.021

NRT, 2020. Flight Information | NARITA INTERNATIONAL AIRPORT OFFICIAL WEBSITE [WWW Document]. URL https://www.narita-airport.jp/en/flight/today#section-1 (accessed 2.12.20).

Picquout, A., Lavigne, F., Mei, E.T.W., Grancher, D., Noer, C., Vidal, C.M., Hadmoko, D.S., 2013. Air traffic disturbance due to the 2010 Merapi volcano eruption. Journal of Volcanology and Geothermal Research 261, 366–375. https://doi.org/10.1016/j.jvolgeores.2013.04.005

Poulidis, A.P., Takemi, T., Shimizu, A., Iguchi, M., Jenkins, S.F., 2018. Statistical analysis of dispersal and deposition patterns of volcanic emissions from Mt. Sakurajima, Japan.

Atmospheric Environment 179, 305–320. https://doi.org/10.1016/j.atmosenv.2018.02.021

Smith, I.E., Arnedos, M., 2007. The evolution of adjuvant endocrine therapy: Developments since St Gallen 2005. Breast 16, 4–9. https://doi.org/10.1016/j.breast.2007.07.001

Smith, J.F., 2010. Regional Cooperation, Coordination, and Communication between Airports during Disasters. Transportation Research Record: Journal of the Transportation Research Board 2177, 132–140. https://doi.org/10.3141/2177-16

Toregas, C., Swain, R., ReVelle, C., Bergman, L., 1971. The Location of Emergency Service Facilities. Operations Research. https://doi.org/10.1287/opre.19.6.1363

# APPENDIX A

**Table A2-1** Aircraft Stands Utilization result from GA and GRASP: by Affected Aircraft and Aircraft Stand Sizes.

| Airport Name | ICAO Code | IATA Code | Maximum Capacity | | | | Available capacity — Assumption of non-occupancy stand rate = 79% of Max Capacity (Table A2) | | | | Genetic Algorithm (GA) | | | | | | | Greedy Randomized Adaptive Search Procedure (GRASP) | | | | | | |
|---|---|---|---|---|---|---|---|---|---|---|---|---|---|---|---|---|---|---|---|---|---|---|---|
| | | | Small | Medium | Large | Total Capacity | Small | Medium | Large | Total Capacity | Rank | Small | Medium | Large | Total | Overall capacity usage per available cap | % of All Affected Aircrafts | Rank | Small | Medium | Large | Total | Overall capacity usage per available cap | % of All Affected Aircrafts |
| Chūbu Centrair Airport | RJGG | NGO | 6 | 30 | 44 | 80 | 5 | 24 | 35 | 64 | 1 | 0 | 24 | 35 | 59 | 92.2% | 22.6% | 4 | 0 | 10 | 2 | 12 | 18.8% | 4.6% |
| Kansai Airport | RJBB | KIX | 12 | 45 | 10 | 67 | 9 | 36 | 8 | 53 | 2 | 0 | 31 | 8 | 39 | 73.6% | 14.9% | 3 | 0 | 11 | 2 | 13 | 24.5% | 5.0% |
| Osaka Airport | RJOO | ITM | 0 | 33 | 27 | 60 | 0 | 26 | 21 | 47 | 3 | 0 | 26 | 12 | 38 | 80.9% | 14.6% | 5 | 0 | 11 | 1 | 12 | 25.5% | 4.6% |
| Niigata Airport | RJSN | KIJ | 14 | 10 | 5 | 29 | 11 | 8 | 4 | 23 | 4 | 1 | 8 | 4 | 13 | 56.5% | 5.0% | 8 | 0 | 7 | 2 | 9 | 39.1% | 3.5% |
| Sendai Airport | RJSS | SDJ | 33 | 10 | 4 | 47 | 26 | 8 | 3 | 37 | 5 | 1 | 8 | 3 | 12 | 32.4% | 4.6% | 6 | 0 | 8 | 3 | 11 | 29.7% | 4.2% |
| Shizuoka Airport | RJNS | FSZ | 6 | 7 | 4 | 17 | 5 | 6 | 3 | 14 | 6 | 2 | 6 | 3 | 11 | 78.6% | 4.2% | 7 | 1 | 6 | 3 | 10 | 71.4% | 3.8% |
| Kobe Airport | RJBE | UKB | 0 | 10 | 4 | 14 | 0 | 8 | 3 | 11 | 7 | 0 | 7 | 3 | 10 | 90.9% | 3.8% | 11 | 0 | 4 | 3 | 7 | 63.6% | 2.7% |
| Fukushima Airport | RJSF | FKS | 10 | 5 | 3 | 18 | 8 | 4 | 2 | 14 | 8 | 2 | 4 | 2 | 8 | 57.1% | 3.1% | 16 | 0 | 4 | 2 | 6 | 42.9% | 2.3% |
| Komatsu Airport | RJNK | KMQ | 2 | 6 | 3 | 11 | 2 | 5 | 2 | 9 | 9 | 0 | 5 | 2 | 7 | 77.8% | 2.7% | 12 | 0 | 5 | 2 | 7 | 77.8% | 2.7% |
| Toyama Airport | RJNT | TOY | 12 | 6 | 1 | 19 | 9 | 5 | 1 | 15 | 10 | 1 | 5 | 1 | 7 | 46.7% | 2.7% | 17 | 0 | 5 | 1 | 6 | 40.0% | 2.3% |
| Nagoya Airport | RJNA | NKM | 73 | 5 | 2 | 80 | 58 | 4 | 2 | 64 | 11 | 0 | 4 | 2 | 6 | 9.4% | 2.3% | 18 | 0 | 4 | 2 | 6 | 9.4% | 2.3% |
| Hanamaki Airport | RJSI | HNA | 19 | 5 | 2 | 26 | 15 | 4 | 2 | 21 | 12 | 0 | 4 | 2 | 6 | 28.6% | 2.3% | 22 | 0 | 4 | 1 | 5 | 23.8% | 1.9% |
| Matsumoto Airport | RJAF | MMJ | 11 | 3 | 1 | 15 | 9 | 2 | 1 | 12 | 13 | 3 | 2 | 1 | 6 | 50.0% | 2.3% | 13 | 4 | 2 | 1 | 7 | 58.3% | 2.7% |
| Yamagata Airport | RJSC | GAJ | 6 | 5 | 1 | 12 | 5 | 4 | 1 | 10 | 14 | 1 | 3 | 1 | 5 | 50.0% | 1.9% | 23 | 0 | 4 | 1 | 5 | 50.0% | 1.9% |
| Misawa Airport | RJSM | MSJ | 21 | 3 | 2 | 26 | 17 | 2 | 2 | 21 | 15 | 1 | 1 | 2 | 4 | 19.1% | 1.5% | 28 | 0 | 2 | 2 | 4 | 19.1% | 1.5% |
| Noto Airport | RJNW | NTQ | 4 | 3 | 1 | 8 | 3 | 2 | 1 | 6 | 16 | 1 | 2 | 1 | 4 | 66.7% | 1.5% | 33 | 0 | 2 | 1 | 3 | 50.0% | 1.2% |
| Okayama Airport | RJOB | OKJ | 6 | 5 | 2 | 13 | 5 | 4 | 2 | 11 | 17 | 0 | 2 | 2 | 4 | 36.4% | 1.5% | 38 | 0 | 1 | 1 | 2 | 18.2% | 0.8% |
| Shonai Airport | RJSY | SYO | 7 | 4 | 1 | 12 | 6 | 3 | 1 | 10 | 18 | 0 | 3 | 1 | 4 | 40.0% | 1.5% | 29 | 0 | 3 | 1 | 4 | 40.0% | 1.5% |
| Takamatsu Airport | RJOT | TAK | 18 | 7 | 3 | 28 | 14 | 6 | 2 | 22 | 19 | 0 | 1 | 2 | 3 | 13.6% | 1.2% | 24 | 0 | 4 | 1 | 5 | 22.7% | 1.9% |
| Nanki-Shirahama Airport | RJBD | SHM | 6 | 3 | 1 | 10 | 5 | 2 | 1 | 8 | 20 | 0 | 2 | 1 | 3 | 37.5% | 1.2% | 34 | 0 | 2 | 1 | 3 | 37.5% | 1.2% |
| Odate-Noshiro Airport | RJSR | ONJ | 4 | 4 | 1 | 9 | 3 | 3 | 1 | 7 | 21 | 0 | 2 | 1 | 3 | 42.9% | 1.2% | 30 | 0 | 3 | 1 | 4 | 57.1% | 1.5% |
| Tokushima Airport | RJOS | TKS | 10 | 4 | 2 | 16 | 8 | 3 | 2 | 13 | 22 | 0 | 1 | 1 | 2 | 15.4% | 0.8% | 25 | 0 | 3 | 2 | 5 | 38.5% | 1.9% |
| Kōchi Airport | RJOK | KCZ | 12 | 6 | 3 | 21 | 9 | 5 | 2 | 16 | 23 | 0 | 0 | 2 | 2 | 12.5% | 0.8% | 14 | 0 | 5 | 2 | 7 | 43.8% | 2.7% |
| Matsuyama Airport | RJOM | MYJ | 16 | 7 | 4 | 27 | 13 | 6 | 3 | 22 | 24 | 0 | 1 | 1 | 2 | 9.1% | 0.8% | 35 | 0 | 2 | 1 | 3 | 13.6% | 1.2% |
| Hiroshima Airport | RJOA | HIJ | 3 | 6 | 3 | 12 | 2 | 5 | 2 | 9 | 25 | 0 | 1 | 0 | 1 | 11.1% | 0.4% | 39 | 0 | 2 | 0 | 2 | 22.2% | 0.8% |
| Aomori Airport | RJSA | AOJ | 13 | 3 | 3 | 19 | 10 | 2 | 2 | 14 | 26 | 0 | 1 | 0 | 1 | 7.1% | 0.4% | 31 | 0 | 2 | 2 | 4 | 28.6% | 1.5% |
| Tottori Airport | RJOR | TTJ | 18 | 3 | 1 | 22 | 14 | 2 | 1 | 17 | 27 | 0 | 1 | 0 | 1 | 5.9% | 0.4% | 36 | 0 | 2 | 1 | 3 | 17.7% | 1.2% |
| Kōnan Airport | RJBK | 0 | 61 | 3 | 0 | 64 | 48 | 2 | 0 | 50 | 28 | 0 | 0 | 0 | 0 | 0.0% | 0.0% | 40 | 0 | 2 | 0 | 2 | 4.0% | 0.8% |
| Miho-Yonago Airport | RJOH | YGJ | 10 | 5 | 2 | 17 | 8 | 4 | 2 | 14 | 29 | 0 | 0 | 0 | 0 | 0.0% | 0.0% | 37 | 0 | 3 | 0 | 3 | 21.4% | 1.2% |
| Fukuoka Airport | RJFF | FUK | 36 | 40 | 20 | 96 | 28 | 32 | 16 | 76 | 30 | 0 | 0 | 0 | 0 | 0.0% | 0.0% | 19 | 1 | 4 | 1 | 6 | 7.9% | 2.3% |
| Kagoshima Airport | RJFK | KOJ | 23 | 9 | 3 | 35 | 18 | 7 | 2 | 27 | 31 | 0 | 0 | 0 | 0 | 0.0% | 0.0% | 9 | 0 | 7 | 2 | 9 | 33.3% | 3.5% |
| Kitakyūshū Airport | RJFR | KKJ | 18 | 9 | 3 | 30 | 14 | 7 | 2 | 23 | 32 | 0 | 0 | 0 | 0 | 0.0% | 0.0% | 20 | 0 | 5 | 1 | 6 | 26.1% | 2.3% |
| Kumamoto Airport | RJFT | KMJ | 28 | 6 | 2 | 36 | 22 | 5 | 2 | 29 | 33 | 0 | 0 | 0 | 0 | 0.0% | 0.0% | 15 | 0 | 5 | 2 | 7 | 24.1% | 2.7% |
| Miyazaki Airport | RJFM | KMI | 3 | 16 | 6 | 25 | 2 | 13 | 5 | 20 | 34 | 0 | 0 | 0 | 0 | 0.0% | 0.0% | 10 | 1 | 4 | 3 | 8 | 40.0% | 3.1% |
| Nagasaki Airport | RJFU | NGS | 8 | 7 | 3 | 18 | 6 | 6 | 2 | 14 | 35 | 0 | 0 | 0 | 0 | 0.0% | 0.0% | 2 | 6 | 6 | 2 | 14 | 100.0% | 5.4% |
| Oita Airport | RJFO | OIT | 3 | 5 | 3 | 11 | 2 | 4 | 2 | 8 | 36 | 0 | 0 | 0 | 0 | 0.0% | 0.0% | 26 | 0 | 4 | 1 | 5 | 62.5% | 1.9% |
| Yamaguchi Ube Airport | RJDC | UBJ | 8 | 6 | 3 | 17 | 6 | 5 | 2 | 13 | 37 | 0 | 0 | 0 | 0 | 0.0% | 0.0% | 21 | 0 | 4 | 2 | 6 | 46.2% | 2.3% |
| New Chitose Airport | RJCC | CTS | 10 | 45 | 15 | 70 | 8 | 36 | 12 | 56 | 38 | 0 | 0 | 0 | 0 | 0.0% | 0.0% | 1 | 0 | 17 | 2 | 19 | 33.9% | 7.3% |
| Fukui Airport | RJNF | FKJ | 1 | 0 | 0 | 1 | 1 | 0 | 0 | 1 | 39 | 0 | 0 | 0 | 0 | 0.0% | 0.0% | 42 | 0 | 0 | 0 | 0 | 0.0% | 0.0% |
| Iwami Airport | RJOW | IWJ | 0 | 3 | 0 | 3 | 0 | 2 | 0 | 2 | 40 | 0 | 0 | 0 | 0 | 0.0% | 0.0% | 41 | 0 | 2 | 0 | 2 | 100.0% | 0.8% |
| Izumo Airport | RJOC | IZO | 5 | 5 | 1 | 11 | 4 | 4 | 1 | 9 | 41 | 0 | 0 | 0 | 0 | 0.0% | 0.0% | 32 | 0 | 4 | 0 | 4 | 44.4% | 1.5% |
| Saga Airport | RJFS | HSG | 10 | 5 | 1 | 16 | 8 | 4 | 1 | 13 | 42 | 0 | 0 | 0 | 0 | 0.0% | 0.0% | 27 | 0 | 4 | 1 | 5 | 38.5% | 1.9% |
| *Total* | | | *566* | *402* | *200* | *1168* | *446* | *320* | *159* | *925* | | *13* | *155* | *93* | *261* | | *100%* | | *13* | *189* | *59* | *261* | | *100%* |

**Table A2-2** Arrival and departure flight per hour at 5 affected airports, aircraft stand occupancy rate, and an assumption of shelter airport available capacities.

| Hour_Periods | | Number of Flight per hour | | | | | | | | | | | | | | | | | | | | | Average Cumulative Flight |
| | | Oshima Airport | | | | Chofu Airport | | | | Narita Airport | | | | Ibaraki Airport | | | | Haneda Airport | | | | |
| Start | End | Arrival | Departure | Cumulative | Total | Arrival | Departure | Cumulative | Total | Arrival | Departure | Cumulative | Total | Arrival | Departure | Cumulative | Total | Arrival | Departure | Cumulative | Total | |
|---|---|---|---|---|---|---|---|---|---|---|---|---|---|---|---|---|---|---|---|---|---|---|
| 12:00:00 AM | 12:59:00 AM | 0 | 0 | 1 | 0 | 0 | 0 | 4 | 0 | 0 | 0 | 2 | 0 | 0 | 0 | 2 | 0 | 0 | 0 | 132 | 0 | 28 |
| 1:00:00 AM | 1:59:00 AM | 0 | 1 | 0 | 1 | 0 | 1 | 3 | 1 | 0 | 0 | 2 | 0 | 0 | 0 | 2 | 0 | 0 | 3 | 129 | 3 | 27 |
| 2:00:00 AM | 2:59:00 AM | 0 | 0 | 0 | 0 | 0 | 0 | 3 | 0 | 0 | 0 | 2 | 0 | 0 | 0 | 2 | 0 | 2 | 0 | 131 | 2 | 28 |
| 3:00:00 AM | 3:59:00 AM | 0 | 0 | 0 | 0 | 0 | 0 | 3 | 0 | 0 | 0 | 2 | 0 | 0 | 0 | 2 | 0 | 2 | 0 | 133 | 2 | 28 |
| 4:00:00 AM | 4:59:00 AM | 0 | 0 | 0 | 0 | 0 | 0 | 3 | 0 | 0 | 0 | 2 | 0 | 0 | 0 | 2 | 0 | 3 | 0 | 136 | 3 | 29 |
| 5:00:00 AM | 5:59:00 AM | 0 | 0 | 0 | 0 | 0 | 0 | 3 | 0 | 0 | 0 | 2 | 0 | 0 | 0 | 2 | 0 | 7 | 0 | 143 | 7 | 30 |
| 6:00:00 AM | 6:59:00 AM | 0 | 0 | 0 | 0 | 0 | 0 | 3 | 0 | 8 | 0 | 10 | 8 | 0 | 0 | 2 | 0 | 7 | 37 | 113 | 44 | 26 |
| 7:00:00 AM | 7:59:00 AM | 0 | 0 | 0 | 0 | 0 | 0 | 3 | 0 | 11 | 4 | 17 | 15 | 0 | 1 | 1 | 1 | 8 | 68 | 53 | 76 | 15 |
| 8:00:00 AM | 8:59:00 AM | 0 | 0 | 0 | 0 | 0 | 0 | 3 | 0 | 14 | 4 | 27 | 18 | 0 | 1 | 0 | 1 | 45 | 51 | 47 | 96 | 15 |
| 9:00:00 AM | 9:59:00 AM | 0 | 0 | 0 | 0 | 0 | 0 | 3 | 0 | 19 | 17 | 29 | 36 | 2 | 0 | 2 | 2 | 42 | 48 | 41 | 90 | 15 |
| 10:00:00 AM | 10:59:00 AM | 0 | 0 | 0 | 0 | 0 | 2 | 1 | 2 | 12 | 23 | 18 | 35 | 2 | 1 | 3 | 3 | 45 | 40 | 46 | 85 | 14 |
| 11:00:00 AM | 11:59:00 AM | 0 | 0 | 0 | 0 | 0 | 1 | 0 | 1 | 13 | 20 | 11 | 33 | 0 | 1 | 2 | 1 | 48 | 54 | 40 | 102 | 11 |
| 12:00:00 PM | 12:59:00 PM | 0 | 0 | 0 | 0 | 3 | 0 | 3 | 3 | 10 | 13 | 8 | 23 | 1 | 0 | 3 | 1 | 35 | 55 | 20 | 90 | 7 |
| 1:00:00 PM | 1:59:00 PM | 0 | 0 | 0 | 0 | 0 | 2 | 1 | 2 | 13 | 14 | 7 | 27 | 1 | 3 | 1 | 4 | 56 | 57 | 19 | 113 | 6 |
| 2:00:00 PM | 2:59:00 PM | 0 | 0 | 0 | 0 | 0 | 0 | 1 | 0 | 19 | 12 | 14 | 31 | 0 | 0 | 1 | 0 | 41 | 45 | 15 | 86 | 6 |
| 3:00:00 PM | 3:59:00 PM | 1 | 0 | 1 | 1 | 3 | 0 | 4 | 3 | 31 | 5 | 40 | 36 | 0 | 1 | 0 | 1 | 41 | 38 | 18 | 79 | 13 |
| 4:00:00 PM | 4:59:00 PM | 0 | 0 | 1 | 0 | 0 | 0 | 4 | 0 | 24 | 12 | 52 | 36 | 0 | 0 | 0 | 0 | 37 | 34 | 21 | 71 | 16 |
| 5:00:00 PM | 5:59:00 PM | 0 | 0 | 1 | 0 | 0 | 0 | 4 | 0 | 19 | 37 | 34 | 56 | 1 | 0 | 1 | 1 | 39 | 50 | 10 | 89 | 10 |
| 6:00:00 PM | 6:59:00 PM | 0 | 0 | 1 | 0 | 0 | 0 | 4 | 0 | 12 | 25 | 21 | 37 | 0 | 1 | 0 | 1 | 45 | 45 | 10 | 90 | 7 |
| 7:00:00 PM | 7:59:00 PM | 0 | 0 | 1 | 0 | 0 | 0 | 4 | 0 | 14 | 7 | 28 | 21 | 1 | 1 | 0 | 2 | 42 | 50 | 2 | 92 | 7 |
| 8:00:00 PM | 8:59:00 PM | 0 | 0 | 1 | 0 | 0 | 0 | 4 | 0 | 7 | 9 | 26 | 16 | 2 | 0 | 2 | 2 | 53 | 28 | 27 | 81 | 12 |
| 9:00:00 PM | 9:59:00 PM | 0 | 0 | 1 | 0 | 0 | 0 | 4 | 0 | 5 | 15 | 16 | 20 | 0 | 0 | 2 | 0 | 63 | 12 | 78 | 75 | 20 |
| 10:00:00 PM | 10:59:00 PM | 0 | 0 | 1 | 0 | 0 | 0 | 4 | 0 | 1 | 11 | 6 | 12 | 0 | 0 | 2 | 0 | 37 | 4 | 111 | 41 | 25 |
| 11:00:00 PM | 11:59:00 PM | 0 | 0 | 1 | 0 | 0 | 0 | 4 | 0 | 0 | 2 | 4 | 2 | 0 | 0 | 2 | 0 | 7 | 1 | 117 | 8 | 26 |
| Max_Capacity | | 9 | | | | 24 | | | | 266 | | | | 8 | | | | 228 | | | | % Avg Occupancy |
| Min_Occupancy | | 0 | 0 | 0 | 0 | 0 | 0 | 0 | 0 | 7 | 5 | 7 | 16 | 0 | 0 | 0 | 0 | 35 | 28 | 2 | 71 | 2 |
| % Min_Occupancy per cap | | 0% | 0% | 0% | 0% | 0% | 0% | 0% | 0% | 3% | 2% | 3% | 6% | 0% | 0% | 0% | 0% | 15% | 12% | 1% | 31% | 1% |
| Max_Occupancy | | 1 | 0 | 1 | 1 | 3 | 2 | 4 | 3 | 31 | 37 | 52 | 56 | 2 | 3 | 3 | 4 | 56 | 57 | 46 | 113 | 21 |
| **% Max_Occupancy per cap | | 11% | 0% | 11% | 11% | 13% | 8% | 17% | 13% | 12% | 14% | 20% | 21% | 25% | 38% | 38% | 50% | 25% | 25% | 20% | 50% | 21% |
| ***an assumption of 42 shelter airport available capacities, calculated from average(%Max_Occupancy) of 5 affected airports: (1-0.21) | | | | | | | | | | | | | | | | | | | | | | 79% |

"The busiest period" (10:00:00 AM – 8:59:00 PM, left margin label)

**Table A2-3** Detail of affected aircraft, occupancy, and availability rate at the study airports with various simulated rate for the proposed models' configurations.

| Occupancy aircraft stand, Decrement/Increment rate at ±5% | | -20% | | -15% | | -10% | | -5% | | Baseline * | | 5% | | 10% | | 15% | | 20% | |
|---|---|---|---|---|---|---|---|---|---|---|---|---|---|---|---|---|---|---|---|
| Airborne aircraft — Observable affected aircraft (CARATS dataset) — Number of affected aircraft | | 86 | | 91 | | 96 | | 102 | | 107 | | 112 | | 118 | | 123 | | 128 | |
| On-ground aircraft at 5 affected airports / Affected Airports | Affected Airport Capacity | Max stand occupancy rate (baseline -20%) | Number of affected aircraft (baseline -20%) | Max stand occupancy rate (baseline -15%) | Number of affected aircraft (baseline -15%) | Max stand occupancy rate (baseline -10%) | Number of affected aircraft (baseline -10%) | Max stand occupancy rate (baseline -5%) | Number of affected aircraft (baseline -5%) | Max stand occupancy rate * (baseline) | Number of affected aircraft | Max stand occupancy rate (baseline +5%) | Number of affected aircraft (baseline +5%) | Max stand occupancy rate (baseline +10%) | Number of affected aircraft (baseline +10%) | Max stand occupancy rate (baseline +15%) | Number of affected aircraft (baseline +15%) | Max stand occupancy rate (baseline +20%) | Number of affected aircraft (baseline +20%) |
| Oshima | 9 | 8.80% | 1 | 9.40% | 1 | 9.90% | 1 | 10.50% | 1 | 11% | 1 | 11.60% | 1 | 12.10% | 1 | 12.70% | 1 | 13.20% | 1 |
| Chofu | 24 | 13.60% | 3 | 14.50% | 3 | 15.30% | 4 | 16.20% | 4 | 17% | 4 | 17.90% | 4 | 18.70% | 4 | 19.60% | 5 | 20.40% | 5 |
| Haneda | 228 | 16.00% | 36 | 17.00% | 39 | 18.00% | 41 | 19.00% | 43 | 20% | 46 | 21.00% | 48 | 22.00% | 50 | 23.00% | 52 | 24.00% | 55 |
| Narita | 266 | 30.40% | 81 | 32.30% | 86 | 34.20% | 91 | 36.10% | 96 | 38% | 101 | 39.90% | 106 | 41.80% | 111 | 43.70% | 116 | 45.60% | 121 |
| Ibaraki | 8 | 16.00% | 1 | 17.00% | 1 | 18.00% | 1 | 19.00% | 2 | 20% | 2 | 21.00% | 2 | 22.00% | 2 | 23.00% | 2 | 24.00% | 2 |
| Total number of affected aircraft | | 122 | | 130 | | 138 | | 146 | | 154 | | 161 | | 168 | | 176 | | 184 | |
| Grand total of affected aircraft | | **208** | | **221** | | **234** | | **248** | | **261** | | **273** | | **286** | | **299** | | **312** | |

**Table A2-4** Detail of available aircraft stands (non-occupancy stands) at 42 shelter airports.

| Occupancy aircraft stand, Decrement/Increment rate at ±5% ⓪ | -20% | -15% | -10% | -5% | Baseline * | 5% | 10% | 15% | 20% |
|---|---|---|---|---|---|---|---|---|---|
| Overall capacity of 42 shelter airports ③ | | | | | 1,168 | | | | |
| Average aircraft stand occupancy rate ($c_j$) ** | 16.80% | 17.90% | 18.90% | 20.00% | 21% | 22.10% | 23.10% | 24.20% | 25.20% |
| Average aircraft stand availability rate | 83% | 82% | 81% | 80% | 79% | 78% | 77% | 76% | 75% |
| **Average available capacity** | **972** | **960** | **947** | **935** | **925** | **910** | **898** | **886** | **874** |

* the maximum aircraft stand occupancy was calculated from the maximum cumulative number of aircraft stand occupancy at 5 affected airports, refer to

**Table A2-5** Aerodrome Design and Operations, Aerodrome reference code in Annex 14 - volume 1: by ICAO.

| | Runway | | Aero plane | | |
|---|---|---|---|---|---|
| Code Name | Aero plane reference field length | Code Letter | | Wingspan | Outer main gear wheel span |
| 1 | Less than 800 m | A | | < 15 m | < 4.5 m |
| 2 | 800 m up to but not including 1200 m | B | | 15 m but < 24 m | 4.5 m but < 6 m |
| 3 | 1200 m up to but not including 1800 m | C | | 24 m but < 36 m | 6 m but < 9 m |
| 4 | 1800 m and over | D | | 36 m but < 52 m | 9 m but < 14 m |
| | | E | | 52 m but < 65 m | 9 m but < 14 m |
| | | F | | 65 m but < 80 m | 14 m but < 16 m |

# CHAPTER 3

An Improvement on Shelter Airport Selection
Model During Large-scale Volcanic Disasters: A
case study of Hakoneyama Japan

# An Improvement on Shelter Airport Selection Model During Large-scale Volcanic Disasters: A case study of Hakoneyama Japan

## ABSTRACT

Through the movement of passengers and cargo, air transportation contributes to economic growth and prosperity. As it expands in size and complexity, it becomes more susceptible to disruptions caused by weather conditions and natural disasters, such as volcanic eruptions. The eruptions of the Eyjafjallajökull and Merapi volcanoes caused significant problems in Europe and central Indonesia concerning air traffic and the economy in 2010. Numerous active volcanoes in Japan could severely disrupt the country's airspace and damage aircraft. The study is aimed at the challenge of determining how to select an airport as a safe place to land during an aircraft evacuation in the event of a volcanic eruption. Airside, airline, and historical data were used to design the shelter airport selection model. Later, it was used to discover an approximate solution for aircraft evacuation using a genetic algorithm (GA).

## KEYWORDS

Large-scale Volcanic Disasters, Shelter Airport Selection Criterions, Genetic Algorithm

**Motivations:**

- Impact of natural disaster on air transportation in Japan, especially volcanic eruption.
- Aircraft engine is vulnerable to volcanic ash particles, aircraft evacuation to the safe airport is crucial.
- Additional airport and airline information could help improve shelter airport selection model to select the suitable airport for better supporting their operations from the early to post stage of disaster

**Objectives:**
The study aims to improve shelter airport selection model, which could select the suitable shelter airport for aircraft evacuation with mini flight time using addition airport and airlines information.

**Case study:** Hakonayama, Japan

**Study gaps:**
Airport and airlines flight schedule used in the study came from early of 2021 which may not reflect the current situation of air traffic volume (before COVID-19 pandemic).

**Data collections:**
- CARATS flight dataset on March 7th-13rd, 2016 provided by MLIT (the latest data available at the time of study)
- Japan airport information provided by aviation Information Service Center (AIS), MLIT
- Airports weekly schedule flight data
- Airlines weekly schedule flight data and partners/alliances information

**Methodologies:**
- Model development
- Genetic Algorithm (GA)
- Model validation and comparison
- Sensitivity analysis
- Differentiation analysis using One-Way ANOVA

## 3.1. INTRODUCTION AND BACKGROUND

By transporting passengers and cargo, air transport contributes to economic growth and prosperity. Due to the low fares offered by low-cost carrier airlines (LCCs) and stronger economies, the world's air passenger numbers surpassed four billion for the first time in 2017 and have continued to grow (IATA, 2018). However, as air transport becomes larger and more complex, its performance becomes more susceptible to weather conditions and natural disasters, such as volcanic eruptions. Recently, the aircraft industry faced a perilous situation created by volcanic eruptions and their associated ash cloud. In 2010, the eruptions of the Eyjafjallajökull and Merapi volcanoes in Iceland and central Indonesia severely impacted air travel and the economy (Langmann et al., 2012; Picquout et al., 2013). According to the International Civil Aviation Organization (ICAO), volcanic ash particles consist of chemical compound which melted at the temperature below the operating temperature of modern turbine engine. Those melted chemical compound and its sharpness can seriously damage the aircraft body, external mechanics, and engines. Thus, in any ash cloud density level, all aircraft must avoid interaction with volcanic ash particles and rocks by flying into or parking within the volcanic eruption impacted areas and airspace. (ICAO, 2012). The ICAO has also established guidelines for the safe operation of all aviation parties at early, during, and pos-stage specifically for volcanic eruptions, which including the designation of Tokyo volcanic Ash Advisory Center (VAAC) and the Japan Meteorological Agency (JMA) to provide detail of status and forecasting impact of volcanic ash clouds throughout EAST ASIA airspace.

According to the IATA annual report released in June 2019, Japan had the world's fifth-largest airline industry and one of the busiest airspaces. The country, however, has been struck by a number of natural disasters, including earthquakes and volcanic eruptions, which pose a threat to the country's aviation systems. To handle an emergencies disruption such as this, ICAO had developed the airport and aerodrome emergency planning in Annex 3, Annex 14, Doc 9691 AN/954, and Doc 9137-Part 7 (ICAO, 2018, 2016, 2007, 1991). It is the process of preparing an airport to deal with an emergency that occurs at or near the airport, such as an aircraft, airport building, airport service facilities, passenger, natural and man-made incident/accident, and so on. The goal of airport emergency planning is to reduce the effects of a disaster, especially in terms of preserving lives and maintaining aircraft operations. Since aircraft is the high value asset in aviation industry, it has been proposed that, as soon as airports receive the notice from those parties, in-flight and on-ground aircraft be directed to evacuate or divert to safe designated facilities (airports/alternate destinations) outside the impacted area, if practicable.

The facility selection during to disaster is one of the "Disaster Management (DM)" activities to help impacted entity, which can be people, cargo, animal, etc. to effectively and efficiently avoid or recover from the effect of disaster through four consecutive stages: mitigation, preparation, response, and recovery (Akgün et al., 2015; Coppola, 2015). Therefore, an appropriate facility location selection model may lead to probability reduction of disaster occurrence, decreasing hazardous degree, increasing chance of survival and recovery, and minimizing financial and other loss at the early, during, and pos-stage of disaster.

The Shelter selection optimization model was created for unexpected catastrophes to pick the shelters located near effected places for shelter location selection for evacuation. The primary goals are responsiveness and cost-effectiveness, which are accomplished by lowering overall evacuation costs in particularly time or total distance (Toregas et al., 1971) travelled to demand sites (an affected area and candidate facilities). The use of total minimization or minisum in optimization models for facility selection in distributing humanitarian assistance supplies during natural disasters such as hurricanes, floods, and earthquakes has become commonplace (Horner

and Downs, 2010; Lin et al., 2012). Furthermore, a Genetic Algorithm (GA) approach has been adopted by Kongsomsaksakul et al. in 2005 (Kongsomsaksakul et al., 2005) and Hu et al. in 2014 (Hu et al., 2014) to meet massive catastrophe engine s to handle the complex issue of identifying objective multi-criteria optimal facility selection of flood and earthquake disposal refuges. However, the optimization model for selecting a shelter airport for aircraft evacuation is infrequently available.

The aircraft optimization model research for disruption events began in 1984 (Teodorović and Guberinić, 1984), when one or more aircraft became unavailable. Later that year, Argüello et al. introduced a metaheuristic approach to aircraft recovery optimization by utilizing a Greedy Randomized Adaptive Search Procedure (GRASP) to re-plot aircraft flight paths for the grounding of one or more aircraft. Additionally, aircraft recovery optimization problems have been addressed using the metaheuristic method based on tabu and local search (Andersson, 2006; Løve et al., 2001). These models enabled the development of a novel solution that met the study's objective and constraints.

Many studies in air transportation have identified criteria or restrictions for emergency airport selection during natural catastrophe disruptions, which can be used in the aircraft recovery and shelter facility location selection optimization model. For example, Madas and Zografos recommended that the classification, capacity, size and air traffic need for the airport should be assessed before determining whether to distribute an airport slot in congested areas in an optimum manner. (Madas and Zografos, 2010). In addition, in the case of major airport closures, Voltes-Dorta et al. examined the vulnerability of the European air transport network (Voltes-Dorta et al., 2017). According to the study, airport capacities, alliance/partner airline operations, and airline operations at designated airports all significantly influence aircraft and passenger relocation during a disruption. Other research has addressed these factors (Lordan et al., 2015; Lordan and Klophaus, 2017).

Some studies also recommended using enclosed areas and airspace to represent places damaged by terrible weather or disasters and employing heuristic algorithms in the optimization model to find a viable strategy to avoid those disrupted areas (Krukhmalev and Pshikhopov, 2017). The approach for selecting airport shelters for aviation during volcanic eruptions was proposed in early 2021 for genetic algorithms (Arreeras and Arimura, 2021). The selection model employed an entry of the affected region, the airport capacity and flight schedule data as constraints. In addition, the model was set up to reduce the overall travel time of all affected planes to the chosen shelter airport while keeping the regular airport flight schedule. The model had been compared its performance to the other similar meta-heuristic algorithm Greedy Randomized Adaptive Search Procedure (GRASP), which found the model applied on GA outperformance the GRASP in finding the approximate feasible solution with limited computation time. However, the other proposed characteristics were not considered in the early 2021 study, which could help design a more practical shelter airport option for airline recovery following a disruption event.

Therefore, this research aims to improve the previous model by combining additional airline data and generating new model restrictions. By extended airport and airline perspective on the airport selection model for aircraft evacuation, a new proposed model might give a realistic and viable option for aircraft evacuation to aviation authorities and other stakeholders, at all levels (local, national, international) such as International Civil Aviation Organization (ICAO), Civil Aviation Bureau, Ministry of Land, Infrastructure, Transport and Tourism (MLIT) of Japan, airports, airlines, etc.

The following is a breakdown of how the research is structured. The model's conceptual and assumption details, which comprised the model's objective function, indices, parameter, constraints setting, and handling technique in the form of mathematical equations, were provided in section 3. The proposed model's performance was validated against the research's objective and restrictions and compared to the previous model of early 2021 in section 4 and the case study in section 5.

In addition, the new proposed model was evaluated on the case study of Hakone volcano in Japan using a historical flight dataset (CARATS) to evaluate the proposed model outcome in a real-world situation in section 5. The sensitivity analysis on the various scenarios of occupancy rate, which directly impacts air traffic congestion and the available stands at shelter airport candidates, was established and observed. In the computational result section 6, the study also employed the one-way Analysis of Variance (ANOVA) test to see any variations between the scenarios' selection patterns. In section 7, the study comes to a close with recommendations for future research.

## 3.2.    METHODS AND MATERIALS

The parts that follow address a conceptual model and assumptions, genetic algorithm (GA) encoding, a historical flight dataset, suggested model descriptions, and pseudocodes:

### 3.2.1    Genetic Algorithm (GA)

The Genetic Algorithm (GA) is a kind of metaheuristic. It belongs to the evaluation algorithm introduced by Goldberg and Holland in 1988, which is a high-level process or heuristic meant to identify, develop, or choose a heuristic that may offer a sufficiently correct solution to an optimization issue. It is a Darwinian-based optimization method and genetic principles. GA is typically used to generate and evaluate solutions iteratively via crossover, mutation, and an evaluation function against the constraint on the problem. While GA does not guarantee that the global optimal solution will be found, a near-optimal and sufficiently feasible solution can be found (Blum and Roli, 2003).

The proximity search method has been applied to GA to determine the shortest distance and flight time between two points to solve the study's objective problem. The path between two points on the earth's surface is called a geodesic or curve line, and distances are calculated using Latitude and Longitude (Gade, 2010; Sinnott, 1984). Therefore, the haversine formula for determining the flight distance was employed in this research. It was dividing the flight distance by the average commercial aircraft cruising speed (880 kilometres per hour) from its present location to the chosen airports.

### 3.2.2    Constraints Handling Method

The optimization algorithms' constraint handling method allows the search result from decision space to be accepted or rejected based on the problem's objective and constraint bounds (Maier et al., 2019). It also has several features, such as preserving feasibility, penalizing, and differentiating between feasible and infeasible solutions (Michalewicz, 1996). The penalizing strategy, also known as the penalty function, is the most popular and efficient way to manage a problem's constraint in an optimization process.

The penalty function measures to the extent that fitness is not attainable because of the number of constraint breaches in one solution. The static penalty function is what it's called (Smith

and Coit, 2004). The high degree of infeasibility value of a solution increases as the number of constraint violations rises, and the solution is excluded from the decision space. The penalty function is specified in equation (b) as a simple fitness function $F(\vec{x})$ (Deb, 2000) that is defined as the sum of the objective function $f(\vec{x})$ and extra flight duration that is proportional to the degree of constraint violation $|g_i(\vec{x})|$ from the penalty function:

$$F(\vec{x}) = f(\vec{x}) + \sum_{j=1}^{J} R_j \, |g_i(\vec{x})|^2 \qquad\qquad (b)$$

where, | | denotes the absolute value if the operand is negative, it returns zero; else, it returns a value of zero. $R_j$ is the penalty parameter for violating the $j^{th}$ inequality constraint. The parameter aims to increase the magnitude of the constraint violation, $g_i(\vec{x})$ of similarity of magnitude as the objective function value $f(\vec{x})$.

Additionally, this study employs the penalty coefficient introduced by Homaifar et al. Homaifar et al. (Homaifar et al., 1994) to denote constraints with varying degrees of violation in the multi-constraints problem. Each constraint is assigned a unique coefficient $R_{nm}$ to denote the penalty coefficient associated with the $n^{th}$ constraint ($n=1,…,n$) and the $m^{th}$ violation level ($m=0,..,m$), which is used to define the severity of a constraint relative to the others in the problem. Thus, identical coefficient values indicate the same level of violation.

### 3.2.3 The Historical flight dataset: Japan air space's aircraft profile

CARATS flight datasets are historical flight records of Japan's four area control centres (ACC): Tokyo, Fukuoka, Naha, and Sapporo. In **Table 3.1**, example of flight data for individual aircraft is shown, including the date, a 10-second timestamp, latitude and longitude, altitude, and the aircraft model provided by Japan MLIT (MLIT, 2018). Instead of generating their positions randomly, the study uses this flight dataset to ensure the current position of affected aircraft in the simulation model and calculations. In addition, each aircraft's direction, flight route, and destination are determined using the aircraft movements and timestamps, allowing any possibly affected aircraft to be identified. Furthermore, the aircraft type data (AC type) is also utilized to determine the size of the aircraft so that it can be matched to available aircraft parking stands at the shelter airport.

**Table 3.1.** Historical Flights dataset given by Japan MLIT as an example of CARATS

| Time | Flight_ no. | Latitude | Longitude | Altitude | AC_type |
|---|---|---|---|---|---|
| 18:00:07 | FLT2236 | 33.887928 | 130.633698 | 34000 | B77L |
| 18:00:17 | FLT2236 | 33.877226 | 130.616886 | 33977 | B77L |
| 18:00:26 | FLT2236 | 33.866403 | 130.60072 | 33994 | B77L |
| 18:00:36 | FLT2236 | 33.855695 | 130.584217 | 34000 | B77L |

In this study, the CARATS flight data in March 2016, 7th-13rd (Mon-Sun) from 0.00AM-11.59PM (24hrs) of the latest data available at the study period was used. According to the data with the number of non-duplicated flight counting across multiple ACCs, Japan's airspace handled ~4,244 flight a day or ~177 flights an hour on average, see Table 3.2. Additionally, the non-duplicated flight volume for each hour-timeframe would reflect the actual flight that appeared in the airspace at that hour. However, because certain aircraft flights' duration may span multiple hour intervals, their flight_no(s) could appeared multiple times throughout the day. Thus, the sum of all hours could not be used to represent the air traffic volume for an entire day. They were, nonetheless, the particular flight would be counted as a single flight across 24-hour period. The 7-days data had shown the busy air traffic lied between 8:00AM to 9:59PM (11-hour timeframe),

with average and maximum flight volume per hour of ~426 and ~692 flights respectively, as illustrated in Figure 3.1 below.

**Table 3.2** the 7 days of CARATS dataset observation: number of non-duplicated aircraft flight per day.

| Date of data | Weekday | Total FLT_No. per day | Average FLT_No. per hr. |
|---|---|---|---|
| 7-Mar-16 | Monday | 4,191 | 175 |
| 8-Mar-16 | Tuesday | 4,039 | 168 |
| 9-Mar-16 | Wednesday | 4,216 | 176 |
| 10-Mar-16 | Thursday | 4,283 | 178 |
| 11-Mar-16 | Friday | 4,305 | 179 |
| 12-Mar-16 | Saturday | 4,307 | 179 |
| 13-Mar-16 | Sunday | 4,369 | 182 |
| **Average** | | **4,244** | **177** |
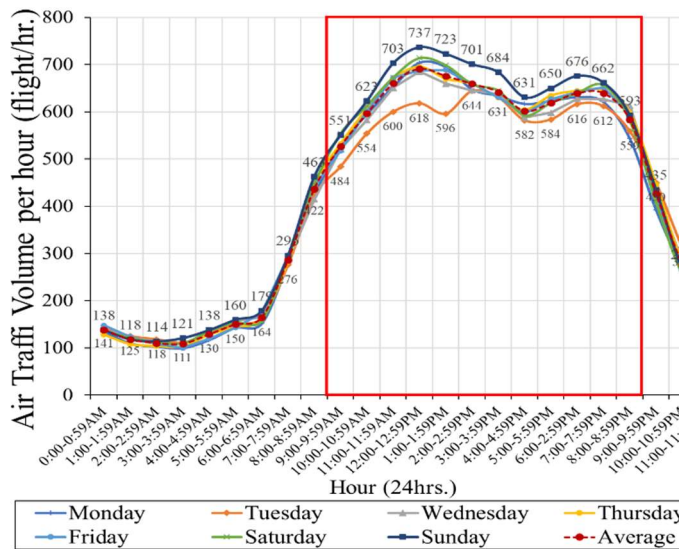


**Figure 3.1** The actual air traffic volume within particular hour and the busy time frame by non-duplicated flight number.
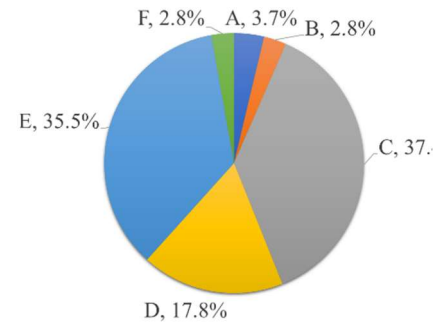
**Figure 3.2** Ratio of aircraft size by wingspan.

Furthermore, the data observation had revealed the aircraft sizes by wingspan ratio, which the majority was aircraft was group C (medium-size aircraft) 37.4% followed by group E (large-size aircraft) 35.5%, and group D (medium-large size) 17.8%, see Figure 3.2. However, the aircraft sizes were grouped into 3 main groups correspond to aircraft parking sizes at the airport, which are small (aircraft size A and B), medium (aircraft size C and D), and large (aircraft size E-F). These aircraft number and sizes ratio were used to simulate the number of affected aircrafts especially for on-ground aircraft at the affected airports in the case study.

## 3.3.   PROPOSED MODELS

For emergency evacuation and selection planning of airports based on traffic control, the GA computational model is developed. The concept aims to reduce flight times for aircraft to safe

airports from their existing positions. Aside from the model's evaluation by evacuation time, the suggested model has also been tested for the best shelter airport selection solution by considering aircraft assignment criteria from airside and airline viewpoints.

These viewpoints were transformed to model constraints in mathematical formulas, which were then utilized in the design of GAs via computational programming. The model considered the airport's available aircraft handling capability, which distinguishes it from the scheduled flight handling capacity of the regular airport. As a result, it may be possible to reduce disruption to regular airport and airline operations at shelter airports. The following are the model construction assumptions, including objective function, constraints, and algorithm's operators, which are presented in mathematical equations, parameters, and variables:

### 3.3.1　The Assumptions of Airport Selection

1. *Location of the shelter airport candidates and their capacities:* the airport must locate outside the volcanic eruption area and affected aircraft assignment cannot exceed airport available capacity.
2. *Airport available aircraft parking stands by aircraft sizes*: although the runway length is one of the critical factors in the shelter airport selection, which is related to the distance of each size of aircraft used for taking off and landing (ICAO, 2016). Therefore, instead of selecting a shelter airport with a suitable runway of the selected airport, the model matched each aircraft by its size and selected the exact size of the available stand, otherwise a larger size stand.
3. *Shelter airport's type:* all affected aircraft must be assigned to the correct type of airport. An international flight aircraft assigns to an international airport, in which international immigration and customs units are available. A domestic flight aircraft can be assigned to both international and domestic airports.
4. *Shelter airport's classification:* The affected aircraft are assigned to the hub and the regional class airport first otherwise to the local and military airports, respectively, to ensure sufficient aircraft handling capability of the selected airport. Refer to airport classification by AIS (MLIT, 2019).
5. *Airline operation and partners at the shelter airport:* The affected aircraft are assigned to the shelter airport, which its airline or partner airlines operate. This procedure could help the affected aircraft's airlines handling aircraft and passengers transit to other flights within its airlines or other partner airlines (Voltes-Dorta et al., 2017).
6. *Original flight route airport assignment:* If the affected aircraft is a domestic flight, an aircraft should be assigned to its original flight route airport, allowing airlines to manage the aircraft recovery more efficiently after the disaster from their original flight route airports.

### 3.3.2　The Indices, Parameters, Decision Variables

*Index sets*

$I$　　　Set of impacted aircrafts; $i \in I$
$J$　　　Set of potential shelter airports; $j \in J$
$S_i$　　Set of impacted aircraft sizes; $s \in \xi$, associated with $I$
$A$　　　Set of impacted airports; $a \in A$
$C_i$　　Set of airlines code associated with $I$
$N_i$　　Set of impacted aircraft flight type; international or domestic, associated with $I$
$F_j$　　Set of Airport types associated with $J$ (International, Domestic)

| $D_i$ | Set of Partner airlines of affected aircraft $I$ |
|---|---|
| $L_j$ | Set of Airport classification associated with $J$ |
| $G_j$ | Set of Operate airlines $c_i$ at shelter airport $j$ |
| $K_{ij}$ | Set of original flight route airport of affected aircraft $i$, associated with $J$ |

*Parameters*

| $M_j$ | Maximum aircraft parking stands of a selected airport; $j \in J$ |
|---|---|
| $OC_j$ | The occupancy rate of at the potential shelter airports $j \in J$ |
| $NC_j$ | The non-occupancy rate at the shelter airport $j \in J$ |
| $P(\rho)_j$ | Free medium-size stands, at the selected $j \in J$ |
| $P(\tau)_j$ | Free large size stands, at the selected $j \in J$ |
| $\rho_{sj}$ | Set to 1 as no medium-size aircraft $s \in \xi$ has been allocated to a medium- or large-size aircraft stand at the selected $j \in J$, 0 otherwise. |
| $\tau_{sj}$ | Set to 1 as no large-size aircraft $s \in \xi$ has been allocated to a large-size aircraft stand at the selected airport $j \in J$, 0 otherwise. |
| $H_j$ | Penalty or extra flight time value is assigned to each aircraft $i \in I$, the capacity constraint to control GA from exceeding the capacity of selected airport $j \in J$. |
| $t_{ij}$ | Each impacted aircraft's flight time $i \in I$ to airport $j \in J$ |
| $W_{nif}$ | Set to 1 as international flight aircraft $n_i$, assigned to airport type international $F_j$, 0 otherwise. |
| $OD_{ijk}$ | Set to 1 as impacted domestic flight aircraft $n_i$, assigned to airport j, which in the original flight route airport $k_{ij}$, 0 otherwise. |
| $SO_{ijcg}$ | Set to 1 as impacted aircraft $i$ is assigned to airport $j$ and affected aircraft's airline $c_i$ is operating airline $g_j$ at shelter airport $j$, 0 otherwise. |
| $PN_{ijcd}$ | Set to 1 as impacted aircraft $i$ is assigned to airport $j$ and affected aircraft's airline $c_i$ has partner airlines $d_{ij}$ operate at airport $j$, 0 otherwise. |
| $V_{hub_{il}}$ | Non-negative value of impacted aircraft $i$ assigned to a hub (1st class) airport $L_{ij}$. |
| $V_{reg_{il}}$ | Non-negative value of impacted aircraft $i$ assigned to a regional (2nd class) airport $L_{ij}$. |
| $V_{loc_{il}}$ | Non-negative value of impacted aircraft $i$ assigned to a local (3rd class) airport $L_{ij}$. |
| $V_{mil_{il}}$ | Non-negative value of impacted aircraft $i$ assigned to a military airport $L_{ij}$. |
| $SV_{ijl}$ | Non-negative value of all selected class of shelter airport $L_{ij}$. |

*Decision variables*

| $X_j$ | Set to 1 as selected airport $j$, in the impacted airport $a \in A$, 0 otherwise. |
|---|---|
| $E_{ij}$ | Designated impacted aircraft $i \in I$ to airport $j \in J$ |
| $T_{ij}$ | Total travel duration of all designated aircrafts $i \in I$ to airports $j \in J$ |

### 3.3.3   The study Objective and Constraints Function

*Objective function*

Concentrate on minimizing the total travel duration of impacted aircraft from their current flight location to potential airports.

$$minT_{ij} = \sum_j \sum_i t_{ij} + H_j \qquad\qquad \forall i,j \qquad\qquad (1)$$

*Constraints*

    *Evacuate to the safe airport outside the affected area:* the selected airport for each affected aircraft must not locate in the affected area of the volcanic eruption.

$$X_j \notin A \tag{2a}$$

$$\sum_{j \in J} X_j = 0 \,. \qquad\qquad\qquad \forall j \tag{2b}$$

    *The airport capacity restrictions:* according to the aircraft size assignment and airport capacity constraints described in Section 3.1, The impacted aircraft may be allocated to the same or a bigger stand than its size. Small-size aircraft can be allocated to any stand size, in contrast to medium large-size aircraft. As a result, the constraint has been narrowed to aircraft of medium and large size that are not allocated to smaller stands, as illustrated in constraints 3b and 3c. Additionally, the selected airport's entire fleet of assigned aircraft must not exceed the number of available or unoccupied parking spaces at the airport (3d).

$$NC_j = M_j\left(1 - OC_j\right) \tag{3a}$$

$$\sum_{s \in \xi} \rho_{sj} = 0 \qquad\qquad\qquad \forall s \tag{3b}$$

$$\sum_{s \in \xi} \tau_{sj} = 0 \qquad\qquad\qquad \forall s \tag{3c}$$

$$\sum_{i \in I} E_{ij} \leq NC_j \qquad\qquad\qquad \forall j \tag{3d}$$

    *Shelter airport's type:* all affected aircraft must be assigned to the correct airport type – constraint (4). The international flight aircraft assigns to the international airport, in which international immigration and customs facilities are available. Domestic flight aircraft, on the other hand, can be assigned to any type of shelter airport.

$$\sum_{n \in N} W_{nif} > 0 \qquad\qquad\qquad \forall n \tag{4}$$

    *Shelter airport's classification:* constraint (5a), requires that the impacted aircraft *I* be assigned first to a 1st class (hub) or the 2nd class (regional) airport, and then to a 3rd class (local) or military airport to ensure the shelter airport's aircraft handling facilities and capabilities, which act as non-negative conditions for decision variables.

$$V_{hub_{il}} \geq V_{reg_{il}} > V_{loc_{il}} > V_{mil_{il}} \qquad\qquad \forall i \tag{5a}$$

$$SV_{ijl} = \sum_{i \in I} V_{hub_{il}} + \sum_{i \in I} V_{reg_{il}} + \sum_{i \in I} V_{loc_{il}} + \sum_{i \in I} V_{mil_{il}} \tag{5b}$$

    *Airline operation and partners at the shelter airport:* the impacted aircraft should be allocated to the shelter airport, airline $c_i$, or the partner airlines $d_{ij}$ operates, representing as non-negative or binary conditions of decision variables.

$$NC_j \geq \sum_{i \in I} SO_{ijcg} + \sum_{i \in I} PN_{ijcd} > 0 \qquad\qquad \forall i \tag{6}$$

    *Original flight route airport assignment:* If the affected aircraft is domestic, it should be assigned to its original flight route airport. This procedure could help manage the aircraft recovery after the disaster efficiently from their original flight route airports, representing non-negative or binary conditions of decision variables.

$$N_{dom_i} \geq \sum_{i \in I} OD_{ijk} > 0 \qquad\qquad\qquad \forall i \tag{7}$$

### 3.3.4 Penalty function

Penalty function represents constraint violation degree provider according setting constraints to penalize infeasible solution generated by model, which force the infeasible solution to be eliminated. According to goal of evacuation and objective function of this study is evaluated by total flight time for aircraft to move of current position to the selected shelter airports, an additional flight time provided by the penalty function $H_j$ (8) for any solution depended on degree of constraints violation. It represents additional waiting time for an aircraft before it can be allowed to evacuate to selected constraint violated airport. However, the addition flight does not reflect a real flight time each aircraft takes to the designated aircraft, it is for evaluation process to select the best feasible solution only. Thus, the additional flight time $H_j$ can be calculated by multiplying the sum of all constraint violations by the constant a where $a \geq 1$, the average duration an aircraft regularly took for landing, take-off and turnaround operations. It generally takes an hour on average, depending on the aircraft's size (Airbus, 2005; ICAO, 2013; Mota et al., 2017).

$$H_j = |a * [R_{nm}(\sum_{i \in I} E_{ij} - NC_j) + R_{nm} \sum_{i \in I} W_{nif} + R_{nm}SV_{ijl} + R_{nm}(\sum_{i \in I} SO_{ijo} + \sum_{i \in I} PN_{ij})]| \tag{8}$$

where:

- $a$ is the constant value of the average length of the LTO operation cycle and turnaround operations of an aircraft, $a \geq 1$.
- $n$ is $n^{th}$ constraint ($n=1,…,n$).
- $m$ is $m^{th}$ violation level ($m=0,..,m$).
- $R$ is non-negative value relate to $n^{th}$ constraint and $m^{th}$ violation level setting.

### 3.3.5 Genetic Algorithm Operators

In this study, a Python-based tool for examining algorithms that deal with fundamental operators and settings known as DEAP was utilized in this research (De Rainville et al., 2012). Algorithm 1 shows the specifics of the process flow and settings for the GA.
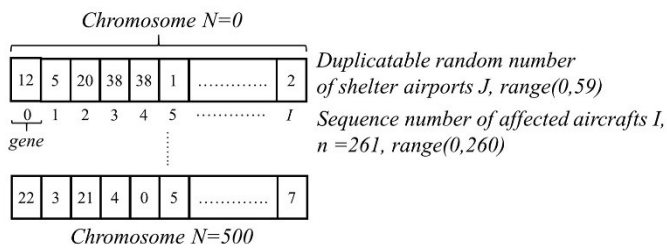


**Figure 3.3.** The GA chromosome encoding.

*Chromosome encoding:* As illustrated in Figure 3.3, the list of designated airports $j \in J$ was stored on chromosome N. A chromosome holds $I$ genes, which are responsible for every impacted aircraft $i \in I$, each gene is randomly generated ranged from 0-59 of the potential airport id $j \in J$. For instance, 261 impacted aircrafts required to be evacuated to one of 60 potential safe airports. Genes in a single chromosome contain numbers indicated to a single shelter airport id and can be duplicated.

*Initial population*: Following DEAP on the number of appropriate initial chromosomal populations, $N$ was set to 500 chromosomes. The smaller number or larger initial chromosome caused a longer computational duration of GA in finding the approximate solution.

*Chromosome evaluation and fitness function*: All chromosomal flight time was computed as a fitness value, which is the value between the overall flight time ($\sum_i \sum_j T_{ij} + H_j$) of all the genes that have been determined using the formula of a haversine distance divided by an average commercial aircraft speed per hour and extra flight time $P_{ij}$ generated by penalty function as specified in section 3.3.4.

*Crossover and mutation*: The two-points crossover technique was used. Via the operator "cxTwoPoints", the crossover process chooses two crossbands $i$ in chromosome N, using the random sequence integer $i \in I$ selection, and switches genes between two parents, maintaining the initial gene values of the chromosome and offering the child chromosome variety. In contrast, the mutation technique employed by the "mutUniformInt" operator is a crossover approach with a random integer chance of 5% between 0 and 59. This resulted in a change in the gene's value from the initial value within the range of $J$.

*Chromosome replacement*: A steady-state method was used in the research, in which population size is fixed in proportion to the number of initial chromosomes produced. This was done using a tournament manager (selTurnament, toursize=3). Thus, the better and more eligible offspring replaced the original parent chromosomes after each successive round of the assessment procedure.

*Chromosome decoding*: In the final stage, the chromosome should include a list of chosen airports $j \in J$ for all impacted aircraft $i \in I$, subsequently transformed between aircraft and selected airports into distances and flight times. The lowest fitness value chromosome (the shortest overall flight time) is selected as the optimal option depending on the goal function.

**Algorithm 1** Pseudocode of the proposed model applied with genetic algorithm

---

**Input:** $J$ represents a collection of potential airports; $M$ represents a set of the airport capacity, and $I$ represents a set of impacted aircraft;

**Output:** A list of the closest $X_j$ designated shelter airports for each $E_{ij}$ impacedted aircrafts;

**Initialize Populations:** 500 randomly generated solutions with 60 random candidate airports $j \in J$ of all affected aircraft $i \in I$.

| | |
|---|---|
| 1 | **Evaluate** assess the suitability of each solution with the lowest total fight time (fitness value) **do** |
| 2 |   **calculate** travel duration of impacted aircraft $i \in I$ to all designated airport $j \in J$; using haversine formula; |
| 3 |     **Repeat Until** condition of termination is fulfilled; 500 iterations **do** |
| 4 |       **Select** parents' solution; the 3 best chromosomes with the lowest fitness value |
| 6 |       **Crossover** two-point crossover operator pairs of parents; |
| 7 |       **Offspring mutation** to randomly alter the solution value by using the mutUniformInt operator; |
| 8 |       **Evaluate** assess the suitability of each solution with the lowest fitness value **do** |
| 9 |         **calculate** travel duration for population $E_{ij}$; |
| 10 |         **Foreach** $E_{ij}$ of aircraft $i$ to designated airport $j$ **do** |
| 11 |           **check** at shelter airport $j$ verify sum of allocated aircraft; $\sum_j E_{ij}$, compare to the available capacity $NC_j$, at airport $j$; |
| 12 |           **if** $\sum_j E_{ij} < NC_j$; exit; |
| 13 |           **else then** |
| |             **calculate** of the extra time (penalty) for aircraft $i$ allocated to airport $j$, depending to its degree of restrictions breach; |

$$P_{ij} = \left| a * \left[ R_{nm}\left(\sum_{i \in I} E_{ij} - NC_j\right) + R_{nm} \sum_{i \in I} W_{inter_{if}} + R_{nm} SV_{ij} + \right. \right.$$
$$\left. \left. R_{nm}\left(\sum_{i \in I} SO_{ijo} + \sum_{i \in I} PN_{ij}\right) \right] \right|$$

| | |
|---|---|
| | exit; |
| 14 | End for |
| 15 | **Select** the 3 best solutions: minimum fitness by total flight time |
| 16 | **Record** the selected solutions in the list of the best available solutions |
| 17 | **Fill up** the solution list with the new best solution for the next iteration |
| 18 | **Terminate** |

## 3.4.   MODEL VALIDATION

In this section, the proposed model's performance has been validated according to the study's objective, constraints described in section 3.3.3, on the same dataset and parameters setting, and compared with the previous model by Arreeras and Arimura in early 2021, which had been proved its performance to the other similar meta-heuristic algorithm such as Greedy Randomized Adaptive Search Procedure (GRASP) in finding the approximate feasible solution, as illustrated in **Figure 3.4** .
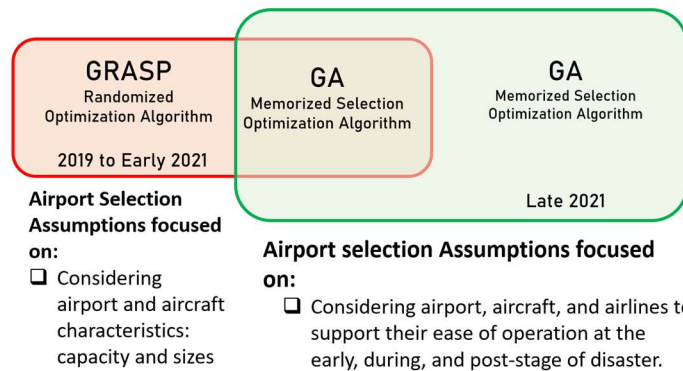


**Figure 3.4** Conceptual of the proposed model validation and comparison

### 3.4.1   Model Performance Validation and Comparison Results

The proposed model's performance had been validated according to the objective function (1) and constraints (2-7) in section 3.3.3. The same genetic algorithm parameters setting, considered the best setting from the previous study (Arreeras and Arimura, 2021), was applied to the proposed model. These settings include the following: a) initial population = 500, b) running iteration = 500, c) crossover probability = 1.0 d) mutation probability = 0.45, e) the number of affected aircraft = 261, and 42 shelter airports.

        When the new study's constraints were implemented, the model's performance was enhanced compared to the previous model from early 2021. However, as shown in Figure 3.5, the overall flight time of the proposed model is longer than the previous model, at 172.4 hours compared to 123.6 hours. All the selected shelter airports in a safe area (constraint 2) with no aircraft assigned exceeded the shelter airport available capacity limitation (constraint 3a,3b). As described in constraints 4 and 5, the new model might assign affected aircraft to appropriate airport types with enough accommodations based on their trip type.
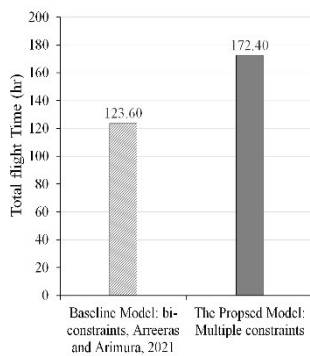
**Figure 3.5.** Total flight comparison (objective function)
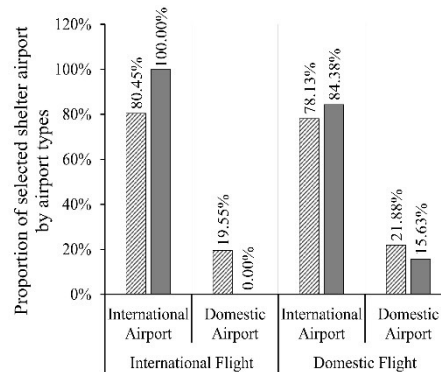
**Figure 3.6.** Selected airport by affected flight type with airport types (Constraint 4)
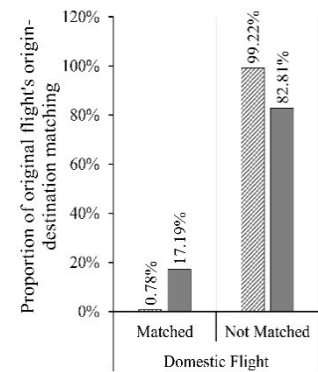
**Figure 3.7.** Selected airport by affected flight type with the original flight's route matching (constraint 7)
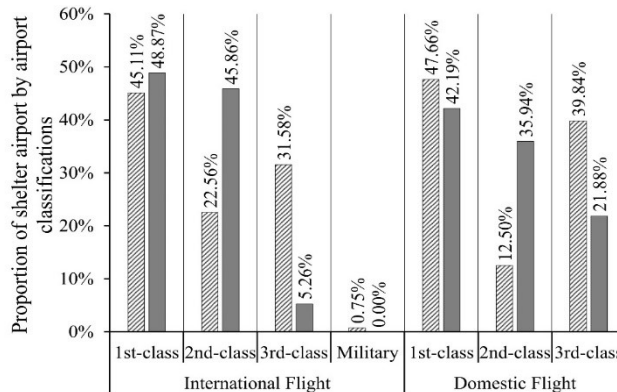


**Figure 3.8.** Selected airport by affected flight type with airport classifications (constraint 5)
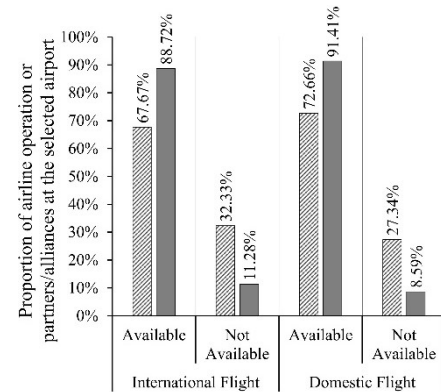
**Figure 3.9.** Selected airport by affected flight type with airline operation or partner/alliance (constraint 6)

As a result, as shown in Figure 3.6 and Figure 3.8, the model assigned a higher number of aircraft to the international airport, both first-class and second-class airports, followed by the domestic airport, third-class and military-class airports. Furthermore, over 90% of the impacted planes have been assigned to the shelter airport used by its airline or partner airlines for international and domestic flights, as illustrated in Figure 3.9. Finally, as shown in Figure 3.7, 17.19% of the affected aircraft could be returned to their original flight path airports, compared to 0.78% in the previous model.

## 3.5. CASE STUDY

This section examines the Hakone Volcano, situated near major air transport hub in the country's most busy airspace (i.e., Haneda and Narita airport international airport). Historical recodes of volcanic ashfall, wind profile, air traffic, airport location, and infrastructure were studied to identify the region, airport and aircraft impacted by its eruption.



|      (a)      |      (b)      |
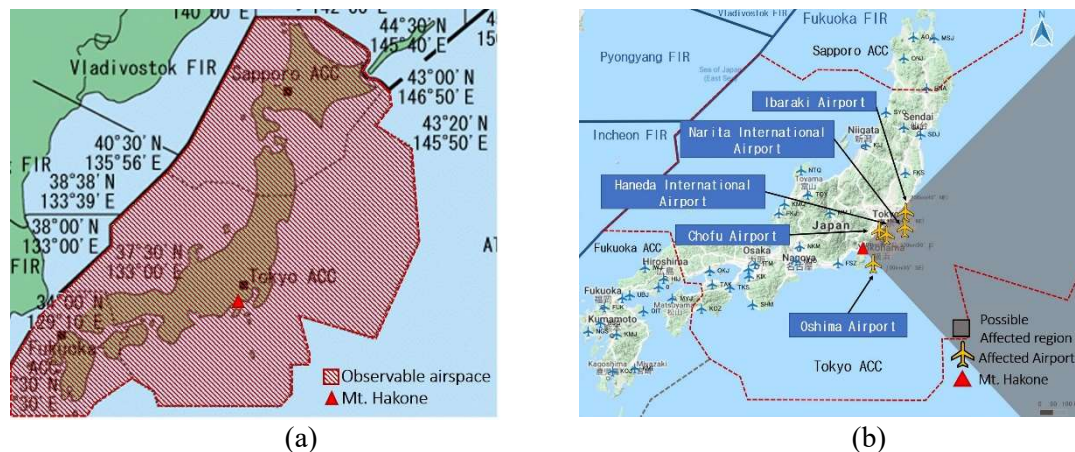
**Figure 3.10.** The CARATS flight data observable airspace (a) and Map of potential areas and airports concerned (b) refer to the previous study on shelter airport selection (Arreeras and Arimura, 2021)

### 3.5.1 The Volcano's Location and Potentially Affected Area

Observations of ashfall on Sakurajima volcano in southern Japan from 2009 to 2015 revealed the ashfall pattern during the eruption period. Typically, the height of the plume of an explosion was between 2 and 5km, with detectable ashfall occurring at distances of 70 to 100km from the vent.(JMA, 2019a). The spreading direction of the ashfall was greatly affected by seasonal winds. (Poulidis et al., 2018). At the same time as the latest CARATS flight data used in the research, wind directions to Kanto moved east, north-east and south-east to the Pacific Ocean, with varying wind speeds from 9.3 km per hour to 30 km per hour, both day and night (JMA, 2019b). The impacted region was simulated from the geolocation of the Hakone (35°14'00" N, 139°01'15" E) volcano and stretched between 45°NE and 45°SE to the north and south of the Pacific Ocean to cover the possible impacted area due to the varying of seasonal wind., as shown in **Figure 3.10**b.

### 3.5.2 The Airports and Airspace Affected

The airport geo-coordinates by the Aviation Information Services agency (AIS) of Japan (MLIT, 2019) were mapped on the ash cloud coverage area, which could identify five affected airports. Three airports that is Oshima, Chofu, and Haneda (Tokyo), were located within the minimum range of ashfall. The other two were within a 200-kilometre radius of the vent, posing a risk of ashfall within 2-7 hours and 5-16 hours, respectively, following the eruption. As illustrated in **Figure 3.10**, Japan's main domestic and international hubs were two out of the 5 airports in the simulated impacted region: Haneda (Tokyo) and Narita international airport.

### 3.5.3 The Number of Affected Aircrafts

*Ground-based aircraft*: the number of occupied aircraft stands per hour was utilized to determine the number of on-ground aircraft. Aircraft parking stands occupancy rates fall between the maximum number of arrivals and departures that each hour can handle and the cumulative number of flights. According to the data from the flight schedules published in June 2020, the week's busiest day at the affected airports is Sunday. The occupancy rate on that day ranged from 11% to 65%, depending on the airport (Central-Air, 2020; HND, 2020; IBR, 2020; NRT, 2020). Together with the aircraft size ratio from CARATS dataset mentioned in section 2.3, It was estimated that ~203 aircrafts were impacted on the ground at those five airports. See Table 3.3.

*Airborne aircraft*: The research focused only on inbound airborne aircraft to the impacted airports using Geo-coordinates, flight's time stamp, and aircraft size extracted from CARATS data mentioned in section 3.2.3. In the hour of eruption, inbound flights to the five airports impacted were 107 aircraft, which had to be transferred to safe shelter airports. The total number of aircraft seen on both ground and airborne was thus 310 aircraft. See Table 3.3.

**Table 3.3.** The simulated number of impacted aircraft from AIS and CARATS.

| Observed Location | Airport | ICAO Code | Max capacity [1] | Max Occupancy Rate | Affected aircraft | Affected aircraft by Aircraft's size ratio | | | Total |
|---|---|---|---|---|---|---|---|---|---|
| | | | | | | 29.6% | 63.4% | 7.0% | |
| | | | | | | L | M | S | |
| On-ground: at affected airports (AIS) | Oshima | RJTO | 9 | 11% | 1 | 0 | 1 | 0 | |
| | Chofu | RJTF | 24 | 17% | 4 | 1 | 3 | 0 | |
| | Haneda | RJTT | 228 | 63% | 143 | 42 | 91 | 10 | **203** |
| | Ibaraki | RJAH | 8 | 38% | 3 | 1 | 2 | 0 | |
| | Narita | RJAA | 266 | 20% | 52 | 16 | 33 | 3 | |
| Airborne (CARATS) | | | | Inbound[1] to the impacted airports | | 32 | 73 | 2 | **107** |
| | | | | | **Grand Total** | **92** | **203** | **15** | **310** |

[1]Civil Aircraft: private and commercial aircraft

### 3.5.4 The Sheltering Airports and Available Capacity

The shelter airport selection criteria were based on the assumptions of airport selection for the model construct, which included a) location of the shelter airport candidates, b) sufficient available stands by aircraft sizes, c) airport type, d) airport classification, and e) airline operation and partners at the shelter airport, mentioned in section 3.3.1.

This study chose 60 airports in Japan as shelter airport candidates, increasing from the previous research's 42 shelter airports. The 18 extra airports coincided with the original flight itineraries (origin and destination airports) of the observed aircraft, allowing afflicted aircraft to return to their original airports. The available capacity was calculated by averaging the maximum cumulative occupied stands' rate ($OC_j$) of arriving and departing aircraft at the five impacted airports on Sunday; according to the quarterly flight schedule, the week's busiest day began in June 2020. As shown in Table 3.4 and Table A3-1, 30% of aircraft parking spaces were occupied on average on the busiest day. As a result, non-occupancy parking stands accounted for 70% of each airport's capacity, which could be used to accommodate aircraft in the event of an emergency evacuation. As a result, out of a total capacity of 1,528, 1,070 stands were available (combined all sizes of aircraft). See Table 3.5 for more information.

**Table 3.4.** Details of occupancy rate at five affected airports, and an assumption for shelter airport

| Airport Name | Oshima | Chofu | Haneda | Ibaraki | Narita | Avg. Occupied stand and ratio |
|---|---|---|---|---|---|---|
| Airport Capacity | 9 | 24 | 228 | 8 | 266 | |
| Minimum Occupied stands per hr.[2] | 0 | 0 | 2 | 0 | 2 | 1 |
| % Min Occupancy rate per capacity | 0% | 0% | 1% | 0% | 1% | 0% |
| Maximum Occupied stands per hr.[2] | 1 | 4 | 143 | 3 | 52 | 41 |
| % Max Occupancy rate per cap | 11% | 17% | 63% | 38% | 20% | **30%** |
| An assumption of 60 shelter airport non-occupancy rate equal to the average of 5 affected airports, that was 1 - (% average Occupancies rate): (1-0.30) | | | | | | **70%** |

[2]Cumulative flight number per hour between arrival and departure of aircraft.

## 3.6.    COMPUTATIONAL RESULTS

This section discusses the performance of the proposed model concerning the study's objective and constraints. The model ran on the selected GA setting parameters, i.e., crossover and mutation probability from section 3.4.1, which were 1.0, and 0.45. In addition, the sensitivity analysis has also been used to study how changing airspace and airport congestion, represented in the airport occupancy rate ($OC_j$), will impact the model's aircraft assignment pattern and overall results. The proposed model and genetic algorithms were coded in Python 4.1.5 and tested on a personal computer with an Intel® Core™ i7-8700 CPU (3.20GHz.) and 32.0 GB of RAM.
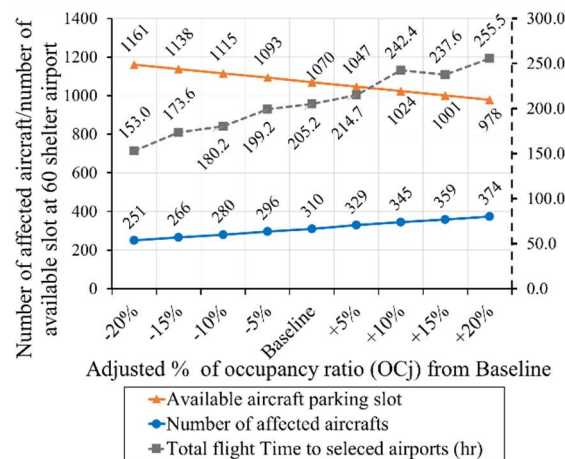


**Figure 3.11.** Sensitivity study's results on the total travel duration of impacted aircrafts to designated airports
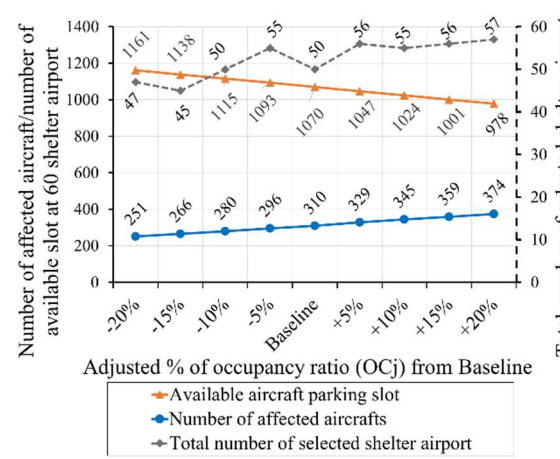
**Figure 3.12.** Sensitivity study's results on the total number of selected airports for imapacted aircraft accommodation

### 3.6.1    Result of the Proposed Model

As a result of the proposed model, 50 shelter airports were chosen to accommodate aircraft for evacuation with a total flight time of 205.2 hours for baseline, as shown in Figure 3.11 and Figure 3.12. The evacuation time for each aircraft ranged from 0.2 to 2.2 hours, with an average of 0.7

hours. The distribution of aircraft to all shelter airports varied from 0.3% to 17.1%, with an average 2.2% of all aircraft being impacted.

The selected shelter airports' maximum capacity is used between 2.2% and 100%, with an average of 36.8% of accessible stands (non-occupancy stands). Consequently, no shelter airport experienced an excess of impacted aircraft. During the model validation stage, the model consistently provided consistent selections based on the constraints. The result also addressed 2 key airports, which handle 30.1% of overall affected aircraft: Chubu Centrair International Airport (RJGG) and Kansai International Airport (RJBB) at handling rate 17.1% and 13.5% of total impacted aircraft, respectively. Other shelter airport would handle around 2.3% to 0.3% of their available aircraft parking stand. Comparing to the previous model in early of 2021, the new proposed model still gave a similar result in term of the critical shelter airports selecting pattern by the models, as illustrated in **Figure 3.13**. See details of impacted aircraft assignment to each shelter airports under various occupied aircraft parking stand rate in Table A 3-3 and Table A 3-4.
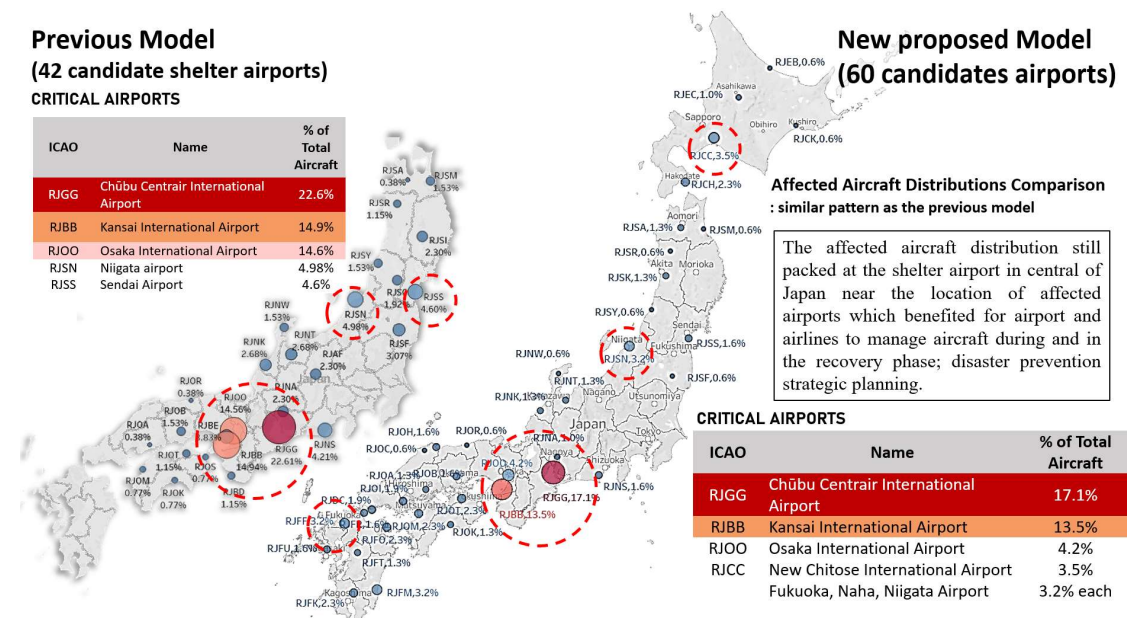


**Figure 3.13** Overview of affected aircraft distribution and selected shelter airports patterns, compared between the previous model in early of 2021 and a new proposed model in this study.

## 3.6.2  Air Traffic Congestion Sensitivity Analysis

In a sensitivity study on air traffic congestion, the occupancy rate ($OC_j$) was utilized to measure airport and airspace congestion levels. This rate might also be used to calculate the number of on-ground and airborne aircraft ($I$) and the available capacity or free stand ($NC_j$) at the impacted and shelter airport candidates. Increased occupancy rate ($OC_j$) indicates that air traffic congestion is increasing, leading to an increasing number of aircraft impacted and a drop in the number of free stands ($NC_j$) or available stands. On the other hand, the falling occupancy rate can be interpreted as a reduction in air traffic congestion, as indicated in Table 3.5 and Figure 3.11, reflected in the lower number of impacted aircraft and increased free stands. Details of changing of occupancy rate reflected on number of impacted aircraft shown in Table A3-2.

**Table 3.5.** Occupancy stands and free (non-occupancy) stands scenarios of 60 shelter airports.

| Scenario's occupancy stands ($OC_j$) | | Baseline[3] | -20% | -15% | -10% | -5% | 5% | 10% | 15% | 20% |
|---|---|---|---|---|---|---|---|---|---|---|
| All available stand of 60 shelter airports | | 1,528 | | | | | | | | |
| Parking occupancy rate (avg.)[4] | | 30% | 24.0% | 25.5% | 27.0% | 28.5% | 31.5% | 33.0% | 34.5% | 36.0% |
| The non-occupancy standing rate: $OC_j$ (avg.) | | 70% | 76% | 75% | 73% | 72% | 69% | 67% | 66% | 64% |
| Capacity by stands sizes | Medium/ Large | 543 | 589 | 562 | 557 | 546 | 523 | 515 | 511 | 495 |
| | small | 532 | 581 | 558 | 550 | 543 | 518 | 509 | 502 | 487 |
| **Average available capacity ($NC_j$)** | | **1,070** | **1,161** | **1,138** | **1,115** | **1,093** | **1,047** | **1,024** | **1,001** | **978** |

[3] The maximum cumulative occupied stand of five airports impacted; refer to Table 3.4.
[4] The max. number of stands at the five impacted airports at 30% on average.

Regarding the proposed adjustments to the airport parking utilization, the sensitivity analysis showed an increase in the occupancy rate ($OC_j$) by +20% from 30% to 36%, led to a reduction in the total number of free stands ($NC_j$) from 1,070 to 978 stands, or from 70% to 64%. Additionally, when the $OC_j$ rate rose, airspace and airport congestion increased, bringing the total number of impacted aircraft to 374 from 310 (baseline in Table 3.3), as illustrated in **Figure 3.11**. Thus, the system was compelled to choose new airports to handle the increasing number of aircraft. As a result, the entire flight duration has risen from 205.2 hours to 255.5 hours, which means the objective function value has changed. Consequently, the number of designated emergency airports for aircraft in distress was expanded from 50 to 57 to serve 374 impacted aircraft, as illustrated in Figure 3.12. On the other hand, reducing the stand occupied's rate by -20% of the baseline increased the number of free stands from 1,070 to 1,161 stands, or from 70% to 76%, respectively. Thus, it was reflecting in reduced affected aircraft 251 from baseline. Consequently, it reduced the number of designated airports from 50 to 47 and dropped total travel duration from baseline to 153.0 hr., as each airport shelter near the impacted aircraft increased with many free stands.
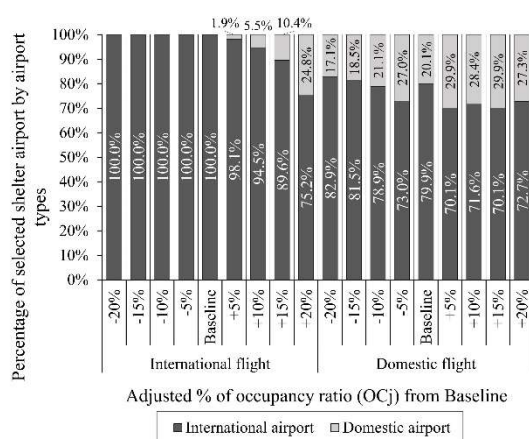


**Figure 3.14.** The proportion of selected airport by criteria: impacted aircraft's flight type and airport types
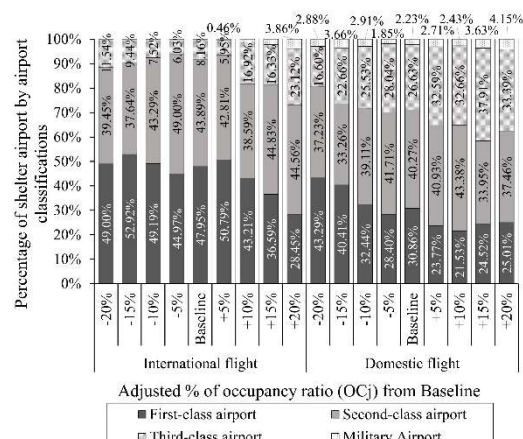


**Figure 3.15.** The proportion of selected airport by criteria: impacted aircraft's flight type and airport Classifications

According to constraint (4), 100% of international flight aircraft and 80% of domestic flight aircraft are assigned to international type airports. However, when the occupancy rate rose from

baseline to +20%, there was a reduction in aircraft stand at each airport shelter. Consequently, the airport's international terminal could not handle the same volume of aircraft as previously. Thus, the system compelled some international flight aircraft (1-5.9%) to use domestic-type airports. This phenomenon occurred as well in domestic aircraft. As a result, domestic airports handled slightly more aircraft as the occupancy rate (level of air traffic congestion) increased from the baseline. Refer to Figure 3.14.

According to constraint (5), Figure 3.15 recommended that affected aircraft be assigned to the most fully equipped and large capacity airport first, followed by the smaller one. As a result, a greater proportion of international aircraft was assigned to first- and second-class airports (34.5–49.4% and 40.9–49.4%, respectively), while the remainder were assigned to third- and fourth-class airports (1.3–16.7%). The military-class airport was not chosen because the model advised against it due to security and civilian accommodation facility readiness concerns. As a result, a sizable portion of the third-available class's capacity remained unutilized.

As the occupancy rate and the number of affected aircraft grew, the system was forced to utilize available stands at third-class airports rather than first-class airports to avoid military airports. Since the first-class airport is primarily an international airport, priority was given to international flight aircraft. Domestic flight aircraft were assigned to second-class airports, followed by first-class and third-class airports in slightly varying proportions of 34-42%, 21-43%, and 16.6-37.9%, respectively, and less than 5% to military-class airports. As with the international flight aircraft, the system was compelled to utilize other underutilized available stands, resulting in an increased occupancy rate, and decreased available stands.

Constraint 6 indicates that the system routed affected aircraft to a shelter airport served by its airline or a partner airline. As shown in Figure 3.16, the model assigned aircraft to those airports at an 80% rate. While the occupancy rate decreased to -20% of baseline, the proportion of appropriately selected airports increased slightly to 90.8%, due to increased parking availability at first- and second-class airports served by most airlines. By contrast, as the occupancy rate increased to 20%, the proportion of adequately selected airports decreased slightly to 70.3%, as available stands at the primary selected airport decreased. As a result, the system is forced to assign overcapacity aircraft to small airports (third and military-class airports) that lack available stands and do not operate by all assigned aircraft's airlines.

In constraint 7, the system may randomly assign the afflicted aircraft to the airport serving their original flight route, either origin or destination, at a rate of 1.9-7.%. Genetic algorithms are a metaheuristic algorithm that uses random variables and evolutionary processes to find a feasible solution to an optimization problem. However, the exact-known solution such as this may need a large number of rounds to acquire. As a result, when applied to GA, the proposed model can rarely find a solution to constraint 7 within the study's 500 iterations. Consider Figure 3.17.

**Table 3.6.** One-way Analysis of Variance (ANOVA) by stand occupancy rate scenarios.

| Source of Variation | SS | df | MS | F | P-value | F crit |
|---|---|---|---|---|---|---|
| Between Groups | 1646.201 | 8 | 205.775 | 1.032 | 0.409 | 1.941 |
| Within Groups | 558512.199 | 2801 | 199.397 | | | |
| Total | 560158.400 | 2809 | | | | |
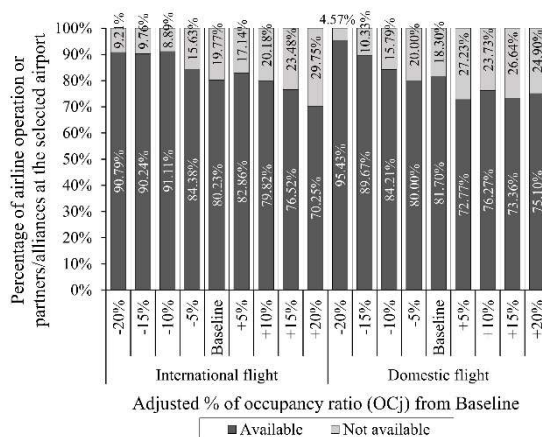
**Figure 3.16.** The proportion of selected airport by criteria: affected aircraft's flight type and airline operation or partner/alliance at the selected airport.
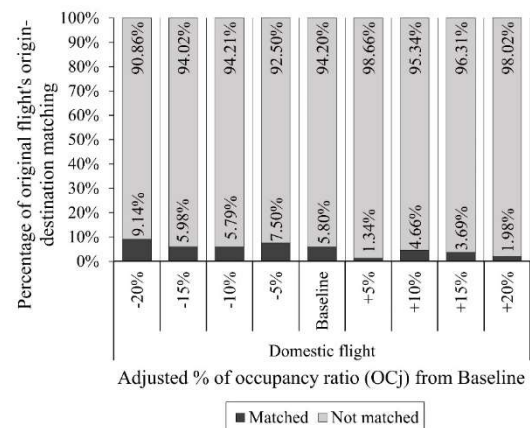
**Figure 3.17.** The proportion of selected airport by criteria: affected aircraft's flight type and original flight's origin-destination matching.

Sensitivity analysis revealed that the proposed model might allocate the aircraft to an appropriate shelter airport according to the research goal and restrictions. A one-way ANOVA was used to assess the difference in the number of aircraft attributed to each shelter airport between nine occupancy rate adjustments. As demonstrated in **Table 3.6** by F=1.032 F crit=1.941, P=0.409 > 0.05, occupancy modifications of 20% from baseline had no significant effect on the shelter airport selection or the number of aircraft assignments. Additionally, it was believed that even in the worst-case scenario of a +20% occupancy rate or a 20% increase in aviation traffic congestion above baseline, the shelter airports would still have adequate space for aircraft evacuation.

## 3.7. CONCLUSION

- The additional airline's constraints enabled the model the find the appropriate shelter airport for airline's flight operations during and after disaster, compared to the previous model.
- The increasing number of selection constraints could create higher number of unsuitable airport, which rise value of objective function from further away airport selection.
- At the worst case of congestion level risen by +20%, available shelter airport still be able to handle the increasing of affected aircraft with no different of pattern of shelter airports selected by affected aircraft.

**Discussion and further study:**

❑ Airport available capacity played a vital role in aircraft evacuation. The airport capacity extension and utilization in an emergency without further facility investment could help on airport and airline operations during disaster.

❑ Scenario analysis on wind directions over time should also being studied, since wind direction can by varied even in the same time period.

The purpose of this work was to present a conceptual model that could be used in conjunction with genetic algorithms (GA) to select a shelter airport during a volcanic eruption to reduce the overall flight time of affected aircraft to the designated shelter airport. Additionally, the study

examined airport and airline criteria to determine the best shelter airport. These additional criteria may aid in selecting an appropriate shelter airport, the improvement of airport and airline performance during the crisis, and the recovery of aircraft flight schedules following the disaster. Additionally, the sensitivity analysis of the aircraft stands occupancy rate, which represented airspace and airport congestion, may result in more practical and realistic recommendations for airport selection and aircraft assignment under various airport and airspace congestion scenarios.

Compared to the previous model studied in early 2021, the new proposed shelter airport selection model performed better across all constraints. In addition, it highlighted and enhanced that the new model could assist airports and airlines in better managing and planning for aircraft evacuations in the face of additional airport and airline constraints. However, both models had given the similarity on the affected aircraft distribution and the shelter airports selection patterns, which enhance the focusing on the particular airport as the critical airports when disaster occur in the similar manner as this study. As noted at the outset of this study, this could lead to a more efficient and cost-effective airport emergency plan at the early, during, and post-natural disaster stages.

However, an increase in the number of shelter airport selection constraints may impact aircraft travel distance and flight time because there are fewer acceptable shelter airports for affected aircraft near its current position. As a result, the longer the computational length and the further away which rises the objective function may be unavoidable.

Furthermore, in the sensitivity analysis, the airport's congestion level and aircraft parking occupancy increased by 20%, resulting in an increase in affected aircraft and a decrease in aircraft handling capacity at the shelter airports. The study, on the other hand, found no difference in the shelter airport selection pattern. Therefore, according to the historical flight schedule and airport data used in this study, the available shelter airports can handle affected airports up to 20% more than the baseline situation.

Although the proposed model, which is based on a broader perspective of airline operations, may provide helpful guidance to all level (local, national, international) of aviation emergency planners and decision-makers, such as International Civil Aviation Organization (ICAO), Civil Aviation Bureau, Ministry of Land, Infrastructure, Transport and Tourism (MLIT) of Japan, airports, airlines, etc. However, the legislation and the operating procedures of airports, airlines and air traffic management make it susceptible to limitations due to the intricacy of the regulation. Furthermore, the growing number of airport selection criteria may complicate and extend the time needed to find adequate answers for algorithms. Therefore, emergency planners and decision-makers must exercise extreme caution in selecting associated factors and constraint coefficient values that accurately reflect the reality, practical operation, and objective of all parties involved. Additional research could be conducted on airline and airport operating chains from the start of the evacuation to the point of recovery, examining all segments of aircraft, passengers, cargo, and flight crew schedules.

## LIMITATIONS AND DISCUSSION

The study's primary limitations were the absence of data on the aircraft's itineraries in the CARATS dataset, historical data on the area covered by volcanic ash clouds, and the range of the Hakone volcano. Additionally, this study's air traffic and flight data may be lower than typical levels due to decreased air quality in this region and internationally due to the COVID 19 epidemic. However, the number of affected aircraft can be determined and changed using secondary data derived from the most recent historical air traffic data and the airports' published

flight schedules to represent the current air traffic situation. In addition, other volcanic historical data could be used to understand better ash cloud behavior, including the changing for wind speed and direction in each season in scenario analysis in the future study.

## ACKNOWLEDGMENTS

## REFERENCES

Airbus, 2005. Airbus A320 Aircraft Characteristics, Airport and Maintenance Planning. Airbus S.A.S. 1–387.

Akgün, I., Gümüşbuğa, F., Tansel, B., 2015. Risk based facility location by using fault tree analysis in disaster management. Omega 52, 168–179. https://doi.org/10.1016/J.OMEGA.2014.04.003

Andersson, T., 2006. Solving the flight perturbation problem with meta heuristics. J. Heuristics 12, 37–53. https://doi.org/10.1007/s10732-006-4833-4

Arreeras, S., Arimura, M., 2021. A Study on Shelter Airport Selection during Large-scale Volcanic Disasters using CARATS Open Dataset. Transp. Res. Part C Emerg. Technol. 129, 103263. https://doi.org/10.1016/j.trc.2021.103263

Blum, C., Roli, A., 2003. Metaheuristics in combinatorial optimization: Overview and Conceptual Comparison. ACM Comput. Surv. 35, 268–308. https://doi.org/10.1145/937503.937505

Central-Air, 2020. 新中央航空株式会社 Time Table [WWW Document]. URL https://www.central-air.co.jp/en/timetable.html (accessed 2.13.20).

Coppola, D.P., 2015. Introduction to International Disaster Management: Third Edition. Introd. to Int. Disaster Manag. Third Ed. 1–733.

De Rainville, F.-M., Fortin, F.-A., Gardner, M.-A., Parizeau, M., Gagné, C., 2012. DEAP, in: Proceedings of the Fourteenth International Conference on Genetic and Evolutionary Computation Conference Companion - GECCO Companion '12. ACM Press, New York, New York, USA, p. 85. https://doi.org/10.1145/2330784.2330799

Deb, K., 2000. An efficient constraint handling method for genetic algorithms. Comput. Methods Appl. Mech. Eng. 186, 311–338. https://doi.org/10.1016/S0045-7825(99)00389-8

Gade, K., 2010. A non-singular horizontal position representation. J. Navig. 63, 395–417. https://doi.org/10.1017/S0373463309990415

Goldberg, D.E., Holland, J.H., 1988. Genetic Algorithms and Machine Learning. Mach. Learn. https://doi.org/10.1023/A:1022602019183

HND, 2020. Tokyo Haneda International Airport (HND/RJTT) | Arrivals, Departures & Routes | Flightradar24 [WWW Document]. URL https://www.flightradar24.com/data/airports/hnd (accessed 2.13.20).

Homaifar, A., Qi, C.X., Lai, S.H., 1994. Constrained optimization via genetic algorithms. Simulation. https://doi.org/10.1177/003754979406200405

Horner, M.W., Downs, J.A., 2010. Optimizing hurricane disaster relief goods distribution: Model development and application with respect to planning strategies. Disasters. https://doi.org/10.1111/j.1467-7717.2010.01171.x

Hu, F., Yang, S., Xu, W., 2014. A non-dominated sorting genetic algorithm for the location and districting planning of earthquake shelters. Int. J. Geogr. Inf. Sci. https://doi.org/10.1080/13658816.2014.894638

IATA, 2018. the Annual Review 2018. IATA J. 68.

IBR, 2020. Flight information | Ibaraki Airport [WWW Document]. URL http://www.ibaraki-airport.net/en/flight.html (accessed 2.12.20).

ICAO, 2018. Annex 3 Meteorological service for international air navigation. to the Convention on International Civil Aviation.

ICAO, 2016. Annex 14: Aerodrome Design and Operations Seventh Edition, International Civil Aviation Organization.

ICAO, 2013. ICAO Environmental Report 2013. ICAO Environ. Rep. 2013.

ICAO, 2012. Flight Safety and Volcanic Ash. Flight Saf. Volcan. Ash 1–46.

ICAO, 2007. International Civil Aviation Organization Manual on Volcanic Ash, Radioactive Material and Toxic Chemical Clouds.

ICAO, 1991. ICAO doc 9137 Airport Sevices Manual - Part 7.

JMA, 2019a. Sakurajima Continuously Monitored [WWW Document]. Janpan Meteorol. Agency. URL https://www.data.jma.go.jp/svd/vois/data/tokyo/STOCK/souran_eng/volcanoes/090_sak urajima.pdf (accessed 8.26.19).

JMA, 2019b. Climat of Kanto/Koshin district [WWW Document]. Janpan Meteorol. Agency. URL https://www.data.jma.go.jp/gmd/cpd/longfcst/en/tourist/file/Kanto_Koshin.html (accessed 9.15.19).

Kongsomsaksakul, S., Yang, C., Chen, A., 2005. Shelter location-allocation model for flood evacuation planning. J. East. Asia Soc. Transp. Stud.

Krukhmalev, V., Pshikhopov, V., 2017. Genetic Algorithms Path Planning, in: Path Planning for Vehicles Operating in Uncertain 2D Environments. Elsevier, pp. 137–184. https://doi.org/10.1016/B978-0-12-812305-8.00004-1

Langmann, B., Folch, A., Hensch, M., Matthias, V., 2012. Volcanic ash over Europe during the eruption of Eyjafjallajökull on Iceland, April-May 2010. Atmos. Environ. 48, 1–8. https://doi.org/10.1016/j.atmosenv.2011.03.054

Lin, Y.H., Batta, R., Rogerson, P.A., Blatt, A., Flanigan, M., 2012. Location of temporary depots to facilitate relief operations after an earthquake. Socioecon. Plann. Sci. 46, 112–123. https://doi.org/10.1016/j.seps.2012.01.001

Lordan, O., Klophaus, R., 2017. Measuring the vulnerability of global airline alliances to member exits. Transp. Res. Procedia 25, 7–16. https://doi.org/10.1016/j.trpro.2017.05.189

Lordan, O., Sallan, J.M., Simo, P., Gonzalez-Prieto, D., 2015. Robustness of airline alliance route networks. Commun. Nonlinear Sci. Numer. Simul. 22, 587–595. https://doi.org/10.1016/j.cnsns.2014.07.019

Løve, M., Sørensen, K., Larsen, J., Clausen, J., 2001. Using heuristics to solve the dedicated aircraft recovery problem, Optimization Online.

Madas, M.A., Zografos, K.G., 2010. Airport slot allocation: A time for change? Transp. Policy 17, 274–285. https://doi.org/10.1016/j.tranpol.2010.02.002

Maier, H.R., Razavi, S., Kapelan, Z., Matott, L.S., Kasprzyk, J., Tolson, B.A., 2019. Introductory overview: Optimization using evolutionary algorithms and other metaheuristics. Environ. Model. Softw. 114, 195–213. https://doi.org/10.1016/j.envsoft.2018.11.018

Michalewicz, Z., 1996. Evolutionary algorithms for constrained parameter optimization problems. Evol. Comput. https://doi.org/10.1162/evco.1996.4.1.1

MLIT, 2019. AIRAC Airports Information [WWW Document]. Japan Aeronaut. Inf. Serv. Cent. URL https://aisjapan.mlit.go.jp/InfoDispAction.do (accessed 6.6.19).

MLIT, 2018. Collaborative Actions for Renovation of Air Traffic Systems (CARATS) [WWW Document]. Minist. land, Infrastruct. Transp. URL http://www.mlit.go.jp/common/001046514.pdf (accessed 6.1.19).

Mota, M.M., Boosten, G., De Bock, N., Jimenez, E., de Sousa, J.P., 2017. Simulation-based turnaround evaluation for Lelystad Airport. J. Air Transp. Manag. 64, 21–32. https://doi.org/10.1016/j.jairtraman.2017.06.021

NRT, 2020. Flight Information | NARITA INTERNATIONAL AIRPORT OFFICIAL WEBSITE [WWW Document]. URL https://www.narita-airport.jp/en/flight/today#section-1 (accessed 2.12.20).

Picquout, A., Lavigne, F., Mei, E.T.W., Grancher, D., Noer, C., Vidal, C.M., Hadmoko, D.S., 2013. Air traffic disturbance due to the 2010 Merapi volcano eruption. J. Volcanol. Geotherm. Res. 261, 366–375. https://doi.org/10.1016/j.jvolgeores.2013.04.005

Poulidis, A.P., Takemi, T., Shimizu, A., Iguchi, M., Jenkins, S.F., 2018. Statistical analysis of dispersal and deposition patterns of volcanic emissions from Mt. Sakurajima, Japan. Atmos. Environ. 179, 305–320. https://doi.org/10.1016/j.atmosenv.2018.02.021

Sinnott, R.W., 1984. Virtues of the Haversine. Sky Telescope 68, 159.

Smith, A.E., Coit, D.W., 2004. Penalty functions, in: Handbook of Evolutionary Computation. https://doi.org/10.1887/0750308958/b386c48

Teodorović, D., Guberinić, S., 1984. Optimal dispatching strategy on an airline network after a schedule perturbation. Eur. J. Oper. Res. 15, 178–182. https://doi.org/10.1016/0377-2217(84)90207-8

Toregas, C., Swain, R., ReVelle, C., Bergman, L., 1971. The Location of Emergency Service Facilities. Oper. Res. https://doi.org/10.1287/opre.19.6.1363

Voltes-Dorta, A., Rodríguez-Déniz, H., Suau-Sanchez, P., 2017. Vulnerability of the European air transport network to major airport closures from the perspective of passenger delays: Ranking the most critical airports. Transp. Res. Part A Policy Pract. 96, 119–145. https://doi.org/10.1016/j.tra.2016.12.009

# APPENDIX A

**Table A3-1** Arrival and departure flight per hour at 5 affected airports, parking slot occupancy ratio, and an assumption of shelter airport available capacities

| Hour_Periods Start | End | Oshima Arr | Oshima Dep | Oshima Cum | Oshima Tot | Chofu Arr | Chofu Dep | Chofu Cum | Chofu Tot | Haneda Arr | Haneda Dep | Haneda Cum | Haneda Tot | Ibaraki Arr | Ibaraki Dep | Ibaraki Cum | Ibaraki Tot | Narita Arr | Narita Dep | Narita Cum | Narita Tot | Average Cumulative Flight |
|---|---|---|---|---|---|---|---|---|---|---|---|---|---|---|---|---|---|---|---|---|---|---|
| 12:00:00 AM | 12:59:00 AM | 0 | 0 | 1 | 0 | 0 | 0 | 4 | 0 | 0 | 0 | 132 | 0 | 0 | 0 | 2 | 0 | 0 | 0 | 2 | 0 | 28 |
| 1:00:00 AM | 1:59:00 AM | 0 | 1 | 0 | 1 | 0 | 1 | 3 | 1 | 0 | 3 | 129 | 3 | 0 | 0 | 2 | 0 | 0 | 0 | 2 | 0 | 27 |
| 2:00:00 AM | 2:59:00 AM | 0 | 0 | 0 | 0 | 0 | 0 | 3 | 0 | 2 | 0 | 131 | 2 | 0 | 0 | 2 | 0 | 0 | 0 | 2 | 0 | 28 |
| 3:00:00 AM | 3:59:00 AM | 0 | 0 | 0 | 0 | 0 | 0 | 3 | 0 | 2 | 0 | 133 | 2 | 0 | 0 | 2 | 0 | 0 | 0 | 2 | 0 | 28 |
| 4:00:00 AM | 4:59:00 AM | 0 | 0 | 0 | 0 | 0 | 0 | 3 | 0 | 3 | 0 | 136 | 3 | 0 | 0 | 2 | 0 | 0 | 0 | 2 | 0 | 29 |
| 5:00:00 AM | 5:59:00 AM | 0 | 0 | 0 | 0 | 0 | 0 | 3 | 0 | 7 | 0 | 143 | 7 | 0 | 0 | 2 | 0 | 0 | 0 | 2 | 0 | 30 |
| 6:00:00 AM | 6:59:00 AM | 0 | 0 | 0 | 0 | 0 | 0 | 3 | 0 | 7 | 37 | 113 | 44 | 0 | 0 | 2 | 0 | 8 | 0 | 10 | 8 | 26 |
| 7:00:00 AM | 7:59:00 AM | 0 | 0 | 0 | 0 | 0 | 0 | 3 | 0 | 8 | 68 | 53 | 76 | 0 | 1 | 1 | 1 | 11 | 4 | 17 | 15 | 15 |
| 8:00:00 AM | 8:59:00 AM | 0 | 0 | 0 | 0 | 0 | 0 | 3 | 0 | 45 | 51 | 47 | 96 | 0 | 1 | 0 | 1 | 14 | 4 | 27 | 18 | 15 |
| 9:00:00 AM | 9:59:00 AM | 0 | 0 | 0 | 0 | 0 | 0 | 3 | 0 | 42 | 48 | 41 | 90 | 2 | 0 | 2 | 2 | 19 | 17 | 29 | 36 | 15 |
| 10:00:00 AM | 10:59:00 AM | 0 | 0 | 0 | 0 | 0 | 2 | 1 | 2 | 45 | 40 | 46 | 85 | 2 | 1 | 3 | 3 | 12 | 23 | 18 | 35 | 14 |
| 11:00:00 AM | 11:59:00 AM | 0 | 0 | 0 | 0 | 0 | 1 | 0 | 1 | 48 | 54 | 40 | 102 | 0 | 1 | 2 | 1 | 13 | 20 | 11 | 33 | 11 |
| 12:00:00 PM | 12:59:00 PM | 0 | 0 | 0 | 0 | 3 | 0 | 3 | 3 | 35 | 55 | 20 | 90 | 1 | 0 | 3 | 1 | 10 | 13 | 8 | 23 | 7 |
| 1:00:00 PM | 1:59:00 PM | 0 | 0 | 0 | 0 | 0 | 2 | 1 | 2 | 56 | 57 | 19 | 113 | 1 | 3 | 1 | 4 | 13 | 14 | 7 | 27 | 6 |
| 2:00:00 PM | 2:59:00 PM | 0 | 0 | 0 | 0 | 0 | 0 | 1 | 0 | 41 | 45 | 15 | 86 | 0 | 0 | 1 | 0 | 19 | 12 | 14 | 31 | 6 |
| 3:00:00 PM | 3:59:00 PM | 1 | 0 | 1 | 1 | 3 | 0 | 4 | 3 | 41 | 38 | 18 | 79 | 0 | 1 | 0 | 1 | 31 | 5 | 40 | 36 | 13 |
| 4:00:00 PM | 4:59:00 PM | 0 | 0 | 1 | 0 | 0 | 0 | 4 | 0 | 37 | 34 | 21 | 71 | 0 | 0 | 0 | 0 | 24 | 12 | 52 | 36 | 16 |
| 5:00:00 PM | 5:59:00 PM | 0 | 0 | 1 | 0 | 0 | 0 | 4 | 0 | 39 | 50 | 10 | 89 | 1 | 0 | 1 | 1 | 19 | 37 | 34 | 56 | 10 |
| 6:00:00 PM | 6:59:00 PM | 0 | 0 | 1 | 0 | 0 | 0 | 4 | 0 | 45 | 45 | 10 | 90 | 0 | 1 | 0 | 1 | 12 | 25 | 21 | 37 | 7 |
| 7:00:00 PM | 7:59:00 PM | 0 | 0 | 1 | 0 | 0 | 0 | 4 | 0 | 42 | 50 | 2 | 92 | 1 | 1 | 0 | 2 | 14 | 7 | 28 | 21 | 7 |
| 8:00:00 PM | 8:59:00 PM | 0 | 0 | 1 | 0 | 0 | 0 | 4 | 0 | 53 | 28 | 27 | 81 | 2 | 0 | 2 | 2 | 7 | 9 | 26 | 16 | 12 |
| 9:00:00 PM | 9:59:00 PM | 0 | 0 | 1 | 0 | 0 | 0 | 4 | 0 | 63 | 12 | 78 | 75 | 0 | 0 | 2 | 0 | 5 | 15 | 16 | 20 | 20 |
| 10:00:00 PM | 10:59:00 PM | 0 | 0 | 1 | 0 | 0 | 0 | 4 | 0 | 37 | 4 | 111 | 41 | 0 | 0 | 2 | 0 | 1 | 11 | 6 | 12 | 25 |
| 11:00:00 PM | 11:59:00 PM | 0 | 0 | 1 | 0 | 0 | 0 | 4 | 0 | 7 | 1 | 117 | 8 | 0 | 0 | 2 | 0 | 0 | 2 | 4 | 2 | 26 |
| Max_Capacity | | 9 | | | | 24 | | | | 228 | | | | 8 | | | | 266 | | | | % Avg Occupancy |
| Min_Occupancy | | 0 | 0 | 0 | 0 | 0 | 0 | 0 | 0 | 35 | 28 | 2 | 71 | 0 | 0 | 0 | 0 | 7 | 5 | 7 | 16 | 2 |
| % Min_Occupancy per cap | | 0% | 0% | 0% | 0% | 0% | 0% | 0% | 0% | 15% | 12% | 1% | 31% | 0% | 0% | 0% | 0% | 3% | 2% | 3% | 6% | 1% |
| **Max_Occupancy** | | 1 | 0 | 1 | 1 | 3 | 2 | 4 | 3 | 56 | 57 | 46 | 113 | 2 | 3 | 3 | 4 | 31 | 37 | 52 | 56 | 41 |
| **% Max_Occupancy per** | | 11% | 0% | 11% | 11% | 13% | 8% | 17% | 13% | 25% | 25% | 20% | 50% | 25% | 38% | 38% | 50% | 12% | 14% | 20% | 21% | 30% |
| ***an assumption of 42 shelter airport available capacities, calculated from average(%Max_Occupancy) of 5 affected airports: (1-0.21) | | | | | | | | | | | | | | | | | | | | | | 70% |

**Table A3-2** Detail of affected aircraft, occupancy, and availability ratio at the study airports with various simulated ratio for the proposed models' configurations.

| Occupancy aircraft stand, Decrement/Increment rate at ±5% | | | -20% | | -15% | | -10% | | -5% | | Baseline * | | 5% | | 10% | | 15% | | 20% | |
|---|---|---|---|---|---|---|---|---|---|---|---|---|---|---|---|---|---|---|---|---|---|
| Airborne aircraft | Observable affected aircraft (CARATS dataset) | Number of affected aircraft | 86 | | 91 | | 96 | | 102 | | 107 | | 112 | | 118 | | 123 | | 128 | |
| On-ground aircraft at 5 affected airports | Affected Airports | Affected Airport Capacity | Max stand occupancy rate (baseline -20%) | Number of affected aircraft (baseline -20%) | Max stand occupancy rate (baseline -15%) | Number of affected aircraft (baseline-15%) | Max stand occupancy rate (baseline -10%) | Number of affected aircraft (baseline -10%) | Max stand occupancy rate (baseline -5%) | Number of affected aircraft (baseline -5%) | Max stand occupancy rate * (baseline) | Numbr of affected aircraft | Max stand occupancy rate (baseline +5%) | Number of affected aircraft (baseline +5%) | Max stand occupancy rate (baseline +10%) | Number of affected aircraft (baseline +10%) | Max stand occupancy rate (baseline +15%) | Number of affected aircraft (baseline +15%) | Max stand occupancy rate (baseline +20%) | Number of affected aircraft (baseline +20%) |
| | Oshima | 9 | 8.89% | 1 | 9.44% | 1 | 10.00% | 1 | 10.56% | 1 | 11% | 1 | 11.67% | 2 | 12.22% | 2 | 12.78% | 2 | 13.33% | 2 |
| | Chofu | 24 | 13.33% | 4 | 14.17% | 4 | 15.00% | 4 | 15.83% | 4 | 17% | 4 | 17.50% | 5 | 18.33% | 5 | 19.17% | 5 | 20.00% | 5 |
| | Haneda | 228 | 50.18% | 115 | 53.31% | 122 | 56.45% | 129 | 59.58% | 136 | 63% | 143 | 65.86% | 151 | 68.99% | 158 | 72.13% | 165 | 75.26% | 172 |
| | Ibaraki | 8 | 30.00% | 3 | 31.88% | 3 | 33.75% | 3 | 35.63% | 3 | 38% | 3 | 39.38% | 4 | 41.25% | 4 | 43.13% | 4 | 45.00% | 4 |
| | Narita | 266 | 15.64% | 42 | 16.62% | 45 | 17.59% | 47 | 18.57% | 50 | 20% | 52 | 20.53% | 55 | 21.50% | 58 | 22.48% | 60 | 23.46% | 63 |
| | Total number of affected aircraft | | | 165 | | 175 | | 184 | | 194 | | 203 | | 217 | | 227 | | 236 | | 246 |
| | **Grand total of affected aircraft** | | **251** | | **266** | | **280** | | **296** | | **310** | | **329** | | **345** | | **359** | | **374** | |

**Table A 3-3 (1/2)** Proportion of affected aircraft assigned to each shelter airports under various aircraft parking occupied rates.

| AIRPORT_ID | ICAO | Airport |
|---|---|---|
| 0 | RJGG | Chūbu Centrair International Airport |
| 1 | RJBB | Kansai International Airport |
| 2 | RJOO | Osaka International Airport |
| 3 | RJSS | Sendai Airport |
| 4 | RJOI | MCAS Iwakuni |
| 5 | RJNK | Komatsu Airport |
| 6 | RJBK | Kōnan Airport |
| 7 | RJOH | Miho-Yonago Airport |
| 8 | RJSM | Misawa Airport |
| 9 | RJNA | Nagoya Airport |
| 10 | RJOS | Tokushima Airport |
| 11 | RJFF | Fukuoka Airport |
| 12 | RJOA | Hiroshima Airport |
| 13 | RJFK | Kagoshima Airport |
| 14 | RJFR | Kitakyūshū Airport |
| 15 | RJOK | Kōchi Airport |
| 16 | RJFT | Kumamoto Airport |
| 17 | RJOM | Matsuyama Airport |
| 18 | RJFM | Miyazaki Airport |
| 19 | RJFU | Nagasaki Airport |
| 20 | RJSN | Niigata Airport |
| 21 | RJFO | Ōita Airport |
| 22 | RJOT | Takamatsu Airport |
| 23 | RJSC | Yamagata Airport |
| 24 | RJDC | Yamaguchi Ube Airport |
| 25 | RJCC | New Chitose Airport |
| 26 | RJEC | Asahikawa Airport |
| 27 | RJSK | Akita Airport |
| 28 | RJCH | Hakodate Airport |
| 29 | RJCK | Kushiro Airport |
| 30 | RJOAH | Naha Airport/Naha Air Base |
| 31 | RJCW | Wakkanai Airport |
| 32 | RJSA | Aomori Airport |
| 33 | RJNF | Fukui Airport |
| 34 | RJSF | Fukushima Airport |
| 35 | RJSI | Hanamaki Airport |
| 36 | RJOW | Iwami Airport |
| 37 | RJOC | Izumo Airport |
| 38 | RJBE | Kobe Airport |
| 39 | RJAF | Matsumoto Airport |
| 40 | RJBD | Nanki-Shirahama Airport |
| 41 | RJNW | Noto Airport |
| 42 | RJSR | Ōdate-Noshiro Airport |
| 43 | RJOB | Okayama Airport |
| 44 | RJFS | Saga Airport |
| 45 | RJNS | Shizuoka Airport |
| 46 | RJSY | Shōnai Airport |
| 47 | RJOR | Tottori Airport |
| 48 | RJNT | Toyama Airport |
| 49 | RJKA | Amami Airport |
| 50 | RJTH | Hachijōjima Airport |
| 51 | RORG | New Ishigaki Airport |
| 52 | RJEB | Monbetsu Airport |
| 53 | RJCM | Memanbetsu Airport |
| 54 | ROMY | Miyako Airport |
| 55 | RJTQ | Miyakejima Airport |
| 56 | ROCB | Tokachi-Obihiro Airport |
| 57 | RJAN | Niijima Airport |
| 58 | RJAZ | Kōzushima Airport |
| 59 | RJCN | Nakashibetsu Airport |
| | | **Total** |

**Table A 3-4** (2/2) Proportion of affected aircraft assigned to each shelter airports under various aircraft parking occupied rates.

| AIRPORT_ID | ICAO | Airport | Ranking | Medium/Large | Small | Total Available Capacity | % of Available Capacity | % of Affected Aircraft | Ranking | Medium/Large | Small | Total Available Capacity | % of Available Capacity | % of Affected Aircraft | Ranking | Medium/Large | Small | Total Available Capacity | % of Available Capacity | % of Affected Aircraft | Ranking | Medium/Large | Small | Total Available Capacity | % of Available Capacity | % of Affected Aircraft |
|---|---|---|---|---|---|---|---|---|---|---|---|---|---|---|---|---|---|---|---|---|---|---|---|---|---|---|
| | | Adjusted occupied parking stand rate (OCj) | | | | | +5% | | | | | | +10% | | | | | | +15% | | | | | | +20% |
| | | Average occupied parking stand rate(OCj) | | | | | 31.5% | | | | | | 33.0% | | | | | | 34.5% | | | | | | 36.0% |
| | | Average non-occupied parking stand rate (NCj) | | | | | 68.5% | | | | | | 67.0% | | | | | | 65.5% | | | | | | 64.0% |
| 0 | RJGG | Chubu Centrair International Airport | 1 | 2 | 50 | 55 | 98.2% | 16.4% | 1 | 2 | 49 | 53 | 100.0% | 16.4% | 1 | 2 | 49 | 53 | 100.0% | 15.4% | 1 | 2 | 47 | 51 | 100.0% | 13.6% |
| 1 | RJBB | Kansai International Airport | 4 | 38 | 4 | 46 | 91.3% | 2.8% | 4 | 37 | 4 | 45 | 82.2% | 10.7% | 4 | 36 | 4 | 44 | 84.1% | 10.3% | 4 | 35 | 3 | 38 | 88.4% | 10.2% |
| 2 | RJOO | Osaka International Airport | 9 | 8 | 10 | 41 | 19.5% | 2.7% | 10 | 9 | 10 | 40 | 35.0% | 2.9% | 3 | 14 | 14 | 32 | 31.3% | 3.9% | 6 | 10 | 35 | 30 | 26.3% | 2.7% |
| 3 | RJSS | Sendai Airport | 8 | 0 | 9 | 33 | 27.3% | 2.4% | 8 | 9 | 14 | 32 | 28.1% | 2.6% | 8 | 10 | 0 | 32 | 31.3% | 2.8% | 9 | 6 | 14 | 38 | 30.0% | 2.4% |
| 4 | RJOI | MCAS Iwakuni | 10 | 8 | 12 | 52 | 15.4% | 2.4% | 12 | 8 | 6 | 51 | 15.7% | 2.6% | 18 | 5 | 10 | 50 | 20.0% | 2.8% | 14 | 9 | 9 | 49 | 28.6% | 3.7% |
| 5 | RJNK | Komatsu Airport | 2 | 0 | 44 | 18 | 42.9% | 2.9% | 6 | 1 | 0 | 43 | 85.7% | 1.7% | 3 | 1 | 42 | 32 | 85.7% | 1.7% | 6 | 4 | 41 | 30 | 85.7% | 1.6% |
| 6 | RJBK | Kohnan Airport | 2 | 0 | 52 | 44 | 4.5% | 0.6% | 2 | 0 | 52 | 52 | 2.3% | 0.3% | 2 | 2 | 50 | 50 | 7.1% | 0.8% | 2 | 0 | 41 | 41 | 4.9% | 0.5% |
| 7 | RJOH | Miho-Yonago Airport | 3 | 0 | 25 | 29 | 36.4% | 1.2% | 6 | 1 | 0 | 40 | 36.4% | 1.2% | 4 | 0 | 40 | 34 | 27.3% | 0.8% | 4 | 3 | 34 | 40 | 63.0% | 1.1% |
| 8 | RJSM | Misawa Airport | 2 | 0 | 17 | 54 | 11.8% | 0.6% | 2 | 0 | 57 | 40 | 11.8% | 0.6% | 3 | 0 | 17 | 17 | 17.6% | 0.8% | 3 | 0 | 16 | 16 | 18.8% | 0.8% |
| 9 | RJNA | Nagoya Airport | 4 | 0 | 54 | 54 | 5.6% | 1.2% | 3 | 0 | 52 | 52 | 3.8% | 0.8% | 4 | 3 | 52 | 52 | 3.8% | 0.8% | 2 | 0 | 51 | 51 | 7.8% | 1.1% |
| 10 | RJOS | Tokushima Airport | 4 | 0 | 12 | 11 | 36.4% | 1.2% | 3 | 1 | 9 | 19 | 27.3% | 0.9% | 3 | 1 | 12 | 11 | 27.3% | 0.8% | 4 | 0 | 10 | 10 | 40.0% | 1.1% |
| 11 | RJFF | Fukuoka Airport | 9 | 0 | 66 | 66 | 13.6% | 2.7% | 10 | 3 | 0 | 64 | 27.3% | 3.2% | 5 | 13 | 3 | 63 | 52.6% | 2.4% | 4 | 14 | 62 | 62 | 22.6% | 3.7% |
| 12 | RJOA | Hiroshima Airport | 6 | 0 | 18 | 18 | 75.0% | 1.8% | 7 | 0 | 19 | 19 | 75.0% | 1.7% | 7 | 0 | 19 | 19 | 62.5% | 1.4% | 6 | 5 | 19 | 19 | 75.0% | 1.6% |
| 13 | RJFK | Kagoshima Airport | 8 | 0 | 24 | 24 | 33.3% | 2.4% | 7 | 0 | 23 | 23 | 30.4% | 2.0% | 5 | 7 | 23 | 23 | 21.7% | 1.6% | 5 | 7 | 23 | 23 | 30.4% | 1.9% |
| 14 | RJFR | Kitakyushu Airport | 0 | 0 | 20 | 20 | 30.0% | 1.8% | 8 | 0 | 20 | 20 | 40.0% | 2.3% | 4 | 0 | 20 | 20 | 20.0% | 1.1% | 6 | 5 | 20 | 20 | 40.0% | 2.1% |
| 15 | RJOK | Kochi Airport | 6 | 0 | 14 | 14 | 42.9% | 1.8% | 4 | 0 | 29 | 29 | 28.6% | 1.2% | 0 | 0 | 14 | 14 | 35.7% | 1.4% | 9 | 4 | 20 | 20 | 42.9% | 1.6% |
| 16 | RJFT | Kumamoto Airport | 5 | 1 | 21 | 24 | 25.0% | 1.8% | 6 | 1 | 21 | 24 | 20.8% | 1.4% | 23 | 5 | 22 | 23 | 21.7% | 1.4% | 5 | 7 | 23 | 23 | 21.7% | 1.6% |
| 17 | RJOM | Matsuyama Airport | 8 | 0 | 19 | 19 | 42.1% | 2.4% | 6 | 1 | 19 | 19 | 36.8% | 2.0% | 5 | 8 | 18 | 18 | 44.4% | 2.2% | 5 | 7 | 16 | 16 | 29.4% | 1.3% |
| 18 | RJFM | Miyazaki Airport | 9 | 1 | 16 | 17 | 58.8% | 3.0% | 6 | 2 | 15 | 17 | 52.9% | 2.6% | 7 | 0 | 17 | 17 | 62.5% | 1.9% | 4 | 3 | 16 | 16 | 56.3% | 1.6% |
| 19 | RJFU | Nagasaki Airport | 6 | 0 | 12 | 12 | 50.0% | 1.8% | 8 | 0 | 12 | 12 | 50.0% | 1.7% | 12 | 0 | 12 | 12 | 58.3% | 1.9% | 11 | 0 | 11 | 11 | 54.5% | 1.6% |
| 20 | RJSN | Niigata Airport | 20 | 8 | 54 | 54 | 45.0% | 2.7% | 19 | 0 | 19 | 19 | 47.4% | 2.6% | 19 | 0 | 19 | 19 | 52.6% | 2.4% | 18 | 0 | 18 | 18 | 50.0% | 2.4% |
| 21 | RJFO | Oita Airport | 22 | 5 | 7 | 7 | 71.4% | 1.5% | 29 | 4 | 4 | 64 | 57.1% | 1.2% | 18 | 5 | 8 | 25 | 85.7% | 1.7% | 4 | 14 | 25 | 62 | 71.4% | 1.3% |
| 22 | RJOT | Takamatsu Airport | 16 | 6 | 19 | 19 | 31.6% | 1.8% | 16 | 7 | 18 | 19 | 31.6% | 1.7% | 16 | 7 | 19 | 19 | 36.8% | 1.9% | 15 | 6 | 15 | 15 | 38.9% | 1.9% |
| 23 | RJSC | Yamagata Airport | 24 | 3 | 8 | 24 | 37.5% | 0.9% | 23 | 7 | 13 | 23 | 30.4% | 1.2% | 22 | 7 | 8 | 34 | 21.7% | 0.9% | 23 | 5 | 7 | 23 | 30.0% | 1.6% |
| 24 | RJDC | Yamaguchi Ube Airport | 0 | 0 | 13 | 13 | 54.5% | 0.9% | 0 | 0 | 8 | 8 | 54.5% | 0.9% | 34 | 0 | 8 | 34 | 37.5% | 0.8% | 12 | 0 | 12 | 12 | 50.0% | 1.1% |
| 25 | RJCC | New Chitose Airport | 14 | 0 | 48 | 48 | 4.3% | 4.3% | 4 | 12 | 0 | 47 | 25.5% | 3.5% | 4 | 0 | 11 | 46 | 45.5% | 1.4% | 45 | 0 | 45 | 45 | 54.5% | 1.6% |
| 26 | RJEC | Asahikawa Airport | 4 | 3 | 7 | 7 | 42.9% | 0.9% | 4 | 3 | 0 | 17 | 25.5% | 0.9% | 49 | 2 | 16 | 16 | 28.6% | 0.9% | 49 | 2 | 19 | 31 | 42.9% | 0.8% |
| 27 | RJSK | Akita Airport | 3 | 0 | 10 | 10 | 50.0% | 0.9% | 3 | 0 | 10 | 10 | 40.0% | 0.9% | 34 | 0 | 34 | 34 | 40.0% | 0.9% | 34 | 2 | 34 | 34 | 42.9% | 0.8% |
| 28 | RJCH | Hakodate Airport | 4 | 2 | 40 | 40 | 50.0% | 1.2% | 13 | 0 | 10 | 10 | 100.0% | 2.6% | 13 | 8 | 0 | 15 | 100.0% | 2.2% | 15 | 7 | 10 | 10 | 100.0% | 1.9% |
| 29 | RJCK | Kushiro Airport | 6 | 2 | 3 | 3 | 75.0% | 1.2% | 40 | 8 | 8 | 57 | 75.0% | 2.6% | 40 | 8 | 8 | 8 | 75.0% | 1.9% | 43 | 3 | 7 | 11 | 75.0% | 1.9% |
| 30 | ROAH | Naha Airport/Naha Air Base | 6 | 0 | 123 | 123 | 4.9% | 1.8% | 16 | 0 | 120 | 120 | 13.3% | 4.6% | 13 | 8 | 119 | 119 | 6.7% | 2.2% | 14 | 116 | 116 | 116 | 12.1% | 3.7% |
| 31 | RJCW | Wakkanai Airport | 2 | 0 | 3 | 3 | 66.7% | 0.6% | 3 | 0 | 13 | 13 | 30.8% | 0.6% | 59 | 0 | 0 | 0 | 0.0% | 0.0% | 52 | 2 | 3 | 3 | 66.7% | 0.5% |
| 32 | RJSA | Aomori Airport | 3 | 0 | 13 | 13 | 23.1% | 0.9% | 4 | 0 | 13 | 13 | 30.8% | 1.2% | 30 | 4 | 13 | 13 | 30.8% | 1.1% | 34 | 0 | 12 | 12 | 33.3% | 1.1% |
| 33 | RJNF | Fukui Airport | 0 | 0 | 8 | 8 | 0.0% | 0.6% | 1 | 0 | 8 | 8 | 0.0% | 0.6% | 54 | 0 | 1 | 8 | 0.0% | 0.3% | 59 | 0 | 8 | 8 | 0.0% | 0.0% |
| 34 | RJSF | Fukushima Airport | 6 | 0 | 12 | 12 | 25.0% | 0.9% | 0 | 0 | 8 | 8 | 25.0% | 0.9% | 54 | 0 | 12 | 12 | 33.3% | 1.1% | 8 | 0 | 11 | 11 | 45.5% | 1.3% |
| 35 | RJSI | Hanamaki Airport | 3 | 0 | 17 | 17 | 17.6% | 0.9% | 3 | 1 | 12 | 12 | 36.4% | 1.2% | 0 | 1 | 16 | 16 | 36.4% | 1.1% | 0 | 1 | 31 | 31 | 41.3% | 1.3% |
| 36 | RJOW | Iwami Airport | 0 | 0 | 29 | 29 | 50.0% | 0.9% | 1 | 0 | 52 | 52 | 50.0% | 1.2% | 2 | 0 | 25 | 25 | 25.0% | 0.9% | 4 | 0 | 9 | 9 | 20.0% | 0.8% |
| 37 | RJOC | Izumo Airport | 1 | 0 | 7 | 7 | 28.6% | 0.6% | 0 | 0 | 7 | 7 | 0.0% | 0.3% | 0 | 2 | 7 | 7 | 42.9% | 0.9% | 7 | 2 | 7 | 7 | 42.9% | 0.8% |
| 38 | RJBE | Kobe Airport | 2 | 0 | 60 | 60 | 60.0% | 1.8% | 2 | 0 | 15 | 15 | 80.0% | 2.3% | 10 | 0 | 10 | 10 | 100.0% | 2.2% | 9 | 10 | 10 | 10 | 100.0% | 2.4% |
| 39 | RJAF | Matsumoto Airport | 1 | 0 | 11 | 11 | 9.1% | 0.3% | 2 | 0 | 10 | 10 | 20.0% | 0.6% | 10 | 0 | 7 | 7 | 20.0% | 0.6% | 43 | 9 | 7 | 7 | 30.0% | 0.8% |
| 40 | RJBD | Nanki–Shirahama Airport | 3 | 0 | 34 | 34 | 42.9% | 0.9% | 3 | 0 | 46 | 46 | 28.6% | 0.6% | 49 | 3 | 34 | 43 | 75.0% | 0.8% | 52 | 2 | 9 | 43 | 28.6% | 0.8% |
| 41 | RJNW | Noto Airport | 3 | 0 | 6 | 6 | 50.0% | 0.9% | 3 | 0 | 6 | 6 | 50.0% | 0.9% | 6 | 0 | 6 | 6 | 50.0% | 0.8% | 6 | 0 | 6 | 6 | 33.3% | 0.5% |
| 42 | RJSR | Odate–Noshiro Airport | 3 | 0 | 29 | 29 | 42.9% | 0.6% | 1 | 0 | 8 | 8 | 57.1% | 1.1% | 0 | 0 | 7 | 7 | 42.9% | 1.1% | 34 | 0 | 12 | 12 | 57.1% | 1.1% |
| 43 | RJOB | Okayama Airport | 2 | 0 | 8 | 8 | 25.0% | 0.6% | 3 | 1 | 8 | 8 | 50.0% | 1.2% | 1 | 0 | 8 | 8 | 33.3% | 0.3% | 8 | 0 | 8 | 8 | 50.0% | 1.1% |
| 44 | RJFS | Saga Airport | 3 | 0 | 11 | 11 | 27.3% | 0.9% | 4 | 0 | 11 | 11 | 36.4% | 1.2% | 0 | 0 | 11 | 11 | 36.4% | 1.1% | 0 | 0 | 10 | 10 | 40.0% | 1.1% |
| 45 | RJNS | Shizuoka Airport | 5 | 0 | 12 | 12 | 41.7% | 1.5% | 4 | 0 | 12 | 12 | 33.3% | 1.1% | 9 | 0 | 11 | 11 | 36.4% | 1.3% | 11 | 0 | 11 | 11 | 63.6% | 1.9% |
| 46 | RJSY | Shonai Airport | 3 | 0 | 52 | 52 | 33.3% | 0.9% | 1 | 0 | 52 | 52 | 11.1% | 0.3% | 34 | 0 | 9 | 9 | 33.3% | 0.8% | 34 | 0 | 50 | 50 | 50.0% | 1.1% |
| 47 | RJOR | Tottori Airport | 2 | 5 | 15 | 15 | 13.3% | 1.5% | 2 | 5 | 15 | 15 | 6.7% | 0.8% | 2 | 4 | 15 | 15 | 20.0% | 0.8% | 2 | 5 | 15 | 15 | 13.3% | 0.5% |
| 48 | RJNT | Toyama Airport | 5 | 0 | 13 | 13 | 38.5% | 1.5% | 4 | 0 | 13 | 13 | 30.8% | 1.2% | 13 | 0 | 13 | 13 | 30.8% | 1.1% | 13 | 0 | 13 | 13 | 38.5% | 1.3% |
| 49 | RJKA | Amami Airport | 5 | 0 | 29 | 29 | 20.0% | 0.3% | 4 | 0 | 29 | 29 | 30.8% | 0.6% | 22 | 0 | 29 | 22 | 30.8% | 1.1% | 34 | 0 | 4 | 4 | 38.5% | 1.1% |
| 50 | RJTH | Hachijojima Airport | 2 | 0 | 2 | 2 | 100.0% | 0.6% | 2 | 0 | 46 | 46 | 100.0% | 1.2% | 54 | 0 | 2 | 2 | 50.0% | 0.3% | 52 | 0 | 2 | 2 | 100.0% | 0.5% |
| 51 | RJOG | New Ishigaki Airport | 3 | 0 | 34 | 34 | 60.0% | 0.9% | 1 | 0 | 29 | 29 | 80.0% | 1.4% | 22 | 5 | 5 | 5 | 62.5% | 1.4% | 43 | 3 | 5 | 5 | 66.7% | 0.8% |
| 52 | RJEB | Monbetsu Airport | 3 | 0 | 2 | 2 | 50.0% | 0.3% | 0 | 0 | 2 | 2 | 50.0% | 0.3% | 52 | 0 | 2 | 2 | 50.0% | 0.3% | 52 | 0 | 2 | 2 | 100.0% | 0.5% |
| 53 | RJCM | Memanbetsu Airport | 3 | 0 | 11 | 11 | 27.3% | 0.9% | 4 | 0 | 11 | 11 | 36.4% | 1.2% | 40 | 0 | 11 | 11 | 27.3% | 0.8% | 25 | 4 | 11 | 11 | 50.0% | 1.3% |
| 54 | ROMY | Miyako Airport | 2 | 0 | 46 | 46 | 66.7% | 0.6% | 3 | 0 | 49 | 49 | 66.7% | 0.9% | 3 | 0 | 19 | 19 | 66.7% | 0.6% | 3 | 0 | 43 | 43 | 100.0% | 0.8% |
| 55 | RJTQ | Miyakejima Airport | 1 | 0 | 0 | 0 | 0.0% | 0.0% | 3 | 0 | 3 | 3 | 100.0% | 0.6% | 3 | 0 | 3 | 3 | 66.7% | 0.6% | 3 | 0 | 3 | 3 | 0.0% | 0.0% |
| 56 | RJCB | Tokachi-Obihiro Airport | 54 | 0 | 3 | 3 | 0.0% | 0.3% | 54 | 0 | 3 | 3 | 0.0% | 0.3% | 54 | 0 | 0 | 0 | 0.0% | 0.0% | 59 | 0 | 3 | 3 | 0.0% | 0.5% |
| 57 | RJAN | Niijima Airport | - | 0 | 0 | 0 | 50.0% | 0.0% | 0 | 0 | 1 | 1 | 50.0% | 0.0% | 0 | 0 | 1 | 1 | 50.0% | 0.0% | 52 | 1 | 1 | 1 | 100.0% | 0.5% |
| 58 | RJAZ | Kozushima Airport | - | 0 | 0 | 0 | 0.0% | 0.0% | 0 | 0 | 0 | 0 | 0.0% | 0.0% | 0 | 0 | 0 | 0 | 0.0% | 0.0% | 52 | 2 | 0 | 2 | 200.0% | 0.5% |
| 59 | RJCN | Nakashibetsu Airport | 54 | 2 | 2 | 2 | 50.0% | 0.3% | 2 | 0 | 2 | 2 | 50.0% | 0.3% | 2 | 2 | 2 | 2 | 50.0% | 0.3% | 2 | 0 | 2 | 2 | 100.0% | 0.5% |
| **Total** | | | | 329 | 10 | 1041 | 31.6% | 100.0% | | 336 | 9 | 1024 | 33.7% | 100.0% | | 349 | 10 | 1013 | 35.4% | 100.0% | | 363 | 11 | 982 | 38.1% | 100.0% |

# CHAPTER 4

Aircraft Parking Stand Utilization for Aircraft Evacuation Using Two-dimensional Bin Packing Algorithm

# Aircraft Parking Stand Utilization for Aircraft Evacuation Using Two-dimensional Bin Packing Algorithm

## ABSTRACT

The purpose of this article is to provide a strategy for resolving the issue of aircraft stand use at shelter airports during emergencies. The suggested aircraft stand utilization for aircraft assignment employs a two-dimensional packing technique combined with a heuristic approach to maximize aircraft handling capability of the airport while minimizing stand usage. The performance of the proposed model was compared to the conventional aircraft assignment in a case study of Japanese airspace, which has endured various natural disasters, including earthquakes and volcanic eruptions, that endanger national air transport infrastructure. In addition, both the proposed aircraft and the conventional aircraft stand assignment models were employed to assess the capabilities and potential of shelter airports to handle various scenarios of affected aircraft.

## KEYWORDS

Aircraft Stand Utilization, Two-dimensional Bin Packing (2DBP), Large-scale disasters, Evacuation.

**Motivations:**

- ❑ **Increasing number of medium to long-period grounded aircraft** during the disaster could disrupt airport's operation especially, aircraft movement and aircraft parking aircraft management

- ❑ **Aircraft parking utilization for grounded-aircraft to maximize the limited airport's aircraft handling capacity** could relax airport's airside congestion. It's also help minimize number of aircraft parking space and airport used for supporting aircraft evacuation.

**Objectives:**
The study aims to develop aircraft parking space utilization model, which could enhance the limited aircraft parking space to accommodate more number of grounded aircraft during the disaster, using two-dimensional bin packing algorithm (2DBP).

**Case study:** 5 Major airports, Japan

**Study gaps:**
Airport and airlines flight schedule used in the study came from early of 2021 which may not reflect the current situation of air traffic volume (before COVID-19 pandemic).

**Data collections:**
- ❑ Japan airport information provided by aviation Information Service Center (AIS), MLIT
- ❑ Historical Flight data CARATS, MLIT
- ❑ FAA and ICAO regulations on grounded aircraft parking and airport aircraft parking space utilization and restrictions. FAA: The Federal Aviation Administration, ICAO: International Civil Aviation Organization

**Methodologies:**
- ❑ Model development
- ❑ Model validation and comparison
- ❑ Two-dimensional Bin Packing Algorithm (2DBP)

## 4.1. INTRODUCTION AND BACKGROUND

Air transport contributes to economic growth and prosperity by moving passengers and cargo. As it grows in complexity, its performance becomes more exposed to events like weather conditions and natural disasters, such as volcanic eruptions. Airports operating in complex environments must be able to adapt to unpredictable circumstances (Butters, 2010). This can be accomplished

by developing realistic and aircraft-specific emergency plans (AEP). AEP is defined as an assurance intended to protect airport operations, human life, and airport infrastructure in the case of a disaster (Ashford et al., 2011; Kvint, 2010). Forecasting demand, establishing physical infrastructure, and monitoring airport capacity are vital components of maintaining passenger and aircraft flow during an airport disaster response operation (Ashford et al., 2011; Enoma and Allen, 2007; Kenville, 2018).

The capacity of an airport relates to its ability to manage its whole operation. However, the majority of definitions define airport capacity in terms of runway and apron area. Additionally, capacity is defined as the maximum number of operations done in a specified amount of time and on a continuous basis on the ground and in the air (de Neufville and Odoni, 2013; Idrissi and Li, 2006). During a disaster, an unexpected surge of various types of aircraft, including non-operational flights, evacuated flights, and humanitarian planes, can easily exceed the airport's capacity. As a result, airports are likely to operate faster and more quickly to aid in local and national disaster relief efforts. Therefore, proper operation and infrastructure planning are crucial for the smooth operation of airport disaster response operations.

Surge capacity (SC) is described as the ability of a system to withstand unexpected surges in demand that might create substantial capacity management difficulties as a result of disasters. SC is a term that denotes to both the sufficiency of existing resources and the capacity to expand (Hanfling, 2006; WATSON et al., 2013). The perspective can be altered depending on the scale of disasters, the techniques used to gather essential resources, and the evacuee-related surge capacity. For example, assuming that the capacity of the airport is insufficient to fulfil the demand, in this instance, expanding operations to local resources or another unaffected airport may be necessary to fulfil the rise in demand (Adams, 2009). Regardless of SC's various definitions and debates, its characteristics may include people, equipment, space, and systems.

In general, "space" refers to the physical facilities that are employed for many functions during surge operations. Airports must identify exiting expandable areas that can be rapidly converted from normal operations to respond to surge demand. If present facilities are insufficient for surge activities, extra space must be developed (Hick et al., 2004; Rose Adam, 2009). This could be accomplished by providing temporary facilities in the airside sections of the airports or by diverting aircraft to other airports that are not in the affected zone. However, the limitations and constraints associated with the extra facilities may affect the airport's ability to handle the rise in demand. For instance, employing airside spaces to accommodate a rising number of aircraft, apron conditions for aircraft parking (e.g., area size, clearance distance between aircraft, and pavement strength), and aircraft moving conditions (e.g., taxiways, runways, intersections, and clearance distances) could all be effected by the rise in demand.

Bouras et al. (Bouras et al., 2014) and Dorndorf et al. (Dorndorf et al., 2007) conducted surveys on aircraft stand allocation and airport gate assignment. They discovered the problems' objectives varied and depended on one's perspective. The first was as a private and public airport. The objectives were to maximize the use of available gates and terminals and minimize gate conflicts, un-gated flights, and flight delays. Another perspective was of an airline owner. Their objectives were to increase customer satisfaction by minimizing passenger walking distances between gates and from the runway to the gate.

According to Skorupski and Żarów (Skorupski and Żarów, 2021), a review of methods for solving stand allocation problem (SAP) optimization tasks revealed it might be impossible to obtain an optimal solution using exact algorithms applied to real-size airports due to computational complexity. Guépet et al. (Guépet et al., 2015) investigated this topic and demonstrated that it is NP-complete to develop a feasible solution for the SAP. As a result, they

established that the optimization issue is NP-hard and that heuristic techniques must be used in such circumstances. Zhang et al. (Zhang et al., 2017) developed a method for solving bi-criteria SAP using the Biogeography-Based Optimization method. Marinelli et al. (Marinelli et al., 2015) developed a hybrid metaheuristic method for the flying gate assignment problem that included Bee Colony Optimization and Biogeography-Based Optimization. They assert that combining these two metaheuristics results in a novel and robust optimization technique for solving SAP. Dell'Orco et al. (Dell'Orco et al., 2017) introduce a methodology that combines Bee Colony Optimization and Fuzzy Inference Systems. Guépet et al. (Guépet et al., 2015) also use time and spatial decomposition techniques. Cheng et al. (Cheng et al., 2012) use a collection of real flight data to evaluate three metaheuristics performances, including Genetic Algorithm, Simulate Annealing, Tabu Search, and a hybrid technique. Studies conducted by Liu et al. (Liu et al., 2016), Ding et al. (Ding et al., 2005), and Aktel et al. discussed employing those metaheuristic algorithms (Aktel et al., 2017).

Additionally, the SAP operation disruptions studies were examined, and the underlying assumptions and methodologies used to address operational disruptions caused by arrival and departure uncertainty were discussed (Skorupski and Żarów, 2021). The problem was commonly referred to as the gate re-assignment problem, and several models were proposed and evaluated using metaheuristic algorithms in conjunction with gate assignment constraints for addressing when an incoming aircraft's delay causes subsequent incoming aircraft to arrive at the assigned gate late (Gu and Chung, 1999; Narciso and Piera, 2015; Şeker and Noyan, 2012; van Schaijk and Visser, 2017; Yan and Tang, 2007). However, the studies rarely addressed surging aircraft parking demand and aircraft stand utilization in an emergency.

The goal of this work is to propose an aircraft stand utilization model based on two-dimensional bin packing and a heuristic approach for improving airport aircraft handling capacity, space utilization, and minimizing the number of aircraft stands required to accommodate aircraft evacuation without impairing regular flying operations at selected aircraft during an emergency. This study contributes to existing research by giving aviation authorities and related parties, such as air traffic control agencies, airports, and airlines, practical and realistic advice for aircraft stand utilization and critical airports that can accommodate a significant number of affected aircraft during aircraft evacuation.

## 4.2.   METHODS AND MATERIALS

In this section, the proposed aircraft assignment model employs the two-dimensional bin packing algorithm (2DBP) to assign affected aircraft to available aircraft stands at shelter airports. In 2DBP, packing techniques such as the maximal rectangles split (MAXRECT) and the first fit decreasing algorithm (FFD) are used. The bins and items represent the available aircraft parking stands and the affected aircraft of different sizes. The proposed model based on 2DBP aims to increase stand space usage, enabling airports to accommodate more aircraft within their limited capacity.

Two-dimensional bin packing is a heuristic optimization algorithm for solving the two-dimensional packing problem. The algorithm is designed to find the optimal or approximate solution for packing the demanded items with the least amount of bin (container) utilization possible and with no items intersecting or contained inside one another (Jylänki, 2010). Bins and items are usually fixed-orientation rectangles with all edges parallel to the bin's edges; this is referred to as two-dimensional rectangular bin packing (2DRBP). A set of rectangular two-dimensional bins $(\mathcal{B}_1, \mathcal{B}_2, \mathcal{B}_3, ... \mathcal{B}_m)$ is defined by its width and length $(W_j, L_j)$. A set of two-

dimensional rectangle items is denoted as $(\mathcal{R}_1, \mathcal{R}_2, \mathcal{R}_3, \dots \mathcal{R}_n)$. Each item $r \in \mathcal{R}$ has width and length $(w_i, l_i)$, that are not larger than the bin they are packed into, denoted as $0 < w_i \leq W_j$ and $0 < l_i \leq L_j$ (Iori et al., 2021).

In rectangle packing, the algorithm based on the free space slit operation is called guillotine algorithm, in which free space of a bin $\mathcal{B}_j$ is spliced into a list of free rectangles $\mathcal{F}_j = \{f_1, \dots, f_n\}$ after each step of a single item $\mathcal{R}_i$ placement at the bottom-left of a free rectangle $f_i$ in packing sequence. The split operation will then produce two new smaller unused free rectangles $f'$ and $f''$ on each of the possible split axes (horizontal or vertical) and then chooses one of the split axes. The chosen free rectangles' axis, i.e., $f'$ and $f''$, will replace $f_i$ in the list of free rectangles. This process is repeated until there is no more available space to suit the next rectangle; at that stage, the algorithm will open a new empty bin and repeat the process. By using only one axis for free area splitting, the guillotine algorithm suffers a drawback, as the following demand items cannot be freely put in the free space, even though there is sufficient free space remaining. By selecting free rectangles on both the horizontal and vertical axes, the maximal rectangles packing rule was established to overcome this disadvantage and then merges those smaller free rectangles along each axis into a single maximal free rectangle without a split line.

Apart from free space maximization, this study took the item's size into account when determining packing priority. Each aircraft stand is built to support a specific aircraft size, and although some stands may support several aircraft sizes, others may support only a single size. For instance, the smallest aircraft should be capable of parking in any size aircraft stand. In comparison, extra-large-size aircraft can park only in the restricted number of extra-large-stands. Thus, aircraft assignment in decreasing order of size may be critical at a shelter airport where the number of aircraft available for emergency parking is restricted. The following section III discusses the fundamentals of scale when it comes to assigning aircraft to available stands.

When it comes to assigning aircraft based on their size, the first-fit decreasing algorithm (FFD), developed in 1973 (Johnson, 1973) for bin packing problems, is also used to handle aircraft assignment in non-increasing order, regardless of the aircraft's length, width, or area. To maximize area utilization, the FFD also allows demand item $I$ with an $a_i$ size ($a_i$ =$width_i$, $length_i$) that does not exceed the available free space $\mathcal{F}$ to be packed into the lowest opened-index bin $\mathcal{B}$, or the higher indexed bin. If item $I$ fits into any open bin, a new bin will begin with it as the first packed item.

## 4.3. PROBLEM DEFINITION AND SCOPE

To make the most efficient use of the available aircraft parking stand, it is necessary to investigate the airport's handling capability and facilities, especially those related to the aircraft size for which the airport was built. These facilities include the number of available aircraft stands, the pavement strength and dimensions of the stands, the length of the runway, and the availability of additional dedicated area(s). This section discusses airport facilities and capabilities, aircraft parking areas, and aircraft constraints. Later in the section, the assumption about airports' aircraft parking stand constraints was made and used as a criterion for airport selection and for the proposed model construction. The analysis of airport and aircraft stand constraints is as follows:

### 4.3.1 Airport: aircraft handling capability

In an emergency, an airport may be required to accommodate a greater number of aircraft than their normal flight schedule. An airport fitted with extensive aircraft handling facilities is likely

to have a high capacity to accommodate the increased number of aircraft efficiently and without interfering with their scheduled flights. According to the AIS of Japan's airport classification system, first- and second-class airports, called hub or regional airports, with comprehensive aircraft accommodation capabilities could be useful in an emergency. Especially useful is the capacity to handle aircraft of the medium (C), medium-large (D), large (E), and extra-large (F) sizes, as defined by wingspan in Table A 4-4, which constitute a sizable proportion of aircraft (96.2 percent) in Japan's airspace, Table 4.1. These handling facilities are also used to refer to the airport's paved airside areas, such as the apron (both terminal and remote apron), taxiway, and runway. Additionally, such airports are mostly domestic in nature, with international immigration and customs facilities capable of supporting international flights if necessary (MLIT, 2019).

**Table 4.1.** Aircraft size classification ratio by wingspan of observable aircraft in Japan.

| Size Categories | 7,383 Observable airborne aircrafts: CARATS dataset[1] | | |
| --- | --- | --- | --- |
| | ICAO Size Code_Letter | Number of aircraft | % of Total aircraft |
| Small | B | 281 | 3.80% |
| Medium | C | 4,134 | 56.00% |
| Medium-large | D | 783 | 10.60% |
| Large | E | 2,082 | 28.20% |
| Extra-large | F | 103 | 1.40% |
| **Total** | | **7,383** | **100.00%** |

[1]*Total flight from the CARATS flight data in March 2016, the busiest day of the week, Sunday between 10:00 am – 9:00 pm.*

### 4.3.2   Additional airside paved area utilization

Apart from the airport's normal aircraft handling facilities, airport authorities may consider designating a portion of the airside paved areas for parking unscheduled aircraft in an emergency. To ensure protection, it is necessary to evaluate all possible airport designs or facilities, including the pavement, line of sight, communications equipment, glare impacts, and visual aids. Both overflow parking arrangements must have no adverse effect on airport users.

The Federal Aviation Administration (FAA) has published procedures for managing the airside area as a designated parking area in the case of the COVID-19 pandemic in 2020 (FAA, 2020). They also recommend thoroughly exhausting all areas at exit aprons first. If ramps/aprons and taxiways are all used, it is recommended that overflow aircraft be parked so aircraft movement between operations and the terminal area is not hampered, which corresponds to the same study conducted by Japan's Kansai Airport Research Institute (KAR) on exceptional long-term aircraft parking and stand management at shelter airports for aircraft evacuation during natural disasters and the ongoing COVID-19 epidemic in Japan (Hirata, 2021).

Additionally, the FAA has recommended optimizing the use of intermediate taxiways as alternative parking spaces as shows in Figure 4.1. However, since the taxiway is needed to connect the aircraft stand to the runway or other airside areas, it should not be blocked. As a result, the designated taxiway for aircraft parking must avoid parking on intersections and provide clearance space equal to the airport's largest handling aircraft for safety. Correspondingly, the taxiway's strength, width, and clearance from the taxiway to the runway should be considered when considering long-term aircraft parking for aircraft safety and to prevent damage to pavement structure potentially caused by overweight aircraft.

**Figure 4.1** Additional pave area for grounded aircraft parking suggestion by FAA.
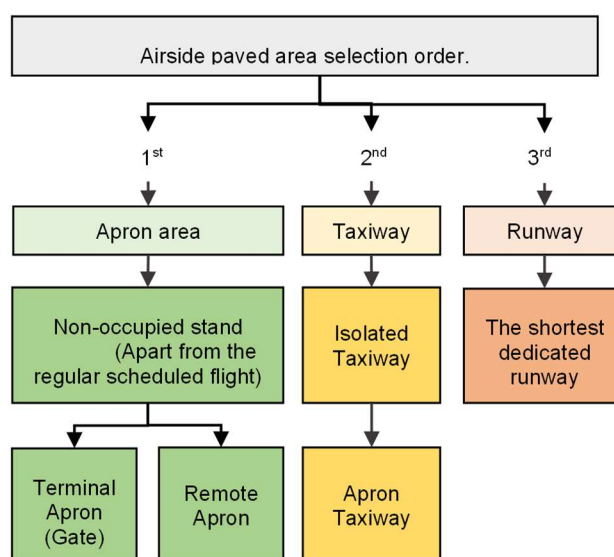


**Figure 4.2**. Airside paved area selection order for surging aircraft parking demand by FAA.

The FAA has previously recommended avoiding parking on runways to the extent possible due to the increased safety risk associated with inadvertent landings on a closed runway during this prolonged period of the situation. Figure 4.2 illustrates the airside paved area selection order in case additional space is needed in an emergency. The airport authorities, however, could use the runway as a dedicated runway for long-term aircraft parking; in this instance, the shortest runway will be recommended. If the dedicated runway is a parallel runway that connects two existing runways and a taxiway. The area at the junction of the runways must also be left open and not used for aircraft parking, with the same clearance space as the dedicated taxiways. This

protocol would maintain aircraft traffic flow and communication on the airport's airside. Thus, the separation distance presents in Aerodrome design manual part 2 on aprons, taxiways, and holding bays doc 9157 by ICAO (ICAO, 2005).

### 4.3.3 Pavement strength and aircraft weight

Each airport has a limited number of aircraft handling capabilities, and capacity is determined by the strength of the airport's pavement and airside space, especially the strength of the pavement. ICAO created the Aircraft classification number-Pavement classification association (ACN-PCN) rating system, which airports must use to determine the strength of their aircraft handling pavement, which includes the area of an apron, ramp, taxiway, and runway, in accordance with ICAO doc 9157 (ICAO, 2005) and Annex 14 on aerodrome design and operations (ICAO, 2016).

The ACN-PCN contains information about the aircraft's single wheel load and the pavement strength conditions. At the airport's particular location, an aircraft with a load equal to or less than the airport pavement strength number can operate safely. Subject to approval by airport authority, an aircraft with a greater ACN number than the PCN number of the airport pavement can be permitted to use the pavement area. Even if some airports have wide usable pavement areas capable of accommodating any aircraft in terms of dimension, e.g., wingspan (width), body length, and aircraft clearance, without regard for pavement load design, it could overload the pavement structure, hastening its deterioration, reducing the pavement's service life, and causing damage to the aircraft (CROW, 2004; ICAO, 2016). The various aircraft stand sizes on the apron area have been equipped with strict ACN-PCN, and only those sizes of aircraft are permitted to operate.

To ensure an aircraft safely, the airport should consider the appropriate aircraft load number and size in relation to the pavement load configuration. The airport ACN-PCN number is expressed in this study on the size of each aircraft stand in relation to the maximum size of aircraft that it can handle, as extracted from the aircraft design document issued by Airport Information of Japan (MLIT, 2019).

### 4.3.4 Dimensions of aircraft and aircraft stand

The physical dimensions and clearance distance of an aircraft are critical when designing aircraft parking stands and allocating aircraft. The wingspan and body length of an aircraft are used to determine its dimensions. Parking clearance distance refers to the minimum acceptable distance between the parked aircraft and other aircraft, structures, or fixed objects. Therefore, parking clearance distance varies according to the size of the aircraft. For instance, a small-medium-size aircraft (ICAO designations A and B) needs 3.0m minimum in clearance distance. 4.5m is needed for a medium-size aircraft (ICAO code C). Larger aircraft, from medium to extra-large (ICAO aircraft codes D, E, and F), require a minimum clearance of 7.5m. The clearance distances for various aircraft sizes are detailed in Table 4.2.

The aircraft stand must have the minimum amount of space and clearance necessary for the aircraft it was built to support. Where a stand is adjacent to an apron taxiway, the minimum separation gap between the taxiway's centerline and the aircraft at the stand must be considered, as shown in Table 4.2 and Figure 4.3. In practice, the stand-aircraft assignment is exclusive, meaning that each aircraft will be assigned to a stand of the same size. For example, a small-size aircraft will be assigned to a small-size stand, and a medium-size aircraft will be assigned to a medium-size stand, see Figure 4.4. According to these requirements, the aircraft stand is designed to accommodate a particular size and weight of an aircraft, or it is designed to accommodate a smaller and lighter aircraft to preserve parking protection and mobility as required.

**Table 4.2.** Aircraft stand size by each aircraft sizes, wingspan, body length, and clearance (ICAO, 2016, 2005).

| Aircraft Dimensions | | | | Aircraft stand size | | |
|---|---|---|---|---|---|---|
| Aircraft code | Maximum wingspan (m) | Maximum body length (m) | Clearance (m) | Wingspan with Clearance (m) | Body length with Clearance (m) | The minimum separation distance between the centreline of the taxiway and aircraft at the stand (m) |
| A | 15 | 17 | 3 | 18 | 20 | 12 |
| B | 24 | 36 | 3 | 27 | 39 | 16.5 |
| C | 36 | 42.1 | 4.5 | 40.5 | 46.6 | 24.5 |
| D | 52 | 61.37 | 7.5 | 59.5 | 68.87 | 36 |
| E | 65 | 70 | 7.5 | 72.5 | 77.5 | 42.5 |
| F | 80 | 74 | 7.5 | 87.5 | 81.5 | 50.5 |



**Clearance requirements**

❑ An aircraft stand should provide the following **minimum clearances** between aircraft using the stand as well as between aircraft and adjacent building or other fixed objects.

❑ **The clearances for code letters D, E and F can be reduced** in the following locations (for aircraft using taxi-in/push-out procedure only):
  ▪ Between the terminal and the nose of an aircraft
  ▪ Over a portion of the stand provided with azimuth guidance by a visual docking guidance system.

❑ **These clearances may, at the discretion of the airport planners, be increased as needed to ensure safe operation on the apron.**

❑ Location of aircraft stand taxilanes and apron taxiways should provide the following minimum separation distance between the center line of these taxiways and ad aircraft at the stand.

ICAO Annex 14 volume 1: Aerodrome Design and Operations, 7th Edition 2016

ICAO Aerodrome Design Manual (Doc 9157): Part 2 Taxiways, Aprons and Holding Bays

**A single aircraft clearance distance**
✓ Taxiway
✓ Runway
✓ Open remote apron area
  where:
    $S$ is an aircraft wingspan (m)
    $C$ is an aircraft clearance from object (m)
    $L$ is an aircraft body length (m)
    $T$ is the minimum separation distance between the centre line of taxiway and aircraft at the stand (m)
    $D$ is the minimum stand width (m), equal to wingspan $S$ plus the required clearance $C$

**A single aircraft clearance distance connect to apron taxiway**
✓ Terminal apron
✓ Remote apron close to Terminal
✓ Ramp apron area

**New Chitose Airport: terminal apron area**

**Figure 4.3.** Aircraft stand (apron) dimensions.

Table 4.3 illustrates the maximum number of aircraft that can be parked alongside other aircraft of the same size in a single stand without exceeding the stand's dimensions. For instance, the A-size stand can accommodate only one A-size aircraft, while the C-size stand can accommodate four A-size aircraft or one B- or C-size aircraft. On the other hand, the extra-large aircraft stand (F-Size) has been built to accommodate an extra-large aircraft (e.g., A380 and B747-8), as well as a range of aircraft sizes, such as 16 A-size, 6 B-size, or 2 C-size, or 1 D-, E-, or F-size aircraft. The bigger the aircraft stand, the more aircraft of different sizes it can accommodate. As a result, an aircraft equipped with F-size stand numbers can play a critical role in emergency aircraft handling during surges in capacity-required situations. Additionally, larger aircraft take up less space in the appropriate aircraft stand; for example, F-size aircraft will park exclusively in the F-size stand. As a result, priority should be given to the largest affected aircraft, followed

by the next largest aircraft, and continuing in descending order to the smallest aircraft. FIGURE 4.4 illustrates this relationship in greater detail.

**Table 4.3.** The matrix of aircraft handling by a single aircraft stand according to size and clearance distance.

| | Aircraft Sizes[2] | | | | | Aircraft Stand Sizes[2] | | | | | |
|---|---|---|---|---|---|---|---|---|---|---|---|
| ICAO Code | Wingspan (m) | Body length (m) | Clearance (m) | Wingspan w Clearance (m) | Body length w Clearance (m) | A | B | C | D | E | F |
| A | 15 | 17 | 3 | 18 | 20 | 1 | 0 | 0 | 0 | 0 | 0 |
| B | 24 | 36 | 3 | 27 | 39 | 1 | 1 | 0 | 0 | 0 | 0 |
| C | 36 | 42.1 | 4.5 | 41 | 47 | 4 | 1 | 1 | 0 | 0 | 0 |
| D | 52 | 61.37 | 7.5 | 60 | 69 | 9 | 2 | 1 | 1 | 0 | 0 |
| E | 65 | 70 | 7.5 | 73 | 78 | 12 | 4 | 1 | 1 | 1 | 0 |
| F | 80 | 74 | 7.5 | 88 | 82 | 16 | 6 | 2 | 1 | 1 | 1 |

[2]Aircraft and aircraft stand sizes use the maximum dimensions of each aircrafts' sizes by their wingspan, body length, and clearance distance refers to the ICAO aircraft's size codes.
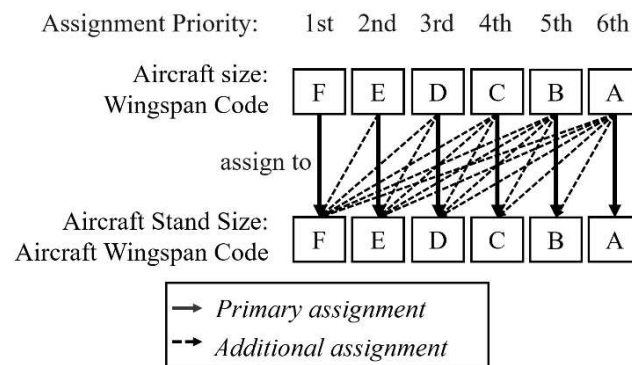


**Figure 4.4.** The aircraft assignment priority by aircraft and stand sizes.

### 4.3.5 Airport selection and parking area utilization assumptions

1) Utilizing the airport's pavement area for middle- to long-term aircraft parking in an emergency, the available area(s) will be prioritized as follows: the aircraft stands (both terminal and remote apron area), followed by taxiway(s) and runway(s).

2) The dedicated runway(s) and taxiway(s) are considered the largest-sized aircraft stand type depending on the largest-size aircraft accommodated by the airport according to runway and taxiway width. For instance, a dedicated runway measuring 3,000 meters in length and 65 meters in width could accommodate an aircraft with a wingspan of 65 meters (size E). The airport itself can handle the size of aircraft. The dedicated runway will be considered as E-size aircraft stand area by dividing the runway space (3,000x65m) with the E stand space plus clearance distance (72.5x77.5m, Table 4.2). As a result, this dedicated runway will accommodate 34 E-size aircraft: (3,000x65m) ÷ (72.5x77.5m) ≈ 34 of the E-size aircraft.

3) The emergency parking runway(s) and taxiway(s) must not interfere with airport operations or aircraft movement to a designated location. The runway on the far side and the shortest should be considered the dedicated runway, not the one in the center or adjacent to an aircraft apron area. When selecting the taxiway(s), it is recommended to avoid the apron-taxiway, as it can obstruct aircraft mobility in the aircraft parking area. Each intersection of the dedicated area (taxiway and runway) must be left open with sufficient room to accommodate the airport's largest operating aircraft.

4) The first- and second-class airports are given preference when it comes to accommodating emergency aircraft due to their ample capacity and capability of handling a greater number of aircraft. Additionally, these airports are served by the majority of domestic and foreign airlines, which benefits their aircraft operations during emergency parking and recovery phases.

5) The affected aircraft will be assigned based on their size. The largest aircraft would be prioritized, followed by the smallest aircraft.

6) To ensure the safety of the stand, aircraft, and surrounding objects, the affected aircraft will be allocated to an aircraft stand that is the same or larger in dimensions (width and length).

## 4.4. PROPOSED MODEL

### 4.4.1 Objective function and constraints

*Sets*

$\mathcal{R}$      set of affected aircraft, $\mathcal{R}_i = \{(w_i, l_i)\}$.

$\mathcal{P}$      set of shelter airports.

$\mathcal{B}_p$      set of aircraft parking stand at shelter airport $p\epsilon\mathcal{P}$, $\mathcal{B}_{j,p} = \{(W_{j,p}, L_{j,p})\}$. $i\epsilon\mathcal{B}_p$.

$\bar{\mathcal{R}}_p$      set of the affected aircraft $r\epsilon\mathcal{R}$ assigned to stand $b_j\epsilon\mathcal{B}_p$ at airport $p\epsilon\mathcal{P}$, $\mathcal{R}_{i,b,p} = \{(x_i, y_i)\}$

$\mathcal{S}_{b,p}$      set of intersected affected aircraft dimensions $\mathcal{R}_i$ and $\mathcal{R}_j$ in aircraft stand at airport $p\epsilon\mathcal{P}, i, j\epsilon\mathcal{R}, i \neq j$.

*Parameters*

$Max\_b_p$ Maximum number of aircraft stands $b\epsilon\mathcal{B}_p$ at airport $p\epsilon\mathcal{P}$.

$OC_p$      Occupancy ratio of maximum aircraft parking stands $Max\_b_p$, at shelter airports $p\epsilon\mathcal{P}$.

$NC_p$      Available non-occupancy parking stands at shelter airport $p\epsilon\mathcal{P}$.

*Decision variables*

$\mathcal{V}_{b,p}$      The non-empty set indicator if there is intersection between of any aircraft $\mathcal{R}_i$ and $\mathcal{R}_j$ assigned into aircraft stand at shelter $b_j\epsilon\mathcal{B}_p$ at airport $p\epsilon\mathcal{P}$.

$\mathcal{X}_p$      Number of aircraft stand usage at airport $p\epsilon\mathcal{P}$.

*Objective function*

Minimize the number of aircraft stands needed for disaster relief by increasing the aircraft stand space utilization.

$$min \sum_b \mathcal{X}_p \qquad\qquad \exists p \qquad (1)$$

***Subject to***

*Shelter airport available capacity limitation:* the available aircraft parking capacity $NC_p$ is determined by occupancy rate $OC_p$ of the airport maximum capacity. The total number of selected aircraft stands must not exceed the available aircraft stands at the selected airport.

$$NC_p = Max\_b_p(1 - OC_p) \qquad\qquad \exists p \qquad (2a)$$

$$\sum_b \mathcal{X}_p \leq NC_p \qquad\qquad (2b)$$

*Parking an aircraft inside the stand:* to avoid blocking the airport's services on the apron area, the assigned aircraft $\bar{r}^i_{j,b,p} = r_i$ must be parked inside the provided aircraft parking stands.

$$r_i = \{(w_i, l_i)\} \qquad\qquad (4a)$$

$$\bar{r}^i_{j,b,p} = \{(x_i, y_i)\} \qquad\qquad (4b)$$

$$\mathcal{B}_{j,p} = \{(W_{j,p}, L_{j,p})\} \qquad\qquad (4c)$$

$$x_i \in \{0, \dots, W_{j,p} - w_i\} \text{ and } y_i \in \{0, \dots, L_{j,p} - l_i\} \qquad (4d)$$

*Non-overlap assigning aircraft:* according to ICAO aircraft parking regulations, to prevent collisions between aircraft parked in the same aircraft parking stand, each aircraft must be parked with the minimum necessary space, which includes a minimum separation distance based on the aircraft's size. Thus, for the protection of parking aircraft, the allocated aircraft's parking space (4b) should not be overlapping with that of other nearby aircraft.

$$\mathcal{V}_{b,p} = (x_i, x_i + w_i) \cap (x_j, x_j + w_j) = \emptyset \text{ OR}, (y_i, y_i + l_i) \cap (y_j, y_j + l_j) = \emptyset$$
$$\forall i, j \in \bar{\mathcal{R}} \qquad (5)$$

### 4.4.2 The affected aircraft allocation framework for stand space utilization

This section describes the proposed construction in detail, outlining the general context, including the input data collection, the pre-computation, and the affected aircraft assigning algorithm for maximizing a single aircraft stand space utilization ratio and minimizing overall stand usage or stand utilization rate for the affected aircraft allocation.

*1)    Input data (explain input data sets)*

Three distinct sets of input data are needed to develop a solution for allocating aircraft to available aircraft stands at airports. The first data set is a collection of shelter airports that have been chosen from the capacity setting for shelter airports discussed in Section III. The shelter airport consists of a limited number of available aircraft stands that are isolated from regularly scheduled flights to prevent disruptions to the airport's normal operations. This is followed by the set of available aircraft stands at the airports with dimensions width (*W*) and length (*L*), which is used to assign an aircraft to an aircraft stand with dimensions equal to or greater than the aircraft itself. The final set is a collection of affected aircraft, each with the same width (*w*) and length (*l*) as the aircraft stand, which is used for area measurements, aircraft positioning, and aircraft intersection within the assigned aircraft stand.

*2)    Constructive heuristic*

A constructive heuristic is based on 2DBP First-Fit Decreasing (FFD) for the aircraft's allocation. The pseudocode of the heuristic algorithm is presented in workflow (

Figure **4.5**) and algorithm 1 while the main procedures of the algorithm are explained below:
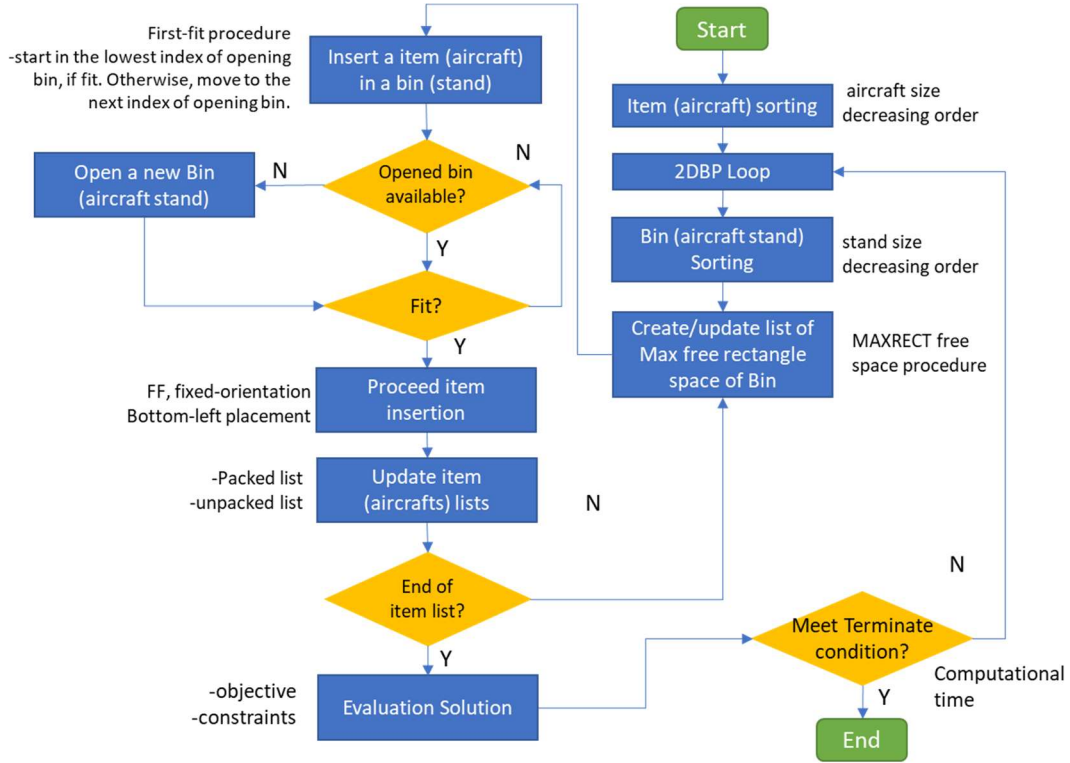


**Figure 4.5** Workflow of 2DBP (MAXRECT) for affected aircraft assignment Algorithm.

### A.    *Sorting affected aircraft*

After uploading the input data sets, the first procedure is to sort the affected aircraft (as items) list according to their sizes in descending order from the largest to the smallest as mentioned in section 4.3.4.

### B.    *Affected aircraft assignment to available aircraft stand solution (First-Fit decreasing FFD algorithm)*

The aircraft assignment loop is the algorithm's key operation. The objective is to generate a solution for allocating the aircraft $\mathcal{R}$ to the appropriate size by using the fewest possible aircraft stands at shelter airports. The procedure begins by sorting the available aircraft stands $\mathcal{B}_p$ in descending order by size at the selected airport $p$ in the list of shelter airport $\mathcal{P}$ in descending order. According to ICAO's guidelines on aerodrome design and operation for aircraft stand size and pavement strength in Annex 14, aircraft may be allocated to the same or larger aircraft stand. When it comes to small aircraft, a variety of aircraft stand options are available; for example, A-size aircraft (the smallest aircraft) can be allocated to any of the aircraft stand sizes from A to F. In comparison, the largest aircraft F (for example, the A380 and B748) can only be allocated to the F-size stand. As a result, the largest aircraft size and parking stand must be assigned first, then in decreasing order to the smallest aircraft size, as shown in Figure 4.4.

The largest available size stand $b_{j,p}$ is the first to be assigned aircraft $r_i \in \mathcal{R}$ if the aircraft stand (bin, $b_{j,p}$) has enough space to fit the aircraft's dimensions $r_i = (w_i, h_i)$; if not, the algorithm will break the loop and select the next stand's bin $b_{j+1,p}$. In case there is free space fit

for aircraft $r_i$, the aircraft will be assigned to the stand's bin $b_{j,p}$. Then the MAXRECT split algorithm will take over by removing the assigned area $f_n = r_i$ and splitting the available free space $\mathcal{F}$ of the stand bin $b_{j,p}$ into the possible free rectangles for both vertical $\{f_n'\}$ and horizontal $\{f_n''\}$ axes; this is the free list $\mathcal{F} \leftarrow \mathcal{F} \cup \{f_n', f_n''\} \setminus \{f_n\}$. All free rectangles $f_{n:m}$ in list $\mathcal{F}$ will be compared to determine the maximal rectangle in case any rectangle $f_m$ is located inside $f_n$. The algorithm will remove $f_m$ and update the remaining maximal rectangles to the list $\mathcal{F}$, $\mathcal{F} \leftarrow \mathcal{F} \setminus \{f_m\}$. Finally, the aircraft $r_i$ will be removed from the list of affected aircraft $\mathcal{R} \leftarrow \mathcal{R} \setminus \{r_i\}$.

Then the next aircraft $r_{i+1}$ assignment follows the FFD process to search from the lowest index of opened aircraft stand bin $b_{j,p} \in \mathcal{B}_p$ at candidate airport $p_k \in \mathcal{P}$ for the available space to assign the aircraft if a stand's bin still has space left $\mathcal{B}_p \neq \emptyset$. Otherwise, the algorithm will break the loop and select the next candidate airport $p_k \in \mathcal{P}$ until all aircraft are assigned.

*C.    Solution evaluation*

In each iteration, a generated solution will be evaluated according to the study's objective to find the minimum number of aircraft stand usage of the certain number of affected aircraft. If the value of aircraft stand usage at the solution's current generation is smaller than the value of the previous one, the algorithm will eliminate the previous solution and store the current one. Otherwise, the current solution will be discarded, and the algorithm will move on to the next iteration. In this study, computational duration is used as the algorithm termination trigger, which relates to the number of affected aircraft in the study scenarios.

As the number of aircraft increases, the computational time will rise accordingly. Since the number of affected aircraft is not extensive with a few of constraints in aircraft assignment, at least 0.5 seconds of computational duration per an affected aircraft would be sufficient to get the approximate solutions (Erdoğan, 2017). This study set the duration per aircraft to 1.0 seconds to give the algorithm more time to find the most feasible solution. Therefore, computational duration setting for the scenarios would be 50sec,100sec, 150sec, 250sec, and 300sec based on the number of affected aircraft in each scenario.

**Algorithm 1.** Pseudocode: affected aircraft assignment Algorithm.

| |
|---|
| **PSEUDOCODE**: Affected aircraft assignment Algorithm. |

**INPUT:**
$\mathcal{P}$, a set of shelter airports
$\mathcal{B}_p$, a set aircraft stands at airport $p \in \mathcal{P}$
$\mathcal{R}$, a set of affected aircrafts
$T$, Terminate duration (sec)
**OUTPUT:** Minimum number of aircraft stand usage $\mathcal{X}_{b,p}$ at selected airports $p \epsilon \mathcal{P}$ for all affected aircrafts in list $\mathcal{R}$; $min \sum_b \mathcal{X}_{b,p}$

1   **PROCEDURE s**orting aircrafts in decreasing order using their sizes
2   **PROCEDURE** the affected aircraft assignment loop (First-Fit decreasing FFD applied MAXRECT algorithm)
3       **FOREACH** shelter airport $p \epsilon \mathcal{P}$ **DO**
4       Sorting bins $\mathcal{B}_p$ in decreasing order using their sizes.
5           **WHILE** $\mathcal{B}_p \neq \emptyset$ and Running duration $< T$ **DO** ◁ $\mathcal{B}_p$ equal to $NC_p$, number of non-occupied aircraft stand at the airport
6               **FOREACH** aircraft stand (bin) $b_{j,p} \in \mathcal{B}_p$ **DO**
7                   **INITIALIZE:** set list of all free rectangles $\mathcal{F}_{j,p}$ of an aircraft stand (bin) $b_{j,p} \in \mathcal{B}_p$
8                   **FOREACH** affected aircraft (rectangle) $r_i$ in sequence **DO**
9                       **PACK:**

| | |
|---|---|
| 10 | Decide the free rectangle $f_n \in \mathcal{F}_{j,p}$ for packing the *aircraft rectangle* $r_i$, with no overlapping of any assigned aircrafts in list of inner solution $\overline{\mathcal{R}'}_{j,b,p}$, $\mathcal{V}_{b,p} = \emptyset$ |
| 11 | **IF** the aircraft rectangle $r_i$ cannot fit into free rectangle $f_n$ **THEN** |
| 12 |     **BREAK** restart with a new stand (bin), $b_{j+1,p}$. |
| 13 | **ELSE** |
| 14 |     Decide the orientation for the rectangle and place it at the bottom-left of $f_n$, denote by $\bar{r}^i_{j,b,p}$ the bounding box of $r_i$ in the bin $b_{j,p}$ after, if has been positioned. |
| 15 |     **UPDATE** affected aircraft list $\mathcal{R}$ by remove packed aircraft $r_i$, $\mathcal{R} \leftarrow \mathcal{R} \setminus \{r_i\}$ |
| 16 |     **UPDATE** the assigned aircraft list of inner solution $\overline{\mathcal{R}'}_p$ |
| 17 |     **INCREMENT** an inner-solution stand count $\mathcal{X}'_{b,p}$ by 1 |
| | |
| 18 |     **PROCEDURE** MAXRECT split rule algorithm |
| 19 |     Use the MAXRECT split placement scheme to subdivide $f_n$ into $f_n'$ and $f_n''$. |
| 20 |     Update new two free rectangles $\{f_n', f_n''\}$ into the list and remove the recently assigned aircraft rectangle $\bar{r}^i_{j,b,p}$. |
| 21 |       **SET** $\mathcal{F}_{j,p} \leftarrow \mathcal{F}_{j,p} \cup \{f_n', f_n''\} \setminus \{\bar{r}^i_{j,b,p}\}$, |
| 22 |       **FOREACH** free rectangle $f_n \in \mathcal{F}_{j,p}$ **DO** |
| 23 |       **COMPUTE** $f_n \setminus \mathcal{B}_{j,p}$ and subdivide the result into at most four new rectangles $G_1, \ldots, G_4$. |
| 24 |       **SET** $\mathcal{F}_{j,p} \leftarrow \mathcal{F}_{j,p} \cup \{G_1, \ldots, G_4\} \setminus \{f_n\}$. |
| 25 |       **ENDFOR** |
| 26 |       **FOREACH** Ordered pair of free rectangles $f_n, f_m \in \mathcal{F}_{j,p}$ **DO** eliminate rectangle if any rectangle is inside another than update free rectangle list |
| 27 |         **IF** $f_n$ contains $f_m$ **THEN** |
| 28 |         **SET** $\mathcal{F}_{j,p} \leftarrow \mathcal{F}_{j,p} \setminus \{f_m\}$. |
| 29 |         **ENDIF** |
| 30 |       **ENDFOR** |
| 31 |     **ENDPROCEDURE** *(MAXRECT)* |
| 32 |     **BREAK** select and assign next aircraft $r_{i+1}$ |
| 33 |     **ENDIF** |
| 34 |     **ENDFOR** |
| 35 |   **ENDFOR** |
| 36 |   **PROCEDURE** objective evaluation |
| 37 | Evaluate the feasible of aircraft assignment solution according to objective in minimizing aircraft stand usage at the shelter airport using the inner-solution stand count $\mathcal{X}'_p$ and the algorithm solution stand count $\mathcal{X}_p$. |
| 38 | Elimination the larger stand count value than update with the smaller one. |
| 39 |   **IF** $\mathcal{X}'_p < \mathcal{X}_p$ **THEN** |
| 40 |     **EMPTY** the algorithm-assigned aircraft solution list $\bar{\mathcal{R}}_p$ |
| 41 |     **SET** $\bar{\mathcal{R}}_p \leftarrow \overline{\mathcal{R}'}_p$ |
| 42 |   **ENDIF** |
| 43 |   **ENDWHILE** |
| 44 |   **BREAK** restart with a new shelter airport $p_{k+1} \in \mathcal{P}$. |
| 45 |   **ENDFOR** |
| 46 | **END PROCEDURE** |

## 4.5. CASE STUDY: JAPAN AIRSPACE

This section presents a case study of Japan airspace for aircraft evacuation and aircraft stand utilization at the selected shelter airports. Using the latest CARATS flight data from March 2016, the week's busiest day was on Sunday. There were 419 flights per hour airborne aircraft in Japan's airspace on average. The study discovered that the largest proportion of aircraft was in group C (medium-size) at 56.0% followed by group E (large size) at 28.2%, group D (medium-large size) at 10.6%, group B (small-medium size) at 3.8%, and group F (extra-large size) at 1.4%. This study uses the various number of affected aircraft at 50, 100, 150, 200, 250, and 500 aircraft with the aircraft's size ratio of the observed commercial aircraft in TABLE 4.4, to represent the various aviation impacts during the emergency.

**Table 4.4.** The various simulated number of the affected commercial aircraft by sizes corresponded to the observed Japan historical flight data.

| Size Categories | Observable commercial aircrafts: CARATS dataset[3] | | Simulated number of affected aircrafts by sizes | | | | | |
|---|---|---|---|---|---|---|---|---|
| | ICAO Size Code Letter | % of Total aircraft | 50 | 100 | 150 | 200 | 250 | 300 |
| Small | A | 0.0% | 0 | 0 | 0 | 0 | 0 | 0 |
| Small-medium | B | 3.8% | 2 | 4 | 6 | 8 | 10 | 11 |
| medium | C | 56.0% | 28 | 56 | 84 | 112 | 139 | 168 |
| Medium-large | D | 10.6% | 5 | 11 | 16 | 21 | 27 | 32 |
| Large | E | 28.2% | 14 | 28 | 42 | 56 | 70 | 85 |
| Extra-large | F | 1.4% | 1 | 1 | 2 | 3 | 4 | 4 |
| | **Total** | **100.0%** | **50** | **100** | **150** | **200** | **250** | **300** |

[3]Total flight from the CARATS flight data on March 2016 observation, the busiest day of the week, Sunday between 10:00 am –9:00 pm

The second data set is the chosen shelter airports and their available capacities, including the additional capacities from the dedicated runway(s) and/or taxiway(s) if they are available, with specific size according to which aircraft they are designed to handle. The study explicitly chooses 9 airports as the candidate airports; there are 4 first-class and 5 second-class airports according to the assumption of airport selection in Section 4.3.5, with a combined cumulative of 970 aircraft stands (including all sizes). However, each airport's available capacity is calculated by the average maximum cumulative occupied aircraft stand in the form of occupancy rate (ICAO, 2018) between the arrival and departure flights during the busiest time of the day between 10:00 am and 9:00 pm according to the quarterly's flight schedule of all chosen airports. The occupancy rate was mentioned in the studies of Japan airport selection of aircraft evacuation in 2019 (Arreeras and Arimura, 2021) and 2020 (Arreeras and Arimura, 2020). In the previous study, the average aircraft stand occupancy ratio for the selected candidate shelter airports was set to 30% of airport maximum capacities (the aircraft apron area, aircraft stands at the terminal, and remote and cargo areas), with the dedicated pavement area, i.e., runway(s) and taxiway(s), being excluded. Thus, the total number of available aircraft stands used in this analysis is 948, which includes 681/970 stands from 70% vacant aircraft stands and 267 stands from additional dedicated areas (including all sizes).

In FIGURE 4.6, the chosen airports have intensive capacities increasing from the additional dedicated areas. They are New Chitose Airport (+151.2%), Sendai Airport (+100%), Osaka International Airport (+91.9%), Kumamoto Airport (+90.9%), Naha airport (+65.9%), Fukuoka Airport (+58.3%), Kansai International Airport (+23.7%), Tokyo (Haneda) International Airport

(+14.4%), and Narita International Airport (+7.0%). Details of the candidate airports capacities are shown in Table A 4-1 and Table A4-2.
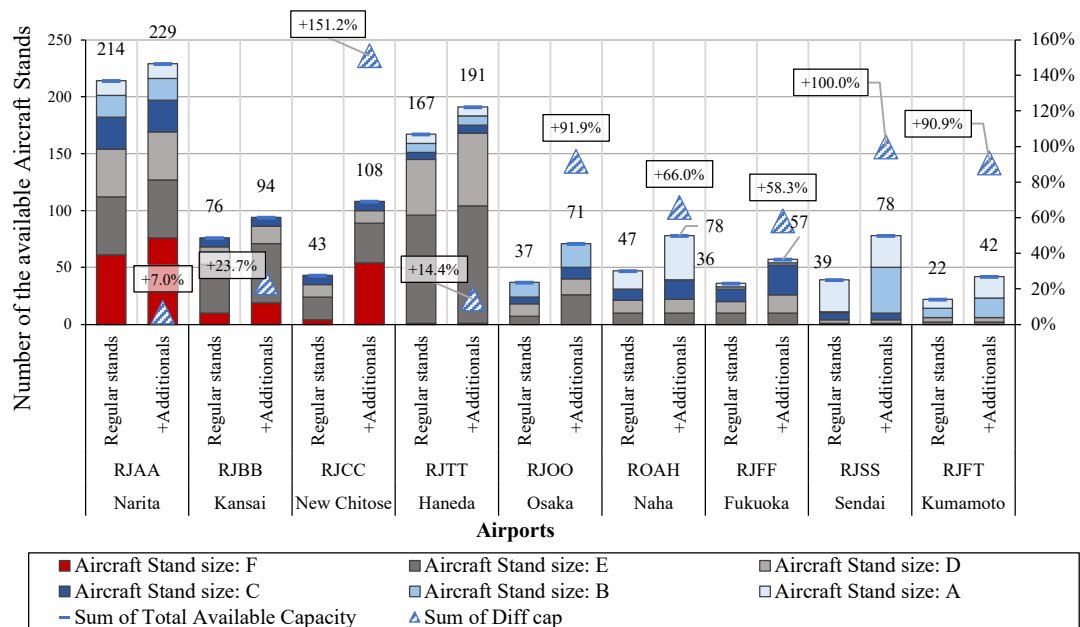


**Figure 4.6.** Case Study: The increased number of aircraft stands from the airports additional dedicated area(s).

## 4.6. COMPUTATIONAL RESULTS

The case study analyzed and compared the results of aircraft stand utilization for models equipped with and without 2DBP. The stand utilization rate and ratio at the airport were used to quantify the models' efficacy in terms of aircraft parking space utilization on a single stand and total usable airside area for emergency aircraft handling.

Additionally, the variant number of aircraft affected was set to approximate the effects of an aviation accident at a stage of 50 to 300 aircraft, with a 50-aircraft increment. Table 4.4 contains a detailed description of the aircraft environment that is impacted. To evaluate an airport's capability to handle aircraft that have varying degrees of disaster effects, and then to compare their results using the same metric as previously discussed, the findings may indicate which airports are critical and how many affected aircraft each airport can handle based on the proposed model. The proposed model had adopted BPP spreadsheet Solver program version 2.22 on Microsoft Excel and VBA developed by Prof Güneş Erdoğan, School of Management, University of Bath, England (Erdoğan, 2017) and tested on a personal computer with an Intel® Core™ i7-8700 CPU (3.20GHz.) and 32.0 GB of RAM.

### Result of the proposed model

The single stand space utilization ratio is the ratio between number of aircraft assigned to a single aircraft stand without violating the stand's restrictions. This ratio can be used to determine the efficiency of a single stand space utilization in handling aircraft. As illustrated in FIGURE 4.7(a), the standard aircraft assignment resulted in a stand space utilization ratio of 1.0. (1:1). In contrast to the proposed model when applied with the 2DBP algorithm, aircraft could be assigned

to a single stand if there is any available space that fits the aircraft's dimensions and clearance distance without violating the stand's restrictions.

In FIGURE 4.7(b), a visual representation of the proposed model's result for aircraft assignment is shown. This designates the proposed model as a many-to-one (M:1) aircraft assignment, implying that the proposed model's space utilization ratio may exceed 1.0 when compared to the conventional assignment method (1:1). The results in Figure 6 show that the space utilization ratio of the 2DBP applied model was higher than the regular assignment method, between 1.03-1.47, depending on the available number of aircraft stands and their sizes.



(a)                                                    (b)
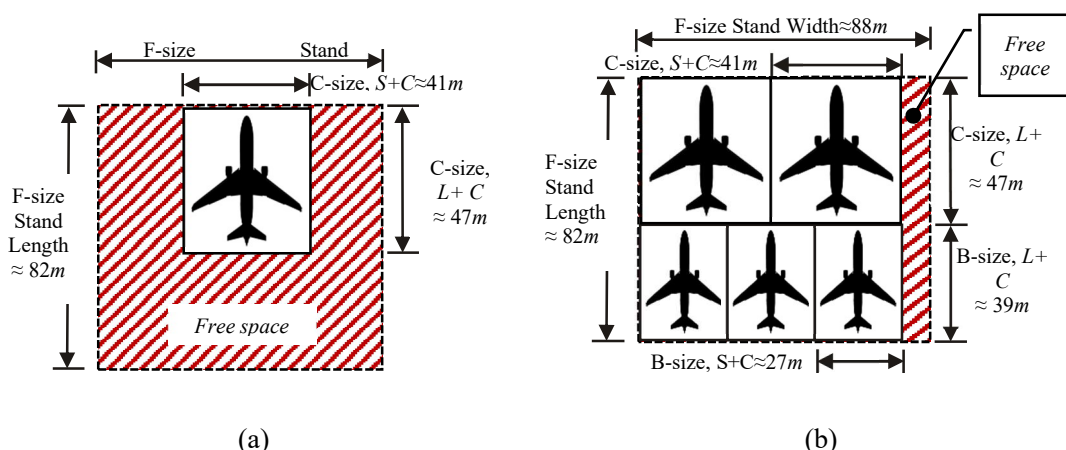
**Figure 4.7.** The result's example on assigning aircrafts into the F-size stand; (a) the regular aircraft assignment one-to-one (1:1) without 2DBP and (b) the proposed model aircraft assignment many-to-one (M:1) generated by 2DBP.

Figure 4.8 demonstrates unequivocally that airports with a greater number of F-size stands (the largest size of aircraft stand) have a higher stand space utilization ratio than airports with fewer F-size stands. For example, the RJBB and RJCC airports have a higher aircraft stand utilization ratio of 1.28 and 1.12, respectively, than the RJTT airport, which has a ratio of 1.04 for regular stands and 1.47 for additional area(s), even though RJTT's total number of available aircraft stands is at least twice that of RJBB and RJCC. This is because RJBB and RJCC have more F-size aircraft stands than RJTT, both on the regular stand (10 and 4 to 1) and on the additional dedicated area(s) (19 and 54 to 1). As mentioned previously in Table 3 and Section III-E, the F-size aircraft stand can accommodate multiple C-size aircraft, which account for most affected aircraft (56 percent) in Japan based on observed air traffic data. In comparison, Tokyo Haneda International Airport (RJTT) was unable to provide the additional area(s) required to accommodate the F-size stand due to the airport's limited apron, taxiway, and runway space. Table A4-2 contains detailed information about the airports' available capacity.

The single stand space utilization ratio may indicate the airport's effectiveness in managing aircraft stand space. A higher stand utilization ratio resulted in a lower airport stand utilization rate, as more aircraft could be handled with fewer stands. However, the airport's capability for aircraft handling is also determined by the number of available stands and dedicated area(s). In Figure 4.8 and Table A 4 3, the ratio of single stand space utilization (red square-marked dash line) at Tokyo Haneda International Airport (RJTT) is smaller than at other airports, such as Narita International Airport (RJAA), Kansai International Airport (RJBB), and New Chitose International Airport (RJCC), which are 1.04, 1.28, and 1.47, respectively. At RJTT, the airport's extensive available capacity has enabled it to handle a significant portion of the affected aircraft,

particularly on the D-size and E-size stands, which can accommodate C- and E-size aircraft, which account for the largest portion of affected aircraft in Japan's airspace, as discussed previously. As a result, RJTT could handle between 91% and 100% of affected aircraft, which is comparable to those with a higher utilization ratio when the number of affected aircraft is less than 200.
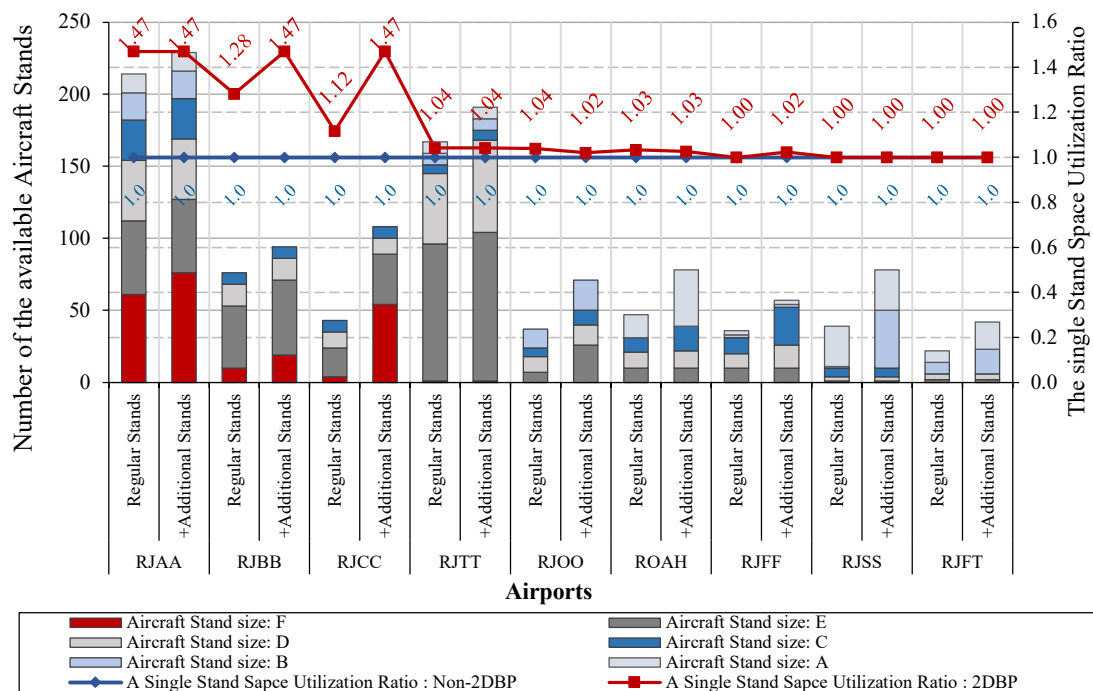


**Figure 4.8**. The regular and additional available airports capacities by stand sizes between Non-2DBP and 2DBP on A Single Stand Space Utilization Ratio

According to the various number of affected aircraft scenarios (50, 100, 150, 200, 250, 300) (the affected aircraft handling rate: Non-2DBP, Figure 4.9), seven of nine airports (RJAA, RJCC, RJBB, RJTT, ROAH, RJFF, and RJOO) can handle between 80% and 100% of the affected aircraft in the 50 aircraft scenario, while others can handle less than 25% of the affected aircraft without applying 2DBP. As the number of affected aircraft increased, each airport's capacity for aircraft handling decreased proportionately.

In Figure 4.9, the example results indicate that at Narita International Airport (RJAA), which has a total of 229 aircraft stands (regular stands plus additional areas), using the regular aircraft assignment method with no 2DBP and a single stand utilization ratio of 1.0, the airport could handle affected aircraft at a rate of 100% for scenarios involving 50, 100, 150, and 200 aircraft. However, once the number of affected aircraft reached 250 and 300, the airport's handling capability decreased to 82.8% and 69.3%, respectively. While the applied 2DBP approach increased the rate of aircraft handling capabilities to 100% (+17.2%) for the 250 aircraft scenario, it then decreased to 81.0% (+11.7%) in the 300 aircraft scenario, or +14.4% on average, compared to the non-applied 2DBP approach.

In comparison, the applied 2DBP approach utilizes fewer aircraft stands than the non-2DBP method to accommodate 50, 100, 150, 200, 250, and 300 aircraft at -7%, -14%, -21%, -28%, -4%, and -1%, respectively, with an average of 13%, as shown in the differentiation of stand utilization rate (%) between applied 2DBP and non-applied 2DBP approaches. Single stand space utilization

ratio is greater than the non-applied 2DBP methods at 1.47, 1.47, 1.47, 1.47, 1.27, and 1.19, respectively, with an average of 1.39 compared to 1.0 for the non-applied 2DBP approach.

Overall, the applied 2DBP aircraft assignment method tends to boost the airport's aircraft stand space usage ratio while decreasing the number of stands utilized (the stand utilization rate). Airports having a greater number of available F-size aircraft stands are denoted by a utilization ratio greater than 1.0 (the yellow square-marked dash line), e.g., RJAA, RJCC, and RJBB airports. According to Figure 7, the handled aircraft rate increased by an average of +14%, +12%, +6%, +1%, and +2%at airports RJAA, RJCC, RJBB, RJTT, and ROAH, respectively, while the stand utilization rate decreased by an average of -13%, -16%, -17%, -3%, and 0% using the applied 2DBP model.
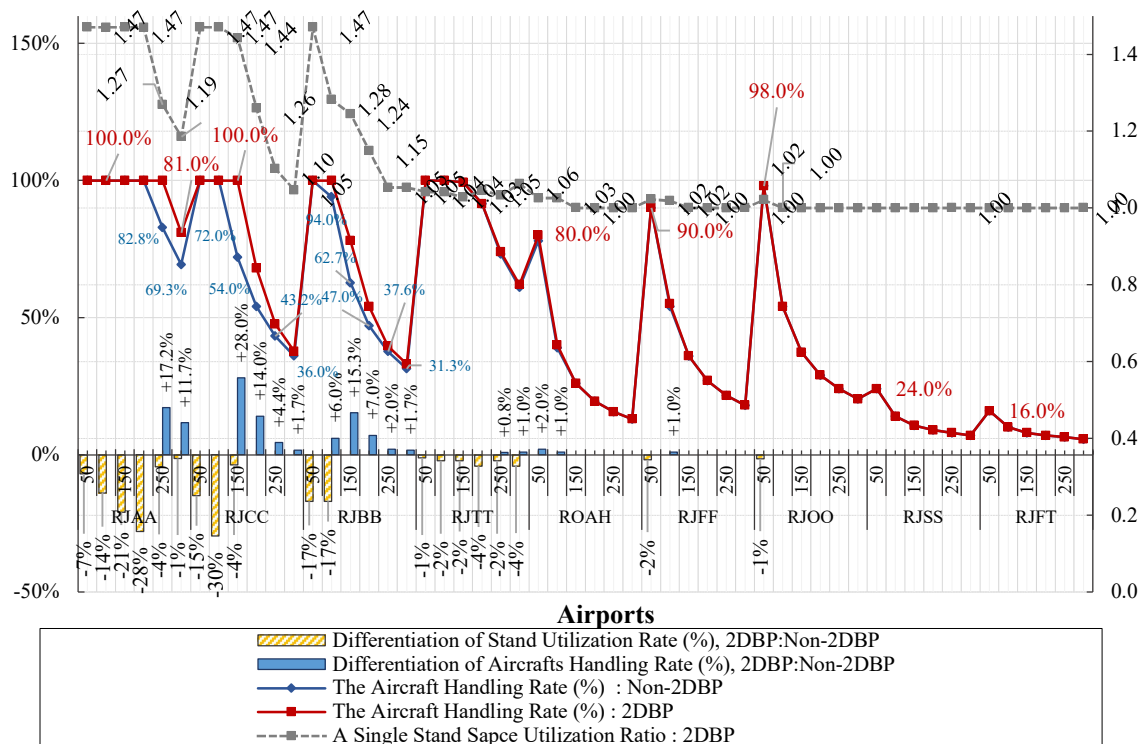


**Figure 4.9.** The Stand Space Utilization Ratio effect on the individual airport's aircraft handling and differentiation of stand utilization rate between non-2DBP and 2DBP applied model on the simulated scenarios.

## 4.7. CONCLUSION

- **Longer time of aircraft parking and parking close together must be consider aircraft safety**, and airport infrastructure safety: aircraft dimensions, clearance, and parking pavement strength must be appropriate.

- By additional dedicated area alone could rise airport's aircraft handling capacity by +7% up to 151%.

- **Two-dimensional Bin Packing algorithm (2DBP) acted as many-to-1 (aircrafts to a stand).** This had increased a single stand aircraft handling capacity by 10-30%.

- **With additional dedicated parking areas and 2DBP, only a few large airports could be sufficient to handling up to 300 affected aircrafts.**

- **The F-size equivalent aircraft stand played a vital role in increase stand handling capacity**, since it can handle at least 2 of C-size aircraft, the majority aircraft size in Japan airspace.

**Discussion and further study:**
- ❑ Limitations of this study was the accuracy information on airport facility (pavement area) of airport design document by AIS.
- ❑ Dedicated area for aircraft parking (taxiway, runway, remote apron) can be change depends on airport authorities and airport planners. However, those decisions should disrupt airport and aircraft operations. Furthermore, the safety of aircraft and airport facility must be concerned.
- ❑ Further study may consider aircraft as polygon not rectangle, which allow aircraft to be packed tight together and leave more free space for more number of aircraft.

In aircraft assignment to the aircraft stand at the airport, regularly there are restrictions between the assigned aircraft and the aircraft stand based on an aircraft's weight, the pavement's strength, an aircraft's dimensions, and clearance distance. An aircraft should park on the same-sized aircraft stand or a larger one to ensure its safety, as well as the safety of surrounding facilities and other aircraft. In an emergency, airport authorities may decide to provide additional area(s) to accommodate the surge of aircraft, particularly non-scheduled aircraft that were required to park for an extended period of time due to the disaster's duration. In this case, the airport's authorities could repurpose some of the airside paved area by prioritizing the use of unused aircraft apron space (terminal and remote aprons), taxiway(s), and runway(s) as dedicated parking areas, in accordance with the FAA's and KAR's recommendation for long-term aircraft parking management in COVID-19. Nonetheless, those designated areas should not interfere with normal airport and airline operations. In comparison to the conventional aircraft stand assignment, the two-dimensional bin packing algorithm used in this study is capable of utilizing aircraft stands (M:1), allowing multiple aircraft to be parked in a single stand without violating ICAO or airport safety regulations (1:1). As a result, the average efficiency of utilizing a single-stand space increases, resulting in a reduced (minimized) number of aircraft stands being used.

According to the findings of this study, the commercial aircraft size ratio in Japan's airspace has a significant effect on the utilization of aircraft stands at candidate shelter airports. As a result, the shelter airport equipped with a large number of stands and dedicated pavement areas will serve as the critical shelter airport during the disaster. Airports with dedicated taxiways and runways, in particular, are likely to have a significant impact on aircraft stand utilization. Since those dedicated areas provide exceptionally large space and can accommodate a range of aircraft sizes from the largest to the smallest, particularly the extra-large size (F) of aircraft stands, it benefits the medium-size aircraft (C), which account for the majority of aircraft in Japan's airspace, by allowing them to pack together in a single stand. Thus, additional dedicated areas such as taxiways and runways contribute significantly to the reduction of airport stand utilization rates, allowing for more aircraft to operate and avoiding airport traffic congestion during an emergency.

## LIMITATION

The study analyzed historical data from MLIT Japan's CARATS flight dataset in 2016. Additionally, during the study period, the number of scheduled operational flights at the target airports may have dropped significantly as a result of the COVID-19 pandemic's impact on airport and flight operations. To accurately simulate and generate results for aviation disaster scenarios, real-time or up-to-date airport and flight data are required. Emphasis should be placed on the airport's airside facilities, occupancy rate, and specific aircraft affected.

## ACKNOWLEDGEMENT

This article was based on exchanges of opinions with the Civil Aviation Bureau of the Ministry of Land, Infrastructure, Transport and Tourism, as well as discussions at the study group of the Kyoto University Disaster Prevention Research Institute "Study on Crisis Management System for Air Transport during Large-Scale Eruption".

## REFERENCES

Adams, L.M., 2009. Exploring the concept of surge capacity. Online Journal of Issues in Nursing 14.

Aktel, A., Yagmahan, B., Özcan, T., Yenisey, M.M., Sansarcı, E., 2017. The comparison of the metaheuristic algorithms performances on airport gate assignment problem. Transportation Research Procedia 22, 469–478. https://doi.org/10.1016/j.trpro.2017.03.061

Arreeras, S., Arimura, M., 2021. A Study on Shelter Airport Selection during Large-scale Volcanic Disasters using CARATS Open Dataset. Transportation Research Part C: Emerging Technologies 129, 103263. https://doi.org/10.1016/j.trc.2021.103263

Arreeras, S., Arimura, M., 2020. An Improvement on Shelter Airport Selection Model During Large-scale Volcanic Disasters: A case study of Hakoneyama Japan. Manuscript submitted for publication.

Ashford, N.J., Mumayiz, S., Wright, P.H., 2011. Airport Engineering, Airport Engineering: Planning, Design, and Development of 21st Century Airports: Fourth Edition. John Wiley & Sons, Inc., Hoboken, NJ, USA. https://doi.org/10.1002/9780470950074

Bouras, A., Ghaleb, M.A., Suryahatmaja, U.S., Salem, A.M., 2014. The Airport Gate Assignment Problem: A Survey. https://doi.org/10.1155/2014/923859

Butters, M., 2010. Flexible airport design. Journal of airport management 4, 321–328. https://doi.org/10.3912/OJIN.Vol14No02PPT03

Cheng, C.-H., Ho, S.C., Kwan, C.-L., 2012. The use of meta-heuristics for airport gate assignment. Expert Systems with Applications 39, 12430–12437. https://doi.org/10.1016/j.eswa.2012.04.071

CROW, 2004. The PCN Runway Strength Rating and Load Control System.

de Neufville, R., Odoni, A.R., 2013. Airport Systems: Planning, Design, and Management. McGraw-Hill Education.

Dell'Orco, M., Marinelli, M., Altieri, M.G., 2017. Solving the gate assignment problem through the Fuzzy Bee Colony Optimization. Transportation Research Part C: Emerging Technologies 80, 424–438. https://doi.org/10.1016/j.trc.2017.03.019

Ding, H., Lim, A., Rodrigues, B., Zhu, Y., 2005. The over-constrained airport gate assignment problem. Computers & Operations Research 32, 1867–1880. https://doi.org/10.1016/j.cor.2003.12.003

Dorndorf, U., Drexl, A., Nikulin, Y., Pesch, E., 2007. Flight gate scheduling: State-of-the-art and recent developments. Omega 35, 326–334. https://doi.org/10.1016/j.omega.2005.07.001

Enoma, A., Allen, S., 2007. Developing key performance indicators for airport safety and security. Facilities 25, 296–315. https://doi.org/10.1108/02632770710753334

Erdoğan, G., 2017. BPP Spreadsheet Solver.

FAA, 2020. Federal Aviation Administration National Part 139 Cert Alert.

Gu, Y., Chung, C.A., 1999. Genetic algorithm approach to aircraft gate reassignment problem. Journal of Transportation Engineering 125, 384–389. https://doi.org/10.1061/(ASCE)0733-947X(1999)125:5(384)

Guépet, J., Acuna-Agost, R., Briant, O., Gayon, J.P., 2015. Exact and heuristic approaches to the airport stand allocation problem. European Journal of Operational Research 246, 597–608. https://doi.org/10.1016/j.ejor.2015.04.040

Hanfling, D., 2006. Equipment, Supplies, and Pharmaceuticals: How Much Might It Cost to Achieve Basic Surge Capacity? Academic Emergency Medicine 13, 1232–1237. https://doi.org/10.1197/j.aem.2006.03.567

Hick, J.L., Hanfling, D., Burstein, J.L., Deatley, C., Barbisch, D., Bogdan, G.M., Cantrill, S., 2004. Health care facility and community strategies for patient care surge capacity. Annals of Emergency Medicine 44, 253–261. https://doi.org/10.1016/j.annemergmed.2004.04.011

HIRATA, T., 2021. Aircraft Evacuation in the Event of a Large-Scale Natural Disaster And temporary parking. KANSAI Airport Review.

ICAO, 2018. International Civil Aviation Organization Manual on Collaborative Air Traffic Flow Management.

ICAO, 2016. Annex 14: Aerodrome Design and Operations Seventh Edition, International Civil Aviation Organization.

ICAO, 2005. Aerodrome Design Manual-Part 2: Taxiways, Aprons and Holding Bays, in: ICAO. p. 156.

Idrissi, A., Li, C.M., 2006. Modeling and optimization of the capacity allocation problem with constraints, in: Proceedings of the 4th IEEE International Conference on Research, Innovation and Vision for the Future, RIVF'06. pp. 107–116. https://doi.org/10.1109/RIVF.2006.1696426

Iori, M., de Lima, V.L., Martello, S., Miyazawa, F.K., Monaci, M., 2021. Exact solution techniques for two-dimensional cutting and packing. European Journal of Operational Research. https://doi.org/10.1016/j.ejor.2020.06.050

Johnson, D.S., 1973. Near-optimal bin packing algorithms. Massachusetts Institute of Technology. Massachusetts Institute of Technology.

Jylänki, J., 2010. A thousand ways to pack the bin-a practical approach to two-dimensional rectangle bin packing. Retrieved From Http://Clb. Demon. Fi/Files/ … 1–50.

Kenville, K.A., 2018. An Analysis of the Strategic Planning Process at Large Hub Airports in the United States, The Collegiate Aviation Review International.

Kvint, V., 2010. The Global Emerging Market, The Global Emerging Market: Strategic Management and Economics. Routledge. https://doi.org/10.4324/9780203882917

Liu, S., Chen, W.H., Liu, J., 2016. Robust assignment of airport gates with operational safety constraints. International Journal of Automation and Computing 13, 31–41. https://doi.org/10.1007/s11633-015-0914-x

Marinelli, M., Palmisano, G., Dell'Orco, M., Ottomanelli, M., 2015. Fusion of Two Metaheuristic Approaches to Solve the Flight Gate Assignment Problem. Transportation Research Procedia 10, 920–930. https://doi.org/10.1016/j.trpro.2015.09.045

MLIT, 2019. AIRAC Airports Information [WWW Document]. Japan Aeronautical Information Service center. URL https://aisjapan.mlit.go.jp/InfoDispAction.do (accessed 6.6.19).

Narciso, M.E., Piera, M.A., 2015. Robust gate assignment procedures from an airport management perspective. Omega 50, 82–95. https://doi.org/10.1016/j.omega.2014.06.003

Rose Adam, 2009. ECONOMIC RESILIENCE TO DISASTERS. Community and Regional Resilience Institute.

Şeker, M., Noyan, N., 2012. Stochastic optimization models for the airport gate assignment problem. Transportation Research Part E: Logistics and Transportation Review 48, 438–459. https://doi.org/10.1016/j.tre.2011.10.008

Skorupski, J., Żarów, P., 2021. Dynamic management of aircraft stand allocation. Journal of Air Transport Management 90, 101964. https://doi.org/10.1016/j.jairtraman.2020.101964

van Schaijk, O.R.P., Visser, H.G., 2017. Robust flight-to-gate assignment using flight presence probabilities. Transportation Planning and Technology 40, 928–945. https://doi.org/10.1080/03081060.2017.1355887

WATSON, S.K., RUDGE, J.W., COKER, R., 2013. Health Systems' "Surge Capacity": State of the Art and Priorities for Future Research. Milbank Quarterly 91, 78–122. https://doi.org/10.1111/milq.12003

Yan, S., Tang, C.H., 2007. A heuristic approach for airport gate assignments for stochastic flight delays. European Journal of Operational Research 180, 547–567. https://doi.org/10.1016/j.ejor.2006.05.002

Zhang, H.H., Xue, Q.W., Jiang, Y., 2017. Multi-objective gate assignment based on robustness in hub airports. Advances in Mechanical Engineering 9, 2017. https://doi.org/10.1177/1687814016688588

# APPENDIX A

**Table A 4-1**. The candidate shelter airports' aircraft available stands capacities for regular stand: by sizes.

| Airport Name | ICAO Code | IATA Code | Airport Classifications | Dedicated Remote Apron | Dedicated taxiway(s) | Dedicated runway(s) | Maximum Capacity by Aircraft Sizes | | | | | | | Regular Available Capacity (Assumption of non-occupancy stand ratio = 70% of Max Capacity (Table A2)) | | | | | | | |
|---|---|---|---|---|---|---|---|---|---|---|---|---|---|---|---|---|---|---|---|---|---|
| | | | | | | | F (Extra-large) | E (Large) | D (Medium-large) | C (Medium) | B (Small-medium) | A (Small) | Total Capacity | F (Extra-large) | E (Large) | D (Medium-large) | C (Medium) | B (Small-medium) | A (Small) | Total Capacity | % of Available capacity |
| Narita | RJAA | NRT | 1 | N | Y | N | 87 | 73 | 60 | 40 | 27 | 18 | 305 | 61 | 51 | 42 | 28 | 19 | 13 | 214 | 70.2% |
| Kansai | RJBB | KIX | 1 | Y | Y | N | 14 | 62 | 21 | 11 | 0 | 0 | 108 | 10 | 43 | 15 | 8 | 0 | 0 | 76 | 70.4% |
| New Chitose | RJCC | CTS | 2 | Y | Y | Y | 5 | 29 | 15 | 12 | 0 | 0 | 61 | 4 | 20 | 11 | 8 | 0 | 0 | 43 | 70.5% |
| Fukuoka | RJFF | FUK | 2 | Y | N | N | 0 | 14 | 14 | 16 | 3 | 4 | 51 | 0 | 10 | 10 | 11 | 2 | 3 | 36 | 70.6% |
| Kumamoto | RJFT | KMJ | 2 | Y | N | N | 0 | 3 | 5 | 0 | 11 | 11 | 30 | 0 | 2 | 4 | 0 | 8 | 8 | 22 | 73.3% |
| Osaka Itami | RJOO | ITM | 1 | Y | N | N | 0 | 10 | 16 | 8 | 19 | 0 | 53 | 0 | 7 | 11 | 6 | 13 | 0 | 37 | 69.8% |
| Sendai | RJSS | SDJ | 2 | Y | N | N | 0 | 2 | 4 | 8 | 2 | 40 | 56 | 0 | 1 | 3 | 6 | 1 | 28 | 39 | 69.6% |
| Haneda | RJTT | HND | 1 | Y | N | N | 2 | 136 | 70 | 9 | 12 | 11 | 240 | 1 | 95 | 49 | 6 | 8 | 8 | 167 | 69.6% |
| Naha | ROAH | OKA | 2 | Y | N | N | 0 | 14 | 15 | 14 | 0 | 23 | 66 | 0 | 10 | 11 | 10 | 0 | 16 | 47 | 71.2% |
| *Total* | | | | | | | *108* | *343* | *220* | *118* | *74* | *107* | *970* | *76* | *239* | *156* | *83* | *51* | *76* | *681* | *70.2%* |

**Table A4-2.** The candidate shelter airports' aircraft available stands capacities for additional dedicated areas: by sizes.

| Airport Name | Airport ICAO Code | Dedicated Remote Apron | Dedicated taxiway(s) | Dedicated runway(s) | Dedicated Remote Apron for emergency long period aircraft parking, not for cargo or near terminal remote apron | | | | | | | Dedicated taxiway(s) | | | Dedicated runway(s) | | | | Total capacity (Regular stands + Additional areas) | | | | | | | |
|---|---|---|---|---|---|---|---|---|---|---|---|---|---|---|---|---|---|---|---|---|---|---|---|---|---|---|
| | | | | | F (Extra-laree) | E (Large) | D (Medium-large) | C (Medium) | B (Small-medium) | A (Small) | Total Capacity | Taxiway length (x1000m) | Taxiway intersections | Considerable as F stand | Runway length (x1000m) | Runway intersects | Considerable as F stand | Considerable as E stand | F (Extra-large) | E (Large) | D (Medium-large) | C (Medium) | B (Small-medium) | A (Small) | Total Capacity | % of Regular Available Capacities |
| Narita | RJAA | N | Y | N | 0 | 0 | 0 | 0 | 0 | 0 | 0 | 1.5 | 3 | 15 | 0 | 0 | 0 | 0 | 76 | 51 | 42 | 28 | 19 | 13 | 229 | 107.0% |
| Kansai | RJBB | Y | Y | N | 1 | 9 | 0 | 0 | 0 | 0 | 10 | 0.94 | 3 | 8 | 0 | 0 | 0 | 0 | 19 | 52 | 15 | 8 | 0 | 0 | 94 | 123.7% |
| New Chitose | RJCC | Y | Y | Y | 4 | 15 | 0 | 0 | 0 | 0 | 19 | 0.95 | 1 | 10 | 3 | 0 | 36 | 0 | 54 | 35 | 11 | 8 | 0 | 0 | 108 | 251.2% |
| Fukuoka | RJFF | Y | N | N | 0 | 0 | 6 | 15 | 0 | 0 | 21 | 0 | 0 | 0 | 0 | 0 | 0 | 0 | 0 | 10 | 16 | 26 | 2 | 3 | 57 | 158.3% |
| Kumamoto | RJFT | Y | N | N | 0 | 0 | 0 | 0 | 9 | 11 | 20 | 0 | 0 | 0 | 0 | 0 | 0 | 0 | 0 | 2 | 4 | 0 | 17 | 19 | 42 | 190.9% |
| Osaka Itami | RJOO | Y | N | Y | 0 | 0 | 3 | 4 | 8 | 0 | 15 | 0 | 0 | 0 | 1.83 | 4 | 0 | 19 | 0 | 26 | 14 | 10 | 21 | 0 | 71 | 191.9% |
| Sendai | RJSS | Y | N | N | 0 | 0 | 0 | 0 | 39 | 0 | 39 | 0 | 0 | 0 | 0 | 0 | 0 | 0 | 0 | 1 | 3 | 6 | 40 | 28 | 78 | 200.0% |
| Haneda | RJTT | Y | N | N | 0 | 8 | 15 | 1 | 0 | 0 | 24 | 0 | 0 | 0 | 0 | 0 | 0 | 0 | 1 | 103 | 64 | 7 | 8 | 8 | 191 | 114.4% |
| Naha | ROAH | Y | N | N | 0 | 0 | 1 | 7 | 0 | 23 | 31 | 0 | 0 | 0 | 0 | 0 | 0 | 0 | 0 | 10 | 12 | 17 | 0 | 39 | 78 | 166.0% |
| *Total* | | | | | *5* | *32* | *25* | *27* | *56* | *34* | *179* | | *7* | *33* | | | *36* | *19* | *150* | *290* | *181* | *110* | *107* | *110* | *948* | *139.2%* |

**Table A 4-3.** Detail of airports stand usage, aircraft stand utilization, the number of assigned aircrafts by aircraft sizes on various number of affected scenarios.

| Airport Name | ICAO Code | F (Extra-large) | E (Large) | D (Medium-large) | C (Medium) | B (Small-medium) | A (Small) | Total | F (Extra-large):~1% | E (Large):~28% | D (Medium-large) | C (Medium) | B (Small-medium) | A (Small):~0% | Total | Non-2DBP (A) | Airport Stands Utilization Rate (%) | 2DBP | Airport Stands Utilization Rate (%) | Differentiation of Stand Usage (%) | Non-2DBP (B) | Aircraft Assignment Efficiency (%) | 2DBP | Aircraft Assignment Efficiency (%) | Differentiation of Assigned Aircrafts (%) | Non-2DBP ratio | 2DBP ratio |
|---|---|---|---|---|---|---|---|---|---|---|---|---|---|---|---|---|---|---|---|---|---|---|---|---|---|---|---|
| Narita | RJAA | 76 | 51 | 42 | 28 | 19 | 13 | 229 | | | | | | | | 50 | 21.8 | 34 | 14.8 | -7.0 | 50 | 100.0 | 50 | 100.0 | +0.0 | 1.0 | 1.47 |
| Kansai | RJBB | 19 | 52 | 15 | 8 | 0 | 0 | 94 | | | | | | | | 50 | 53.2 | 34 | 36.2 | -17.0 | 50 | 100.0 | 50 | 100.0 | +0.0 | 1.0 | 1.47 |
| New Chitose | RJCC | 54 | 35 | 11 | 8 | 0 | 0 | 108 | | | | | | | | 50 | 46.3 | 34 | 31.5 | -14.8 | 50 | 100.0 | 50 | 100.0 | +0.0 | 1.0 | 1.47 |
| Fukuoka | RJFF | 0 | 10 | 16 | 26 | 2 | 3 | 57 | | | | | | | | 45 | 78.9 | 44 | 77.2 | -1.8 | 45 | 90.0 | 45 | 90.0 | +0.0 | 1.0 | 1.02 |
| Kumamoto | RJFT | 0 | 2 | 4 | 0 | 17 | 19 | 42 | 1 | 14 | 5 | 28 | 2 | 0 | 50 | 8 | 19.0 | 8 | 19.0 | 0.0 | 8 | 16.0 | 8 | 16.0 | +0.0 | 1.0 | 1.00 |
| Osaka | RJOO | 0 | 26 | 14 | 10 | 21 | 0 | 71 | | | | | | | | 49 | 69.0 | 48 | 67.6 | -1.4 | 49 | 98.0 | 49 | 98.0 | +0.0 | 1.0 | 1.02 |
| Sendai | RJSS | 0 | 1 | 3 | 6 | 40 | 28 | 78 | | | | | | | | 12 | 15.4 | 12 | 15.4 | 0.0 | 12 | 24.0 | 12 | 24.0 | +0.0 | 1.0 | 1.00 |
| Tokyo | RJTT | 1 | 103 | 64 | 7 | 8 | 8 | 191 | | | | | | | | 50 | 26.2 | 48 | 25.1 | -1.0 | 50 | 100.0 | 50 | 100.0 | +0.0 | 1.0 | 1.04 |
| Naha | ROAH | 0 | 10 | 12 | 17 | 0 | 39 | 78 | | | | | | | | 39 | 50.0 | 39 | 50.0 | 0.0 | 39 | 78.0 | 40 | 80.0 | +2.0 | 1.0 | 1.03 |
| Narita | RJAA | 76 | 51 | 42 | 28 | 19 | 13 | 229 | | | | | | | | 100 | 43.7 | 68 | 29.7 | -14.0 | 100 | 100.0 | 100 | 100.0 | +0.0 | 1.0 | 1.47 |
| Kansai | RJBB | 19 | 52 | 15 | 8 | 0 | 0 | 94 | | | | | | | | 94 | 100.0 | 78 | 83.0 | -17.0 | 94 | 94.0 | 100 | 100.0 | +6.0 | 1.0 | 1.28 |
| New Chitose | RJCC | 54 | 35 | 11 | 8 | 0 | 0 | 108 | | | | | | | | 100 | 92.6 | 68 | 63.0 | -29.6 | 100 | 100.0 | 100 | 100.0 | +0.0 | 1.0 | 1.47 |
| Fukuoka | RJFF | 0 | 10 | 16 | 26 | 2 | 3 | 57 | | | | | | | | 54 | 94.7 | 54 | 94.7 | 0.0 | 54 | 54.0 | 55 | 55.0 | +1.0 | 1.0 | 1.02 |
| Kumamoto | RJFT | 0 | 2 | 4 | 0 | 17 | 19 | 42 | 1 | 28 | 11 | 56 | 4 | 0 | 100 | 10 | 23.8 | 10 | 23.8 | 0.0 | 10 | 10.0 | 10 | 10.0 | +0.0 | 1.0 | 1.00 |
| Osaka | RJOO | 0 | 26 | 14 | 10 | 21 | 0 | 71 | | | | | | | | 54 | 76.1 | 54 | 76.1 | 0.0 | 54 | 54.0 | 54 | 54.0 | +0.0 | 1.0 | 1.00 |
| Sendai | RJSS | 0 | 1 | 3 | 6 | 40 | 28 | 78 | | | | | | | | 14 | 17.9 | 14 | 17.9 | 0.0 | 14 | 14.0 | 14 | 14.0 | +0.0 | 1.0 | 1.00 |
| Tokyo | RJTT | 1 | 103 | 64 | 7 | 8 | 8 | 191 | | | | | | | | 100 | 52.4 | 96 | 50.3 | -2.1 | 100 | 100.0 | 100 | 100.0 | +0.0 | 1.0 | 1.04 |
| Naha | ROAH | 0 | 10 | 12 | 17 | 0 | 39 | 78 | | | | | | | | 39 | 50.0 | 39 | 50.0 | 0.0 | 39 | 39.0 | 40 | 40.0 | +1.0 | 1.0 | 1.03 |
| Narita | RJAA | 76 | 51 | 42 | 28 | 19 | 13 | 229 | | | | | | | | 150 | 65.5 | 102 | 44.5 | -21.0 | 150 | 100.0 | 150 | 100.0 | +0.0 | 1.0 | 1.47 |
| Kansai | RJBB | 19 | 52 | 15 | 8 | 0 | 0 | 94 | | | | | | | | 94 | 100.0 | 94 | 100.0 | 0.0 | 94 | 62.7 | 117 | 78.0 | +15.3 | 1.0 | 1.24 |
| New Chitose | RJCC | 54 | 35 | 11 | 8 | 0 | 0 | 108 | | | | | | | | 108 | 100.0 | 104 | 96.3 | -3.7 | 108 | 72.0 | 150 | 100.0 | +28.0 | 1.0 | 1.44 |
| Fukuoka | RJFF | 0 | 10 | 16 | 26 | 2 | 3 | 57 | | | | | | | | 54 | 94.7 | 54 | 94.7 | 0.0 | 54 | 36.0 | 54 | 36.0 | +0.0 | 1.0 | 1.00 |
| Kumamoto | RJFT | 0 | 2 | 4 | 0 | 17 | 19 | 42 | 2 | 42 | 16 | 84 | 6 | 0 | 150 | 12 | 28.6 | 12 | 28.6 | 0.0 | 12 | 8.0 | 12 | 8.0 | +0.0 | 1.0 | 1.00 |
| Osaka | RJOO | 0 | 26 | 14 | 10 | 21 | 0 | 71 | | | | | | | | 56 | 78.9 | 56 | 78.9 | 0.0 | 56 | 37.3 | 56 | 37.3 | +0.0 | 1.0 | 1.00 |
| Sendai | RJSS | 0 | 1 | 3 | 6 | 40 | 28 | 78 | | | | | | | | 16 | 20.5 | 16 | 20.5 | 0.0 | 16 | 10.7 | 16 | 10.7 | +0.0 | 1.0 | 1.00 |
| Tokyo | RJTT | 1 | 103 | 64 | 7 | 8 | 8 | 191 | | | | | | | | 149 | 78.0 | 145 | 75.9 | -2.1 | 149 | 99.3 | 149 | 99.3 | +0.0 | 1.0 | 1.03 |
| Naha | ROAH | 0 | 10 | 12 | 17 | 0 | 39 | 78 | | | | | | | | 39 | 50.0 | 39 | 50.0 | 0.0 | 39 | 26.0 | 39 | 26.0 | +0.0 | 1.0 | 1.00 |
| Narita | RJAA | 76 | 51 | 42 | 28 | 19 | 13 | 229 | | | | | | | | 200 | 87.3 | 136 | 59.4 | -27.9 | 200 | 100.0 | 200 | 100.0 | +0.0 | 1.0 | 1.47 |
| Kansai | RJBB | 19 | 52 | 15 | 8 | 0 | 0 | 94 | | | | | | | | 94 | 100.0 | 94 | 100.0 | 0.0 | 94 | 47.0 | 108 | 54.0 | +7.0 | 1.0 | 1.15 |
| New Chitose | RJCC | 54 | 35 | 11 | 8 | 0 | 0 | 108 | | | | | | | | 108 | 100.0 | 108 | 100.0 | 0.0 | 108 | 54.0 | 136 | 68.0 | +14.0 | 1.0 | 1.26 |
| Fukuoka | RJFF | 0 | 10 | 16 | 26 | 2 | 3 | 57 | | | | | | | | 54 | 94.7 | 54 | 94.7 | 0.0 | 54 | 27.0 | 54 | 27.0 | +0.0 | 1.0 | 1.00 |
| Kumamoto | RJFT | 0 | 2 | 4 | 0 | 17 | 19 | 42 | 3 | 56 | 21 | 112 | 8 | 0 | 200 | 14 | 33.3 | 14 | 33.3 | 0.0 | 14 | 7.0 | 14 | 7.0 | +0.0 | 1.0 | 1.00 |
| Osaka | RJOO | 0 | 26 | 14 | 10 | 21 | 0 | 71 | | | | | | | | 58 | 81.7 | 58 | 81.7 | 0.0 | 58 | 29.0 | 58 | 29.0 | +0.0 | 1.0 | 1.00 |
| Sendai | RJSS | 0 | 1 | 3 | 6 | 40 | 28 | 78 | | | | | | | | 18 | 23.1 | 18 | 23.1 | 0.0 | 18 | 9.0 | 18 | 9.0 | +0.0 | 1.0 | 1.00 |
| Tokyo | RJTT | 1 | 103 | 64 | 7 | 8 | 8 | 191 | | | | | | | | 183 | 95.8 | 175 | 91.6 | -4.2 | 183 | 91.5 | 183 | 91.5 | +0.0 | 1.0 | 1.05 |
| Naha | ROAH | 0 | 10 | 12 | 17 | 0 | 39 | 78 | | | | | | | | 39 | 50.0 | 39 | 50.0 | 0.0 | 39 | 19.5 | 39 | 19.5 | +0.0 | 1.0 | 1.00 |
| Narita | RJAA | 76 | 51 | 42 | 28 | 19 | 13 | 229 | | | | | | | | 207 | 90.4 | 197 | 86.0 | -4.4 | 207 | 82.8 | 250 | 100.0 | +17.2 | 1.0 | 1.27 |
| Kansai | RJBB | 19 | 52 | 15 | 8 | 0 | 0 | 94 | | | | | | | | 94 | 100.0 | 94 | 100.0 | 0.0 | 94 | 37.6 | 99 | 39.6 | +2.0 | 1.0 | 1.05 |
| New Chitose | RJCC | 54 | 35 | 11 | 8 | 0 | 0 | 108 | | | | | | | | 108 | 100.0 | 108 | 100.0 | 0.0 | 108 | 43.2 | 119 | 47.6 | +4.4 | 1.0 | 1.10 |
| Fukuoka | RJFF | 0 | 10 | 16 | 26 | 2 | 3 | 57 | | | | | | | | 54 | 94.7 | 54 | 94.7 | 0.0 | 54 | 21.6 | 54 | 21.6 | +0.0 | 1.0 | 1.00 |
| Kumamoto | RJFT | 0 | 2 | 4 | 0 | 17 | 19 | 42 | 4 | 70 | 27 | 139 | 10 | 0 | 250 | 16 | 38.1 | 16 | 38.1 | 0.0 | 16 | 6.4 | 16 | 6.4 | +0.0 | 1.0 | 1.00 |
| Osaka | RJOO | 0 | 26 | 14 | 10 | 21 | 0 | 71 | | | | | | | | 60 | 84.5 | 60 | 84.5 | 0.0 | 60 | 24.0 | 60 | 24.0 | +0.0 | 1.0 | 1.00 |
| Sendai | RJSS | 0 | 1 | 3 | 6 | 40 | 28 | 78 | | | | | | | | 20 | 25.6 | 20 | 25.6 | 0.0 | 20 | 8.0 | 20 | 8.0 | +0.0 | 1.0 | 1.00 |
| Tokyo | RJTT | 1 | 103 | 64 | 7 | 8 | 8 | 191 | | | | | | | | 183 | 95.8 | 179 | 93.7 | -2.1 | 183 | 73.2 | 185 | 74.0 | +0.8 | 1.0 | 1.03 |
| Naha | ROAH | 0 | 10 | 12 | 17 | 0 | 39 | 78 | | | | | | | | 39 | 50.0 | 39 | 50.0 | 0.0 | 39 | 15.6 | 39 | 15.6 | +0.0 | 1.0 | 1.00 |
| Narita | RJAA | 76 | 51 | 42 | 28 | 19 | 13 | 229 | | | | | | | | 208 | 90.8 | 205 | 89.5 | -1.3 | 208 | 69.3 | 243 | 81.0 | +11.7 | 1.0 | 1.19 |
| Kansai | RJBB | 19 | 52 | 15 | 8 | 0 | 0 | 94 | | | | | | | | 94 | 100.0 | 94 | 100.0 | 0.0 | 94 | 31.3 | 99 | 33.0 | +1.7 | 1.0 | 1.05 |
| New Chitose | RJCC | 54 | 35 | 11 | 8 | 0 | 0 | 108 | | | | | | | | 108 | 100.0 | 108 | 100.0 | 0.0 | 108 | 36.0 | 113 | 37.7 | +1.7 | 1.0 | 1.05 |
| Fukuoka | RJFF | 0 | 10 | 16 | 26 | 2 | 3 | 57 | | | | | | | | 54 | 94.7 | 54 | 94.7 | 0.0 | 54 | 18.0 | 54 | 18.0 | +0.0 | 1.0 | 1.00 |
| Kumamoto | RJFT | 0 | 2 | 4 | 0 | 17 | 19 | 42 | 4 | 85 | 32 | 168 | 11 | 0 | 300 | 17 | 40.5 | 17 | 40.5 | 0.0 | 17 | 5.7 | 17 | 5.7 | +0.0 | 1.0 | 1.00 |
| Osaka | RJOO | 0 | 26 | 14 | 10 | 21 | 0 | 71 | | | | | | | | 61 | 85.9 | 61 | 85.9 | 0.0 | 61 | 20.3 | 61 | 20.3 | +0.0 | 1.0 | 1.00 |
| Sendai | RJSS | 0 | 1 | 3 | 6 | 40 | 28 | 78 | | | | | | | | 21 | 26.9 | 21 | 26.9 | 0.0 | 21 | 7.0 | 21 | 7.0 | +0.0 | 1.0 | 1.00 |
| Tokyo | RJTT | 1 | 103 | 64 | 7 | 8 | 8 | 191 | | | | | | | | 183 | 95.8 | 175 | 91.6 | -4.2 | 183 | 61.0 | 186 | 62.0 | +1.0 | 1.0 | 1.06 |
| Naha | ROAH | 0 | 10 | 12 | 17 | 0 | 39 | 78 | | | | | | | | 39 | 50.0 | 39 | 50.0 | 0.0 | 39 | 13.0 | 39 | 13.0 | +0.0 | 1.0 | 1.00 |

**Table A 4-4.** Aerodrome design and operations, aerodrome reference code in Annex 14 - volume 1: by ICAO.

| Runway | | Aero plane | | |
|---|---|---|---|---|
| Code Name | Aero plane reference field length | Code Letter | Wingspan | Outer main gear wheel span |
| 1 | Less than 800 m | A | < 15 m | < 4.5 m |
| 2 | 800 m up to but not including 1200 m | B | 15 m but < 24 m | 4.5 m but < 6 m |
| 3 | 1200 m up to but not including 1800 m | C | 24 m but < 36 m | 6 m but < 9 m |
| 4 | 1800 m and over | D | 36 m but < 52 m | 9 m but < 14 m |
| | | E | 52 m but < 65 m | 9 m but < 14 m |
| | | F | 65 m but < 80 m | 14 m but < 16 m |

# CHAPTER 5

Conclusions and Discussions

## SUMMARY OVERVIEW

| | |
|---|---|
| *Main Objective* | " To provide short-term solution for aviation industry during the volcanic disaster by reducing the damage to aircraft by aircraft evacuation and management of airport limited capacity with optimization approach " |

**Question 1:**
**How to select shelter airport for aircraft evacuation** with approximate solution?
Sub question: ?

Chapter 3 →

✓ **The basic constraints for evacuation** (time, distance, and shelter's capacity)
✓ **Historical dataset**: flight (CARATS) and airport facility (AIS) data could help to generate an accuracy results.
✓ **Genetic Algorithm (GA) was applied** to the proposed model had been proofed the higher capability in finding the approximate solution, **compared to GRASP (Randomized heuristic algorithm)**

**Question 2:**
How to improve the shelter airport selection model to suitable shelter airport which could help airport and airline perform their operations during and after the disaster?

Chapter 4 →

✓ **Additional dataset** of airport and airline were added as new constraints of the model applied with GA.
✓ **Comparison between the previous model** and new proposed model had shown better results. However, it generated higher(worst) in objective function value (min flight time), from **stress created by multiple constraints**.

**Question 3:**
How can airport utilize it aircraft parking capacity to handle more grounded aircraft during the disaster without invest more on expanding their facility?

Chapter 5 →

✓ **Airport pavement and aircraft parking regulations had been studied** to understand aircraft parking procedures in an emergency
✓ **Aircraft assignment model was developed using 2DBP algorithm.**
✓ 2DBP and its selected packing procedures had **allowed aircraft to park inside parking stand as M:1 assignment under safety measures.**
✓ **Comparison between conventional (1:1) and 2DBP (M:1),** 2DBP had shown capability in increasing airport parking space utilization, which **led to smaller number of airport and stand needed** for aircraft in an emergency

## SHELTER AIRPORT SELECTION FOR AIRCRAFT EVACUATION

This study has proposed the conceptual models for shelter airport selection and aircraft parking space utilization for aircraft evacuation and grounded aircraft during the disaster, e.g., a volcanic eruption. The main purposes were reduction of evacuation flight time and maximum shelter airport capacity. The models had been tested on a case study of a volcanic eruption at Mt. Hakone in Japan's central and its major airports, with the latest air traffic data in March 2016 (CARATS open dataset) provided by MLIT. In addition, the airport facilities data by AIS and airlines flight schedules at each airport are also used to determine the number of the affected area, airports, the number of affected aircraft and the available aircraft stands for evacuation during the event. Finally, the airborne and on-ground affected aircraft have been simulated in their current positions and selected the appropriate shelter airports for evacuation. Japan's airports were chosen as shelter airports by location outside ash cloud affected area, sufficient runway length for accommodating affected aircraft, and available aircraft stands (non-occupancy stands).
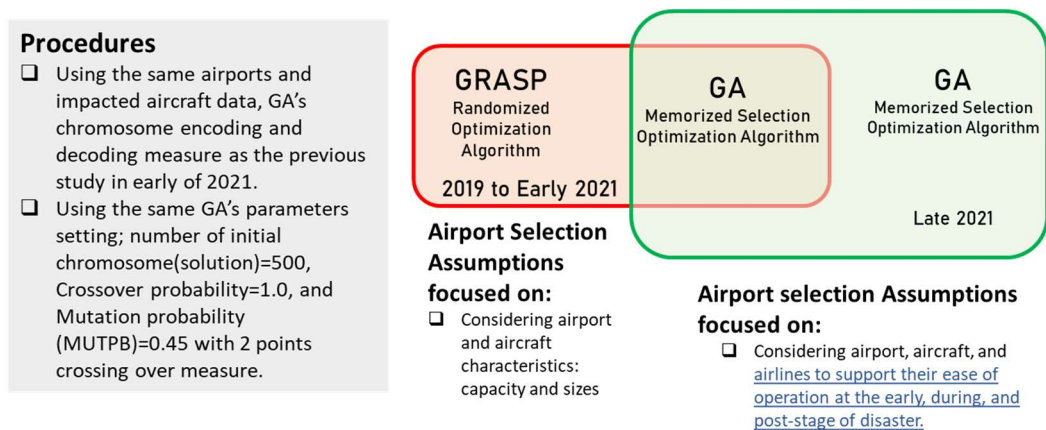
On the first study, a proposed models had applied to the Genetic Algorithm (GA) and Greedy Randomized Adaptive Search Procedure (GRASP) to find the approximate solution of shelter airport selection. Both algorithms proved their capabilities of searching for the approximate solution according to the study objective and subjective of the assigned aircraft to shelter airports with minimum total flight time and not exceeding selected airports' capacities. With the same logical model of aircraft's assignment and running iteration, GA outperformed GRASP to find less total flight time solution for the overall population with fewer selected shelter airports on the case study. Since they were different in the best solution selection mechanism, this gave GA's mechanism the advantage in preserving and passing on the previous best solution to

its offspring through crossover operation while GRASP randomly generate new solution on every iteration with no trace of the previous best solution.

Additionally, the second study examined more one airport and airline criteria to determine the appropriate shelter airport selection solution. These additional criterions could also help improvement of airport and airline performance during the crisis, and the recovery of aircraft flight schedules. Compared to the first proposed model, the new proposed shelter airport selection model performed better across all constraints. It highlighted that the new model could assist airports and airlines in better managing and planning for aircraft evacuations under additional airport and airline constraints, see Figure 5.5.1. As noted at the outset of this study, this could lead to a more efficient and cost-effective airport emergency plan at all stages for disaster management.

**Purpose**
❑ Compare results between the previous selection model and new proposed model under 6 assumptions
❑ Validate the new proposed model whether it could give results correspondent to the assumptions.

**Procedures**
❑ Using the same airports and impacted aircraft data, GA's chromosome encoding and decoding measure as the previous study in early of 2021.
❑ Using the same GA's parameters setting; number of initial chromosome(solution)=500, Crossover probability=1.0, and Mutation probability (MUTPB)=0.45 with 2 points crossing over measure.

**GRASP**
Randomized Optimization Algorithm
2019 to Early 2021

**Airport Selection Assumptions focused on:**
❑ Considering airport and aircraft characteristics: capacity and sizes

**GA**
Memorized Selection Optimization Algorithm

**GA**
Memorized Selection Optimization Algorithm
Late 2021

**Airport selection Assumptions focused on:**
❑ Considering airport, aircraft, and airlines to support their ease of operation at the early, during, and post-stage of disaster.

**Figure 5.5.1** The differentiation framework and comparison between early 2021 and late 2012 models of shelter airport selection for aircraft evacuation

Although the proposed model, which was based on a broader perspective of airline operations, may provide helpful guidance to all level (local, national, international) of aviation emergency planners and decision-makers, such as International Civil Aviation Organization (ICAO), Civil Aviation Bureau, Ministry of Land, Infrastructure, Transport and Tourism (MLIT) of Japan, airports, airlines, etc. However, the legislation and the operating procedures of airports, airlines and air traffic management make it susceptible to limitations due to the intricacy of the regulation. Nevertheless, the studies also revealed the critical shelter airports for aircrafts evacuation. The larger-size airport with a large number of available aircraft stands was likely to act as the critical shelter airport during the disaster event. The alternative adjustment of the proportion of available aircraft stands at shelter airports, along with the proportion of affected aircrafts, will give flexibility to the algorithms' output, which gives the better suggestion on which shelter airports could accommodate a reasonable number of aircraft according to their capacities.

## AIRPORT'S AIRCRAFT PARKING SPACE UTILIZATION FOR GROUNDED AIRCRAFT

The study had developed aircraft parking space utilization model, which could enhance the limited aircraft parking space to accommodate more number of grounded aircraft during the disaster, using two-dimensional bin packing algorithm (2DBP). An increasing number of medium to long-period grounded aircraft during the disaster could disrupt airport's operation especially, aircraft movement and aircraft parking aircraft management. Aircraft parking utilization for grounded aircraft to maximize the limited airport's aircraft handling capacity could relax airport's airside congestion. It's also help minimize number of aircraft parking space and airport used for supporting aircraft evacuation.

For aircraft assigned to the aircraft stand at the airport, there are regular restrictions between the assigned aircraft and the aircraft stand based on an aircraft's weight, the pavement's strength, an aircraft's dimensions, and clearance distance. An aircraft should park on the same-sized aircraft stand or a larger one to ensure its safety and the safety of surrounding facilities and other aircraft. In an emergency, airport authorities may decide to provide an additional area(s) to accommodate the surge of aircraft, particularly non-scheduled aircraft required to park for an extended period of time due to the disaster's duration. In this case, the airport's authorities could repurpose some of the airside paved areas by prioritizing the use of unused aircraft apron space (terminal and remote aprons), taxiway(s), and runway(s) as dedicated parking areas, following the FAA's and KAR's recommendation for long-term aircraft parking management in COVID-19. Nonetheless, those designated areas should not interfere with regular airport and airline operations.

Compared to the conventional aircraft stand assignment, the two-dimensional bin packing algorithm used in this study can utilize aircraft stands (M:1), allowing multiple aircraft to be parked in a single stand without violating ICAO or airport safety regulations (1:1). As a result, the average efficiency of utilizing a single-strand space increases, resulting in a reduced (minimized) number of aircraft stands being used; see Figure 5.5.2 below.
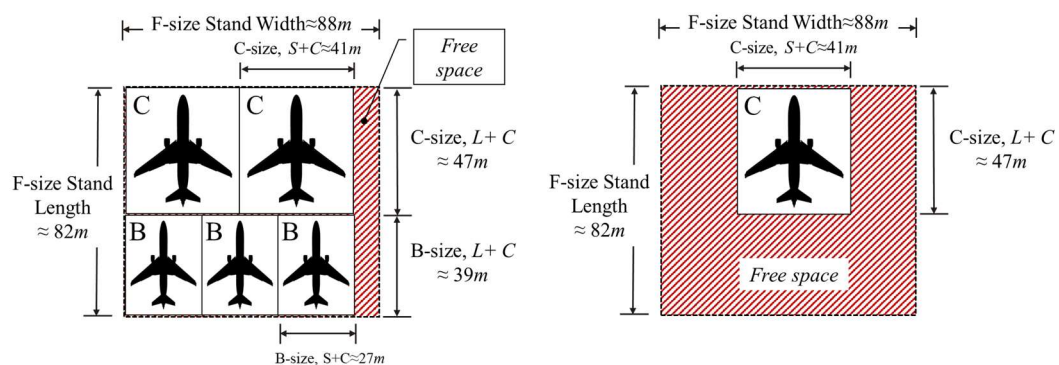


**Figure 5.5.2** The result's example on assigning aircraft into the F-size stand; (right) the regular aircraft assignment one-to-one (1:1) without 2DBP and (left) the proposed model aircraft assignment many-to-one (M:1) generated by 2DBP.

According to the findings of this study, the commercial aircraft size ratio in Japan's airspace has a significant effect on the utilization of aircraft stands at candidate shelter airports. As a result, the shelter airport equipped with a large number of stands and dedicated pavement areas will serve as the critical shelter airport during the disaster. Airports with dedicated taxiways and runways, in particular, are likely to have a significant impact on aircraft stand utilization. Since those

dedicated areas provide exceptionally large space and can accommodate a range of aircraft sizes from the largest to the smallest, particularly the extra-large size (F) of aircraft stands, it benefits the medium-size aircraft (C), which account for the majority of aircraft in Japan's airspace, by allowing them to pack together in a single stand. Thus, additional dedicated areas such as taxiways and runways contribute significantly to the reduction of airport stand utilization rates, allowing for more aircraft to operate and avoiding airport traffic congestion during an emergency.

## LIMITATIONS

This studies' main limitations were subject to the unavailable data as follows: the accurate number of affected aircraft and their itineraries data for both airborne and on-ground, historical data of volcanic ash cloud coverage area, and its range from Mt.Hakone.

Although the number of affected aircraft were observed from the historical data before the pandemic, the aircraft stand occupancy rate and available of aircraft stands at candidate shelter airports in this study may not represent the normal air traffic situation of this region during the COVID-19 pandemic, which caused declined in most airline and airport operations by 90%. Hence, shelter airports' historical flight schedule data before the pandemic are required for the occupancy rate calculation accuracy to reflect the air traffic level's normal situation. However, this study's proposed model has allowed the occupancy rate adjustment to reflect air traffic congestion level close to the level before the pandemic. Therefore, real-time or up-to-date airport and flight data are required to accurately simulate and generate results for aviation disaster scenarios. Emphasis should be placed on the airport's airside facilities, occupancy rate, and specific aircraft affected.

Furthermore, the unavailable ash cloud historical data of Mt.Hakone, the Sakurajima's volcanic ashfall, and ash cloud were studied to understand the ash cloud's behaviour, which was used to predict and determine the possible ash cloud coverage area in the case study. In addition, the changing for wind speed and direction in each season in scenario analysis in the future study.

## SUGGESTIONS FOR FURTHER STUDY

| Shelter Airport Selection Model | Airport Aircraft parking space Utilization Model |
|---|---|
| How to select shelter airport for aircraft evacuation and improve the selection model? | How can airport utilize it aircraft parking capacity to handle more grounded aircraft during the disaster? |
| Variety and accuracy of datasets<br>• Online/real-time and more information of flight dataset<br>• Various behavior and pattern of disaster.<br>• Disaster coverage and impacted areas/facilities and their attributes.<br>Observation items and selection constraints<br>• Evacuation items e.g., people, vehicles, and objects and their attributes.<br>• Selection constrains and restrictions.<br>Result evaluation | Variety and accurate information<br>• Parking/areas utilization constraints and restrictions.<br>Packing algorithm variants<br>• Variety of 2DBP and its variants could be used. (free space management and packing algorithm). |

| | |
|---|---|
| ▪ Economic costs evaluation.<br>Applying on other case study of volcanic eruption or other kind for natural disaster e.g., flooding, earthquake, typhoon, and etc. | ▪ Shapes and orientations of packing item and demand bin (polygon).<br><br>Result evaluation<br><br>▪ Economic costs evaluation.<br><br>Apply of the corresponding disaster scenarios (affected and shelter facilities). |

The studies could give suggestion for the authorities for the airport and aircraft emergency evacuation planning. It's also given a conceptual model of shelter airport selection solution for aircraft's evacuation in the volcanic eruption event using the nearest distances and airport capacity by aircraft size constraints. As mentioned earlier, it still has limitations depending on the regulation's complexity at the airport, airline, and air traffic management. The further applications on airport selection may need to set up more objectives and constraints for the shelter airport selection algorithm to effectively provide a more realistic selection from the beginning of evacuation until recovering for all sections of aircraft, passengers, and cargo and flight crew scheduling.

Nevertheless, an increase in the number of shelter airport selection constraints may impact aircraft travel distance and flight time because there was fewer acceptable shelter airport selection solution for affected aircraft near its current position. It's also resulted in the longer of computational time and conflict among multiple constraints, which unavoidably rises the objective function. Therefore, emergency planners and decision-makers must exercise extreme caution in selecting associated factors and constraint coefficient values that accurately reflect all parties' reality, practical operation, and objective. Finally, all studied models be able to apply on other case studies of disaster types, areas, and airports with additional dataset and model adjustment to give the accurate result accordingly.